Final Report on

EXPERIMENTAL INVESTIGATIONS OF TRIBOLOGICAL AND MECHANICAL PROPERTIES OF FIBRE REINFORCED COMPOSITES

UGC Major Research Project

Report submitted by

NIPU MODAK
PRINCIPAL INVESTIGATOR

UGC Reference No. : F. No. 42-882/2013(SR), 25th March 2013

01.04.2013   to   31.03.2017

Department of Mechanical Engineering
Faculty Council of Engineering & Technology
Jadavpur University
Kolkata, India

Professor
Department of Aerospace Engineering
and Applied Mechanics
Indian Institute of Engineering
Science and Technology, Shibpur
Howrah - 711 103, INDIA

Professor
Department of Aerospace Engineering
and Applied Mechanics
Indian Institute of Engineering
Science and Technology, Shibpur
Howrah - 711 103, INDIA.

1

Final Report on

EXPERIMENTAL INVESTIGATIONS OF TRIBOLOGICAL AND MECHANICAL PROPERTIES OF FIBRE REINFORCED COMPOSITES

UGC Major Research Project

Report submitted by
NIPU MODAK
PRINCIPAL INVESTIGATOR
UGC Reference No. : F. No. 42-882/2013(SR), 25th March 2013
01.04.2013   to   31.03.2017

Department of Mechanical Engineering
Faculty Council of Engineering & Technology
Jadavpur University
Kolkata, India

UNIVERSITY GRANTS COMMISSION
BAHADUR SHAH ZAFAR MARG
NEW DELHI – 110 002

ASSESSMENT CERTIFICATE

(to be submitted with the Final Report)

It is certified that the proposal entitled "**Experimental Investigations of Tribological and Mechanical Properties of Fibre Reinforced Composites**" by (Dr./Prof./Mr./Mrs.) **Nipu Modak** Deptt. of **Mechanical Engineering, Jadavpur University** has been assessed by the **External Experts** committee consisting the following members for submission to the University Grants Commission, New Delhi for financial support under the scheme of Major Research Projects:

Details of Expert Committee:

1.

Professor
Department of Aerospace Engineering
and Applied Mechanics
Indian Institute of Engineering
Science and Technology, Shibpur
Howrah - 711 103, INDIA

2. *Salil Halder*

Professor
Department of Aerospace Engineering
and Applied Mechanics
Indian Institute of Engineering
Science and Technology, Shibpur
Howrah - 711 103, INDIA

The proposal is as per the guidelines.

(REGISTRAR/ PRINCIPAL)

Registrar
JADAVPUR UNIVERSITY
(Seal)

1. INTRODUCTION

1.1 Overview

A composite is a material that is formed by combining two or more materials to achieve some superior properties. Composite materials find use in a variety of applications owing to their high strength, lightness, ease of fabrication, and availability of wider choice of systems (ASM Hand Book, 1992). In view of their superior strength and stiffness properties, they are found to be suitable for structural applications. Composites are used in many mechanical components such as gears, cams, wheels, impellers, brakes, seals, bushes, and bearings. One of the areas where their use has been found to be advantageous is the situation involving contact wear. Polymer based composite materials are increasingly employed in tribological applications owing to their ever increasing demands in terms of stability at higher loads, temperatures, better lubrication, and wear properties.

Major constituents in a glass fiber reinforced composite are the reinforcing fibers and a matrix, which acts as a binder for the fibers. In addition, particulate fillers can also be used with some polymeric matrices primarily to reduce cost and improve their dimensional stability. So, although a judicious selection of matrix and the reinforcing phase can lead to a composite with a combination of strength and modulus comparable to or even better than those of conventional metallic materials (Jang, 1994), the physical and mechanical characteristics can further be modified by adding a solid filler phase to the matrix body during the composite preparation. The fillers play a major role in determining the properties and behavior of particulate reinforced composites. The term 'filler' is very broad and encompasses a very wide range of materials. It is arbitrarily defined as a variety of natural or synthetic solid particulates (inorganic, organic) that may be irregular, acicular, fibrous or flakey. The improved performance of polymers and their composites in industrial and structural applications by the addition of

particulate fillers has shown a great promise and so has lately been a subject of considerable interest.

The present project work thus is undertaken to study the processing, characterization and tribological performance of woven glass fiber reinforced epoxy composites with and without aluminium filler. Attempts have also been made to explore the possible use of aluminium powder as filler materials in these composites.

1.2 literature review

The purpose of this literature review is to provide background information on the issues to be considered in this thesis and to emphasize the relevance of the present study. This treatise embraces various aspects of polymer composites with a special reference to their mechanical, tribological characteristics. Aramide et al. (2012) observed for woven-mat glass polyester composite, the tensile strength, young's modulus, elastic strain and flexural properties increased with increased of the glass fiber V_f but impact strength decreased after a certain V_f of glass fiber. whereas the higher tensile strength and modulus are observed at 40% W_f for the polyester/virgin glass fiber reinforced composite (Araujo et al., 2006). Dandekar et al. (2003) investigated the compression and release response behavior of a woven mat S2 GF-reinforced polyester composites under shock loading and they found that the hugoniot elastic limit (HEL) of composites ranging from 1.3 GPa to 3.7 GPa. Leonard et al. (2009) concluded that 60 V_f of chopped strand mat glass fiber reinforced polyester (CGRP) composites had the maximum improvement of tensile strength, young's modulus, fracture toughness and critical energy release rate. Alam et al. (2010) studied the effect of orientation of chopped strand and roving GFRP composites, the result showed that at 90^0 fiber orientation tensile strength was maximum. The short fiber was found to be reducing the impact strength. The compression, bending and shear behavior of woven mat E glass

fiber reinforced epoxy composites with different fabrics showed that the Z-directional stitching fibers increased the delamination resistance, reduced the impact damage and as well as lowered the bending strength of the composites. The compressive strength of the non-crimp laminate was 15% higher than woven fabric composite (Yang et al., 2000).

The Impact response of woven mat glass fiber reinforced epoxy composites with orthogonal fabric and non-orthogonal fabric of varying weaving angle showed the energy absorption increased with decreased weaving angle (Atas and Liu, 2008). The low-velocity impact damage study of woven E-glass-reinforced vinyl-ester composites with various laminates showed that 3D composites was more resistant to penetration and dissipated more total energy (Baucom and Zikry, 2005). In another experiment, Zaretsky and Perl (2004) investigated the dynamic response of woven GFs-reinforced epoxy composite subjected to impact loading at different velocities. The result showed that the impact strength increased with increased shock wave velocity and the wave speed decreased with decreased pressure. The performance of glass polymer composites can be further improved with the modification of fibers or polymers. Etcheverry and Barbosa (2012) developed a methods for GF/PP adhesion improvement involving the modification of fibers with an aluminium alkyl and hydroxy-α-olefin by growing of the PP chains using direct metallocenic copolymerization. The strength and toughness increased three times and the interfacial strength duplicates in PP/GF composites prepared with in-situ polymerized fibers.

Shokrieh, et al. (2012) developed a model to perform the progressive failure analysis of quasi isotropic composite plates at low temperatures. The effect of low temperature on the failure mechanism of the plates was established. In a similar study, Reis et al. (2013) studied the damage behavior of a composite material based on glass fiber reinforced polymer (GFRP) to predict the rupture force. They developed a model for tensile developed within the framework of continuum

damage mechanics that accounts for the effect of the load rate and temperature of the system.

Mechanical properties of glass polymer composites can also be improved by hybridization of glass fibers with other fibers. The positive hybrid effects exist for flexural strengths of E glass and TR50S carbon fiber reinforced hybrid composites (Dong and Davies, 2013). In the similar study, hybrid composites of kevlar/glass and carbon/glass with different angle ply orientations in epoxy resin, mechanical properties such as tensile strength, tensile modulus, & peak load are greatly influenced by angle ply orientation and 0°/90° orientation showed significant increase in tensile properties as compared to other orientation (Raja and Hari, 2013). The mechanical and electrical properties of Roystonea regia/glass fiber with varying glass fiber loading reinforced epoxy hybrid composites; tensile, flexural, impact and hardness properties of hybrid composites considerably increased with increased glass fiber loading. But electrical conductivity and dielectric constant values decreased with increased glass fiber content (Goud and Rao, 2012). Mansor et al. (2013) used the analytical hierarchy process (AHP) method to select the most suitable natural fiber to be hybridized with glass fiber reinforced polymer composites for the design of passenger vehicle center lever parking brake component and it concluded that the kenaf bast fiber yielded the highest quality and was selected as the best material to formulate the hybrid polymer composites. Almeida et al. (2013) evaluated the effect of hybridizing glass and curaua fibers on the mechanical properties. From the obtained results, it was observed that the tensile strength and modulus increased with glass fiber incorporation. In a study of different hybrid laminates, Petrucci et al. (2013) showed that the mechanical performance of all the hybrid laminates appeared superior to pure hemp and flax fiber reinforced laminates and the best properties were offered by those obtained by adding glass and flax to basalt fiber reinforced laminates. Ramesh et al. (2013) investigated the mechanical properties such as

7

tensile strength, flexural strength and impact strength of sisal–jute–glass fiber reinforced polyester composites They indicated that the incorporation of sisal–jute fiber with GFRP improved the properties and used as a alternate material for glass fiber reinforced polymer composites.

Several reports are available in literatures on the tribological characteristics of glass fiber reinforced thermoplastic polymer composites. The tribological properties of glass fiber reinforced polypropylene (PP) can be significantly improved with a suitable forms of glass fiber reinforcement (Hufenbach et al., 2012). Along with the forms, the quantity of glass fiber as reinforcement and type of the thermoplastic polymer used are also very significant on tribological behavior of the composites (Unal et al., 2006). Bijwe et al. (1989) investigated the tribological behavior of glass-fiber-reinforced polyetherimide composite and found that the specific wear rate was comparable with that of commercially available bearing materials. Similarly, Chen et al. (2006) conducted an experiment on glass fiber reinforced PA66/PPS blend composites and concluded that at a certain GF content, friction coefficient reported lowest value but with the increase of GF content wear volume decreased. In another experiment, Suresha (2008) showed that at dry sliding condition the friction and wear of short glass fiber (SGF) reinforced thermoplastic polyurethane (TPU) composites decreased with increased of SGF wt% depending on load and velocity. Short glass fiber reinforcement in PA66 composites during the sliding against identical materials showed the major benefits of glass fiber reinforcement for reducing the friction coefficient within the matrix softening point (Kukureka et al., 1999). The tribological response of glass and thermoset polymer composites are different than that of thermoplastic polymer composites. Pıhtılı and Tosun (2002) in an investigation of ECGRP composite showed that GF-reinforced polyester matrix composite was more wear resistant than the plain polyester. Further in an reciprocating test, Mathew et al. (2007) established that composites with epoxy

resin showed the best tribological properties among the available thermosets. Suresha et al. (2006) have shown that fiber reinforcements are effective in reducing wear in adhesive situations for glass epoxy composites. In PEEK and GFR reinforced PEEK composites, friction and wear were dependent on the contact pressure and sliding speed under dry pin on disc arrangement (Sumer et al., 2008). In an experiment for short glass fiber reinforced polyamide 6–polyurethane (PA6–PU) block copolymers composites sliding against a chromium steel ball, Li et al. (2010) showed that both friction coefficient and wear rate increased with the increased load and with the increased sliding speed, the friction coefficient decreased and wear rate increased. In epoxy based glass polymer composites, Sampathkumaran et al. (2001) highlighted the effect of load and sliding velocity on the wear loss pattern in sliding wear condition. In an experimental investigation on friction characteristics of GFR-epoxy composite sliding against hard steel, cast iron and aluminium as counterface, El-Tayeb et al. (2005) revealed that for hard steel and cast iron a common trend of increased friction coefficient with increased normal load and decreased friction coefficient with the increased sliding velocities but friction coefficient was maintained at lower level when sliding against aluminium at higher velocities, in comparison of hard steel and cast iron. Suresha et al. (2006) concluded for glass epoxy composite, the friction coefficient was in decrease with the increase in sliding velocity or decrease in the load. and for optimization of tribological characteristics, moderate load and sliding velocity are the preferred choice irrespective of the type of composite.

An investigation of composites of four directionally oriented (biaxial, biaxial non-woven, triaxial and quadraxial) warp knit glass performs and three different thermoset resins (polyester, vinylester and epoxy resin) on a reciprocating sliding test rig. shows that sliding time has a strong effect on the tribological performance (Mathew et al., 2007). Sen et al. (2015) concluded that friction and

wear has a tendency to increase with increase in time based on the investigation using block-on-roller arrangement in dry sliding conditions. Pıhtılı and Tosun (2002) investigated the wear behavior of glass fiber reinforced polyester composite and plane polyester composite against SAE 1030 steel, weight loss of the GFRP specimen is lower than plain polyester specimen depending on the sliding distance. The weight loss in the GFRP and plain polyester specimen did not change for a substantial amount of travel distance (942 m), the weight loss in the plain polyester increased after 942 m drastically, which can be explained by increase in the temperature at the interface and the polyester becoming brittle due to the thermal effect. Suresha at al. (2007) The effect of abrading distances on three-body abrasive wear behavior of glass–epoxy composites has been investigated. The wear volume loss increases with increasing abrading distance. However, the specific wear rate decreases with increase in abrading distance. Sampathkumaran et al. (2001) observed the SEM features of glass fiber–epoxy composites subjected to sliding wear for distances ranging from 500m to 6 km. Results have shown that for the longer run case interface separation is noticed, while for shorter runs matrix debris formation and occasional glass fiber fragmentation are seen. The debris rate was lower for smaller distance and higher for larger distance. Yousif et al. (2008b) investigated interface temperature and frictional behavior of chopped strand mat fiberglass reinforced polyester (CGRP) in three different orientations, at different loads and velocity. Experimental results show that friction and interface temperature are dependent on the orientation pattern, load and velocity and the interface temperature of (AP & P) orientation is similar. Another experiment carried to investigate the wear behaviour of glass fiber reinforced polyester composite, Pıhtılı and Tosun (2002) concluded that increased temp at the interface result in the brittle layer formation which breaks out from the surface and increase wear by acting as abrasive media. Pin on disc experiments of glass fiber reinforced phenolic resin–

based friction material at different shows that the friction coefficient increased with increasing disc temperature up to 300^0C and then decreased above this temperature. The specific wear rate was found to increase with disc temperature (Ozturk et al., 2013). The AP-orientation had more interface temperature (29^0 to 50^0C) compared to P-orientation of chopped strand mat GF reinforced unsaturated polyester composites (Yousif, 2008).

In recent times researchers are trying to explore natural particles as filler in glass polymer composites for a wide variety of industrial applications owing to their good combination of physical and mechanical properties (Debnath et al., 2013). In this direction, Mohan et al. (2011) established that Jatropha oil cake (JOC) filler incorporation into glass fabric-epoxy (G-E) composites enhanced its mechanical properties. In the similar study, Kumar et al. (2013) showed that a fixed weight fraction of mustard cake in varying weight fraction of woven glass fiber reinforced epoxy composites has a very significant role for the superior mechanical properties. Hard particulate fillers consisting of ceramic or metal particles and fibers made of glass are being used these days to improve the performance of polymer composites to a great extent (Sawyer et al., 2003). Various kinds of polymers and polymer matrix composites reinforced with metal particles have a wide range of industrial applications such as heaters, electrodes (Kim et al., 2004), composites with thermal durability at high temperature etc. (Nikkeshi et al., 1998). Similarly, ceramic filled polymer composites have also been the subject of extensive research in last two decades. Incorporation of silicon carbide particles into glass fabric/epoxy as a secondary reinforcement composites leads to an enhancement of their mechanical properties, such as Young's modulus, tensile strength, flexural strength and compression strength (Mohan et al., 2014). The mechanical properties of randomly oriented glass fiber (RGF) reinforced with epoxy resin filled with Al_2O_3, SiC and pine bark dust had

been investigated by Patnaik et al. (2010) and they showed that Incorporation of these fillers modified the tensile, flexural, and impact strengths of the composites. The use of other particle like mica in glass epoxy composite is helpful to improve the hardness and compressive strength of unidirectional E-glass fiber reinforced epoxy resin composites (Srivastava et al., 1992). Similarly, the soft particles i.e particles of mica and tricalcium phosphate in glass epoxy composite further improved the mechanical properties based on the filler contributed to enhance the bonding strength between fiber and epoxy resin (Srivastava and Wahne, 2007). The hybrid composites consisting of bi-directional E-glass-fiber reinforced epoxy filled with different LD slag content (0, 7.5, 15, 22.5 wt%), Pati and Satapathy (2015) proved that LD slag, in spite of being a waste, possesses fairly good filler characteristics as it modifies the strength properties and improves the composite micro-hardness.

Suresha et al. (2006a) investigated the friction and wear behavior of E-GF (woven mat) reinforced epoxy composites with and without SiC particles. The result showed that (5 wt%) SiC particles filled composite had higher coefficient of friction and higher resistance to wear at sliding distance ranging from 2000 m to 4000 m compared to without SiC-filled composites. In between two inorganic fillers, silicon carbide (SiC) and graphite, Graphite filled G-E composite shows lower friction coefficient and SiC filled G-E composite exhibited the maximum wear resistance (Suresha et al., 2006b). Mohan et al. (2014) experimented the tribological behavior of silicon carbide filled glass fabric reinforced-epoxy (SiC-G-E) composites using pin-on-disk test rig at various temperatures, applied loads, and a fixed sliding velocity of 1.5 m/s and for a sliding distance of 5000 m. The wear loss in both the composites increases with increase in temperature/applied load and under the same conditions the specific wear rate increases. However, silicon carbide particulate filled G-E composite exhibits lower wear rate with higher coefficient of friction as compared to virgin G-E composite. Patnaik et al.

(2010) investigated the wear behavior of randomly oriented E-GF-reinforced epoxy composites with particulate-filled like Al_2O_3, SiC and pine bark dust at different loads and the sliding distance ranging from 200 m to 600 m. Among the composites with different wt%, they have concluded that GF (50 wt%)/Epoxy (40 wt%)/Pine bark dust (10 wt%) composite had better wear resistance for all sliding distance. Suresha and Chandramohan (2008) investigated the three-body abrasive wear behavior of woven E-GF-reinforced vinyl ester composites with particulate-filled like SiC and graphite fillers. The experimental result showed that the graphite and silicon-filled composites had more abrasion resistance and lower specific wear rate than unfilled composites. Shivamurthy and Prabhuswamy (2009) investigated the effect of silica content on the sliding wear and coefficient of friction of GE composites at different loads and for a fixed velocity and a constant abrading distance of 1200 m by using pin-on-disc machine. 3 and 6 wt% of SiO_2 filled GE composites exhibits good performance in flexural and slide wear resistance. Further addition of SiO_2 filler are not beneficial for flexural and slide wear performance. Raju et al. (2013) studied the two-body abrasive wear behavior of alumina (Al_2O_3) with different wt% filled glass fabric reinforced epoxy (G-E) composites. Experimental results showed that the presence of Al_2O_3 filler reduced the specific wear rate of G-E composite and the excellent wear resistance was obtained for 10 wt% Al_2O_3 filled G-E composites. Sampathkumaran et al. (2000) carried out a study on the slide wear characteristics of a glass–epoxy composite, filled with either rubber or oxide particles and the block-on-roller test results showed that at high loads the rubber-filled composite had lower wear.

The comparative performance of glass–epoxy (G–E) composites filled with rubber and graphite of two differing levels were conducted by Sampathkumaran et al. (2005). The pin-on-disc test result concluded that for increased load and sliding velocity situations, higher wear loss was recorded and for rubber-bearing samples, the friction coefficient decreased with increased velocity.

Senthilkumar et al. (2012) studied the effect of wt% of aluminium particles in epoxy resin on fatigue strength and thermal conductivity and they concluded that thermal conductivity increased with increased aluminium particles but the fatigue strength decreased. In polymer, aluminium particle quantity is not enough to characterized its properties but particle size is also a very important factor. Chung et al. (2005) established that the mechanical properties including hardness, dimension accuracy and thermal conductivity in micro-scale structures improved by using an epoxy-aluminium particle composite but the hardness and dimension accuracy showed more suitable characteristics with smaller size particle. Whereas, the composite having larger size particle was more heat conducive than that of smaller particles. The use of different coupling agents on surface modification of aluminium particles in aluminium epoxy composites and subsequently its effect of the composite properties are investigated by Zhou and Yu (2011) and Zhou (2011). Zunjarrao and Singh (2006) established that that aluminium particle size, dispersion and silence treatment, all play an important role in determining the enhancement of fracture toughness. Surface silanization and dry particle coating, are the two established technique to reduce the cohesiveness and improve the flowability of fine cohesive aluminium powders as reported by Chen et al. (2010). Chemical functionalization of oxide-passivated aluminium nanoparticles using different acrylic monomers, demonstrate enhanced miscibility and PAM and MPS coatings are effective at inhibiting oxidation at different temperature and working environment (Crouse et al., 2010). Based on combined flowability and CVE characteristics, Jallo et al. (2010) reported that the silane modified material gave the best results followed by the powders dry coated with carbon, titania and silica, respectively. Kim et al. (2012) investigated the effect of surface modification of aluminium powders on the mechanical properties and the results showed that the tensile modulus, strength

and fracture toughness of silane-treated aluminium/epoxy composites were 9%, 12%, and 32% greater, than those of untreated aluminium/epoxy composites. Srivastava and Hogg (1998) presented that aluminium-tri-hydrate filled GFRP composites showed a higher moisture uptake, which resulted in higher values of both mode-I and mode-II, toughness than the polyethylene filled and unfilled GFRP composites. The mechanical behavior of composites containing aluminium particles and micro or nano sized other particles is beneficial to enhance further the mechanical properties (Martin et al., 2007; Mohammed Selleb, 2009). In addition to aluminium particles, presence of micro-sized Ni particles in composite exhibited a higher elastic modulus and static and dynamic compressive strengths than pure epoxy and micro aluminium containing composite (Martin et al., 2007). Along with aluminium particles presence of Cu particles with different volume fraction enhanced the modulus of elasticity, the flexural strength and maximum shear stress increased with increasing the volume fraction of the reinforced particles of aluminium and copper, while the deflection decreased with the increased volume fraction and the reinforcement with copper particles give the best results than the reinforcement with aluminium particles (Mohammed Selleb, 2009).

Several researchers has attempt to explore the mechanical behavior of aluminium filled glass epoxy composites considering different process parameters. In tri-phase materials, composed by an epoxy resin, aluminium particles and milled fibers, Vasconcelos et al. (2005) observed that the mechanical and thermal performances are better than the single materials. This was established through a Charpy impact tests with electronic instrumentation. Hamed (2009) investigated the tensile strength of aluminium powder mixed glass/kevlar/PVC fiber reinforced epoxy composites. He showed that the tensile strength increased with the increased volume fraction of aluminium powder from 20% to 40% and the sample EK had higher tensile strength than all other samples

for both volume fraction. Kim et al. (2012) investigated the effect of surface modification of aluminium powders on the tribological behaviors of aluminium/epoxy composites. The results showed that the wear resistance of silane-treated aluminium/epoxy composites was 56% greater than that of untreated aluminium/epoxy composites. In an experimental study, Peng et al. (2009) investigated effects of $Al(OH)_3$ powder on wear behavior of glass fiber reinforced epoxy composites. The experimental results showed that within a proper content, the addition of $Al(OH)_3$ powder in epoxy could increase the resistance to wear and friction. Several researchers has attempt to explore the tribological behavior of aluminium particle filled glass epoxy composites considering different process parameters. Vasconcelos et al. (2006) studied the tribological behavior of epoxy, aluminium particles and epoxy-aluminium-milled glass by considering thermal conductivity and wear resistance. The study revealed that in the reciprocating test; epoxy, aluminium and glass fiber reinforced composites show lower wear rate than the epoxy at room temperature.

1.3 Knowledge gap in earlier investigations

The literature survey presented above reveals the following knowledge gap in the research reported so far:

o Though much work has been done on a wide variety of glass fibers for polymer composites, very less has been reported on the reinforcing potential of woven E glass fiber in spite of its several advantages over others. Many low-end application areas such as housing, furniture, structural, transport etc. are cited in the literature for woven E glass fiber based products, but there is hardly any mention of their potential use in tribological situations where other type of glass fibers are widely used. Moreover, there is no report available in the literature on the wear characteristics of woven E glass fiber

based polymer composites in different environment when fiber orientation is perpendicular to sliding direction.

o   A number of research efforts have been devoted to the mechanical and wear characteristics of either fiber reinforced composites or particulate filled composites. However, a possibility that the incorporation of both particulates and fibers in polymer could provide a synergism in terms of improved performance has not been adequately addressed so far. Besides, the potential of aluminium powder to be used as fillers material in polymer composites has rarely been reported.

o   The mechanical and tribological properties of aluminium powder as tribo material in polymer composites has not yet been explored much. Very few reports are available. Moreover, aluminium powder filled woven E glass fiber reinforced polymer composites has not yet considered for mechanical and tribological characterization. Though soft metal particle aluminium powder coupled with good combination properties may be utilized as a potential tribo material.

o   Though a number of composite fabrication processes have been followed by the investigators for particulate filled glass polymer composites and conventional hand layup technique is one of the popular one. But conventional hand lay up followed by light compression moulding process never been used for the fabrication of aluminium powder filled woven E glass fiber reinforced epoxy composites.

o   The tribological characterization of particulate filled glass polymer composites has been made by the researchers considering the sliding mode of contact without much attention on the fiber orientation but reciprocating contact mode has rarely been explored. Even for aluminium particulate woven glass polymer composite it is not at all explored yet.

1.4   Objectives of the present work

17

The knowledge gap in the existing literature summarized above has helped to set the objectives of this research work which are outlined as follows:

1) Fabrication of a new class of epoxy based composites reinforced with woven E glass fibers and aluminium particulate fillers with different weight percentages.

2) Determine the Mechanical properties such as tensile strength, density and void fraction, Micro-hardness, Flexural strength, Inter laminar shear strength.

3) Evaluation of the effect of aluminium powder in epoxy and glass epoxy systems on mechanical and tribological properties under reciprocating and sliding contact mode in different conditions through experimentation.

4) Estimation of the effect of woven E glass fiber loading with varying weight percentages in epoxy system on tribological behavior under reciprocating and sliding contact mode in dry condition.

5) Validation of the experimental results through SEM observation and explanation of the possible reason.

2. EXPERIMENTAL DETAILS

2.1 Introduction

This chapter describes the materials and methods used for the processing of the composites under this investigation. It presents in details the mechanical and tribological characterization process of the composites under reciprocating and continuous sliding contact conditions.

2.2 Composite materials

2.2.1 Matrix material

Matrix materials can be of different types like metals, ceramics and polymers. Polymer matrices are most commonly used because of cost efficiency, ease of fabricating complex parts with less tooling cost and they also have excellent room temperature properties when compared to metal and ceramic matrices. Polymer matrices can be either thermoplastic or thermoset. Thermoset matrices are formed due to an irreversible chemical transformation of the resin into an amorphous cross-linked polymer matrix. Due to huge molecular structures, thermoset resins provide good electrical and thermal insulation. They have low viscosity, which allow proper fiber wet out, excellent thermal stability and better creep resistance. Normally, these resins can be formulated to give a wide range of properties upon requirement (Barbero, 2010).

The most commonly used thermoset resins are epoxy, polyester, vinyl ester and phenolics. Among them, epoxy resins are being widely used for many advanced composites due to their excellent adhesion to wide variety of fibers, superior mechanical and electrical properties and good performance at elevated temperatures. In addition to that they have low shrinkage upon curing and good chemical resistance. Due to several advantages of epoxy resin in comparison to other thermoset polymers, the matrix system is chosen as a combination of epoxy resin ARALDITE CY 205 IN with Epoxide Equivalent Weight (EEW) of 5.21 - 5.49 kg/eq. and curing hardener, HY 951 with amine hydrogen equivalent weight (AHEW) of 24 gm/eq., both at room temperature for the present research work. Araldite CY 205 IN is liquid, solvent-free, unmodified Bisphenol A epoxy resin (Chemical Formula: $C_{18}H_{21}ClO_3$) and the hardener Aradur HY 951 is a low viscosity aliphatic amine (Chemical Formula: $C_6H_{18}N_4$) both are procured from Huntsman Advanced Material (India) Pvt. Ltd. Some details of the constituents of matrix material is presented in Table 2.1.

Table 2.1 Properties of epoxy resin and hardener

Material	Trade name and chemical name	Density, (gm/cm³)	Viscosity at 25°C (mPa s)	Flash point (°C)	Parts by wt
Epoxy resin	Araldite CY 205 IN	1.27	9000 – 13000	200	100
Hardener	Aradur HY 951	0.98	10 - 20	110	10

2.2.2 Fiber material

Some commonly used synthetic fibers for composites are glass, carbon and aramid etc. Among them, glass fibers are the most commonly used fibers for engineering composites. Hence, glass fiber is chosen as the reinforcing material in this work. Glass fiber is commercially available in abundance with good mechanical properties; thus is widely used in composite structures (Barbero, 2010). Based upon different applications, glass fibers (silica-oxygen network) are classified into E glass, C glass and S glass fibers. E glass is used as an insulator and mostly used in electrical industry, hence got the name 'E' before the word 'glass'. E-glass also has good mechanical properties in addition to low cost and ease of usability. The letter 'S' in S-glass stands for structural applications. S-glass got different chemical formulation and it has higher strength to weight ratio and higher elongation strain percentage but it is quite expensive. C-glass fibers are advantageous in resisting chemical corrosion. Glass fibers are available in different forms like continuous, chopped and woven fabrics.

In the present work, woven roving fibers, made of 360 gsm, containing E-glass fibers of diameter 5-10 μm, orientation $0/90^0$ have been used as the reinforcing material in the composites. The major constituents of E-glass are silicon oxide (54 wt%), aluminium oxide (15 wt%), calcium oxide (17 wt%), boron oxide (8 wt%) and magnesium oxide (4.5 wt%). E-glass fiber has an elastic modulus of 72.5 GPa and possesses a density of 2.59 gm/cc. The pictorial views of bi- directional roving E-glass fiber mats and the geometry of the fiber orientation
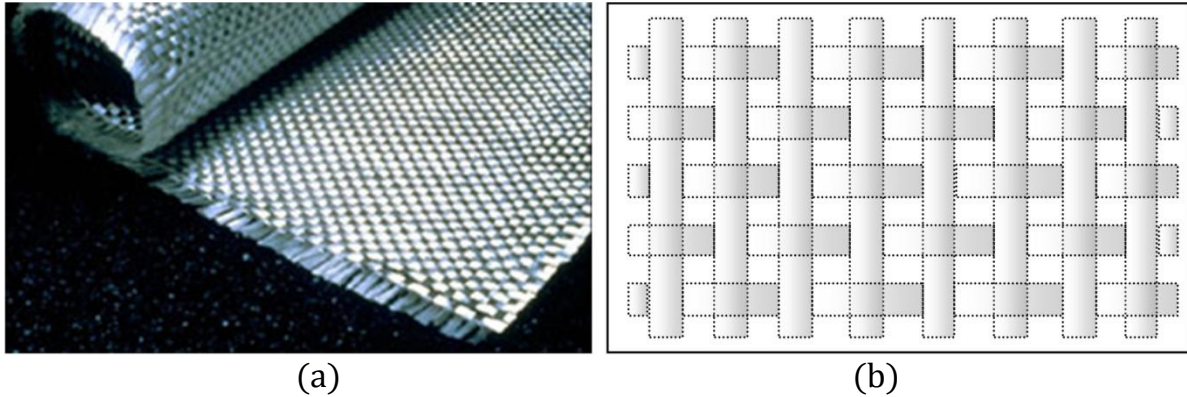
(a)   (b)

Figure 2.1 (a) Woven E glass fabric, (b) geometry of fiber orientation

used for composite fabrication for this study are given in Figure 2.1 and some of the physical and mechanical properties of E glass fiber is presented in Table 2.2.

Table 2.2 Physical and mechanical properties of E glass fiber

Bulk density (g/cm³)	Softening temp. ⁰C	Liquidus temp. ⁰C	Specific heat cal/g/⁰C	Coeff. of linear expansion, (10–6/⁰C)	Tensile strength at 23 ⁰C (MPa)	Young's modulus (GPa)	Filament elongation at break, %
2.54–2.55	830–860	1065–1077	0.192	4.9–6.0	3100–3800	76–78	4.5–4.9

2.2 .3 Particulate filler materials

A variety of natural or synthetic solid particulates, both organic and inorganic is already being commercially used as reinforcing fillers in polymeric composites. While ceramic powders such as alumina (Al_2O_3), silicon carbide (SiC), silica (SiO_2), titania (TiO_2) etc. are widely used as conventional fillers, the use of soft metal particles like aluminium for such purpose is hardly found. Aluminium possesses low weight, high strength, superior malleability, easy machining, and excellent corrosion resistance, good thermal and electrical conductivity. Aluminium is also very easy to recycle (Bhattacharya, 1986). In view of this, in the present work aluminium powder is chosen as particulate fillers to be used in the composites. To make an assessment of their reinforcing potential in terms of wear performance and mechanical properties, aluminium powder with four

different wt% are also considered for comparison. Figure 2.2 shows the aluminium powder in normal and higher magnification.
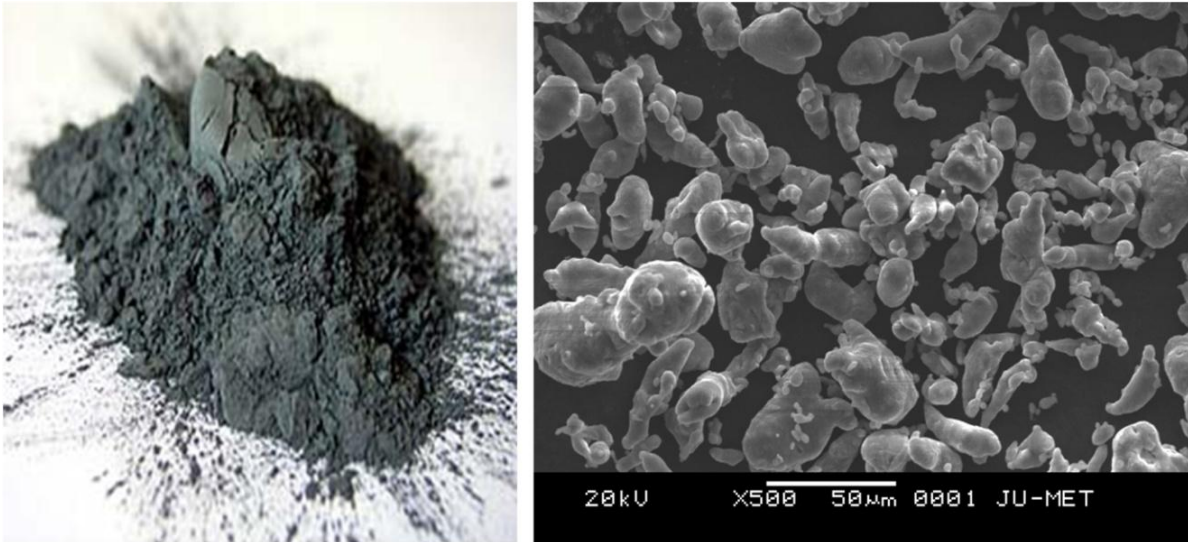

Figure 2.2 (a) Aluminium powder, (b) SEM micrograph of aluminium particles

The fine aluminium powder used in this work has been collected from Loba Chemie Pvt. Ltd., 107, Wodehouse Road, Mumbai-400005, India with assay min. 98.0% and maximum limits of impurities as insoluble in dil HCL 0.005%, iron (Fe) 0.1%, Manganese (Mn) 0.02%, Titanium (Ti) 0.03%, Nitrogen contains (as N) 0.001%, Copper (Cu) 0.02%, Silicon (Si) 0.1%. Some of the important properties of aluminium is presented in Table 2.3.

Table 2.3 Properties of aluminium powder

Colour	Grey
Period	13
Atomic number	13
Atomic mass (amu)	26.981539
Electronegativity	1.61
Space group	Fm-3m
Lattice parameter	Face-Centered Cubic (FCC)
Density (g/cm³)	2.70
Melting point (⁰C)	660.32
Boiling point (⁰C)	2519

Specific heat (Kcal/kg ^{0}C)	0.22
CTE (10^{-6} m/(mK))	22.2
Tensile strength (GPa)	47×10^{-3}
Elastic modulas (GPa)	70
Poision's ratio	0.33
Shear modulus (GPa)	24
Bulk modulus (GPa)	68-70
Hardness	2-2.9

2.2.4 Composite fabrication

Epoxy resin at a ratio of 10:1 by weight as recommended mixed with hardener (HY951) and starred well manually for about ten minutes till the mixture temperature is about to increase and poured into a open mould of fixed dimension and allowed to cure at normal atmospheric condition to fabricate the neat epoxy, 100E with out any particulate filler or reinforcement. The samples B_1–B_3 with different wt% of aluminium filler are fabricated in open mould proces-

(a)

(b)

Figure 2.3 (a) Mould used for composite fabrication, (b) cutting table with tools

ss. In this case, the required quantity of aluminium powder is mixed with the epoxy resin and then the hardener is added. The mixture is shaked well for a particular duration and poured into the mould as sample A. The sample C_1–C_3 with varied amount of fiber reinforcement and 0 wt% of aluminium content is termed as unfilled glass epoxy or simply glass epoxy composite. In composites D_1–D_3 , the quantity of glass fiber has been maintained fixed at 60 wt% for all composites. Aluminium wt% varies as 0, 5, 10, and 15 for each composite. The composition and designation of the composites prepared for this study are listed in Table 2.4. The fabrication of the composite slabs C and D are done by conventional hand-lay-up technique followed by light compression moulding. All C and D composites are fabricated in three steps. On the basis of the mould dimension, certain pre calculation is exercised to determine each constituent quantity. It is essential to maintain the desired wt% of constituents in composites.

Table 2.4 Designations and compositions of the fabricated composites

Sample code	Designation	Composition
A	100E	Epoxy (100 wt%)
B_1	5AlE	Epoxy (95 wt%) + Aluminium (5 wt%)
B_2	10AlE	Epoxy (90 wt%) + Aluminium (10 wt%)
B_3	15AlE	Epoxy (85 wt%) + Aluminium (15 wt%)
C_1	50GE	Epoxy (50 wt%) + Glass Fiber (50wt%)
C_2 (D_o)	60GE (GE)	Epoxy (40 wt%) + Glass Fiber (60wt%)
C_3	70GE	Epoxy (30 wt%) + Glass Fiber (70wt%)
D_1	5AlGE	Epoxy (35 wt%) + Glass Fiber (60wt%) + Aluminium (5 wt%)
D_2	10AlGE	Epoxy (30 wt%) + Glass Fiber (60wt%) + Aluminium (10 wt%)
D_3	15AlGE	Epoxy (25 wt%) + Glass Fiber (60wt%) + Aluminium (15 wt%)

Required numbers of woven fabric of 150 mm×100 mm size is cut with the help of a steel rule and sharp cutter on a wooden platform without disturbing the

actual fiber orientation. For unfilled glass epoxy composite, a dry and clean glass container with a stirrer is put on a weighting machine and reading is set to zero. Epoxy resin, Araldite CY-205 IN is slowly poured to the glass container till the machine display the required reading. Hardener (HY 951) at a ratio 10:1 by weight of resin is added to the epoxy and stirred mechanically for about ten minutes for proper mixing and exothermic reaction is just about to start. In case of aluminium particulate composites, aluminium powder is added to the epoxy resin first and mixed well in continuous stirring process then the hardener is added with the aluminium epoxy mixture. Stirring of the mixture continues for a certain duration based on the exothermic reaction. A specially designed and fabricated HSS mould is used for this purpose to avoid bending during compression. Figure 2.3 show the mould and composite cutting table with tools. The inner sides of the mould are covered with very thin tear resistant plastic film of few microns thickness to perform the similar function of releasing agent to avoid the possibility of infusion of releasing agent into the glass fiber. Unfilled or filled in both the cases, epoxy (resin and hardener) or aluminium mixed epoxy is lapped on the woven fibers uniformly and then the are placed one above the oth-

Table 2.5 Dimensions of the different test samples

Serial no	Name of the test	Sample dimension
1	Density	30 mm× 12 mm× 6 mm
2	Micro hardness	16 mm× 12 mm× 6 mm
3	Tensile strength	150 mm× 12 mm× 6 mm
4	Flexural test	60 mm× 12 mm× 6 mm
5	Inter laminar shear strength (ILSS)	60 mm× 12 mm× 6 mm
6	Reciprocating test	Circular 10 mm dia with 3 mm thickness
7	Sliding test	3 mm× 3 mm c/s with 30 mm height

er into the mould. The whole assembly is pressed in a hydraulic press (20 kg) and is left for 24 (twenty four) hours at this stage at room temperature. The compression ensures that the entrapped air bubbles are completely removed

with the excess resin. After demoulding, post curing is done at room temperature for 48 hour to complete the fabrication process.

Specimens of required dimensions for mechanical and tribological characterization are cut by a diamond cutter. Fine cutting of the samples are carried out with the help of perma grit hacksaw, flat file, sanding block. Final finishing of the surfaces is done with 600 grade and 1000 grade SiC paper. Dimensions of the different samples used for mechanical and tribological characterization is shown in Table 2.5.

2.3 Mechanical testing

2.3.1 Density

The theoretical density (ρ_{ct}) of composite materials in terms of weight fractions of different constituents can easily be obtained following the equation given by Agarwal et al. (2006).

$$\rho_{ct} = \frac{1}{\left(\frac{W_f}{\rho_f}\right)+\left(\frac{W_m}{\rho_m}\right)}$$ (2.1)

where, W and ρ represent the weight fraction and density respectively. The suffixes f and m stand for the fiber and matrix respectively. Since the composites under this investigation consist of three components namely matrix, fiber and particulate filler, the expression for the density has been modified as

$$\rho_{ct} = \frac{1}{\left(\frac{W_f}{\rho_f}\right)+\left(\frac{W_m}{\rho_m}\right)+\left(\frac{W_p}{\rho_p}\right)}$$ (2.2)

where, the suffix p stands for the particulate filler. The actual density (ρ_{ca}) of the composite, however, can be determined experimentally by simple water

immersion technique. The volume fraction of voids (V_v) in the composites is calculated using the following equation:

$$V_v = \frac{\rho_{ct} - \rho_{ca}}{\rho_{ca}}$$ (2.3)

2.3.2 Micro-hardness

Hardness is the resistance of a material to deformation, indentation or scratching. The basic goal of hardness testing is to quantifiably measure the resistance of a material to plastic deformation. The indentation value has high importance for technical applications which reflects the resistance to deformation, which is a complex property and related to modulus, strength, elasticity, plasticity and dimensional stability of a material. Hardness is generally classified into different categories with respect to the depth of indentation (d). When the depth of indentation ranges between 1-50 μm, it is termed as micro hardness. The test methods commonly used for expressing the relationship between hardness and the size of impression are Brinell, Vicker's and Rockwell hardness tests.

Measurement of hardness

Hardness values offer a comparative measurement of a material's resistance to plastic deformation from a standard source, as different hardness techniques have different scales. The Vickers hardness test is very popular among researchers since it is easier to perform compared to other hardness tests and also the hardness calculations are independent of the size of the indenter and load applied. In this study, Vicker's hardness test setup is used to find out the microhardness values of different composites. Microhardness testing is carried out in a UHL micro hardness tester (Model-VMHT MOT, Sl. No. 1002001, Technische Mikroskopie) with a Vickers diamond indenter. Figure 2.4 shows the

Vicker's hardness test setup. The dwell time is kept at 10s while the speed of indentation is set at 50µm/s and indentation load at 1000 gf. It should be mentioned here that as the hardness is measured on the finished test sample surfaces where glass fiber orientation is perpendicular and no separate surface preparation is done, an average of at least three hardness values for each sample is reported.
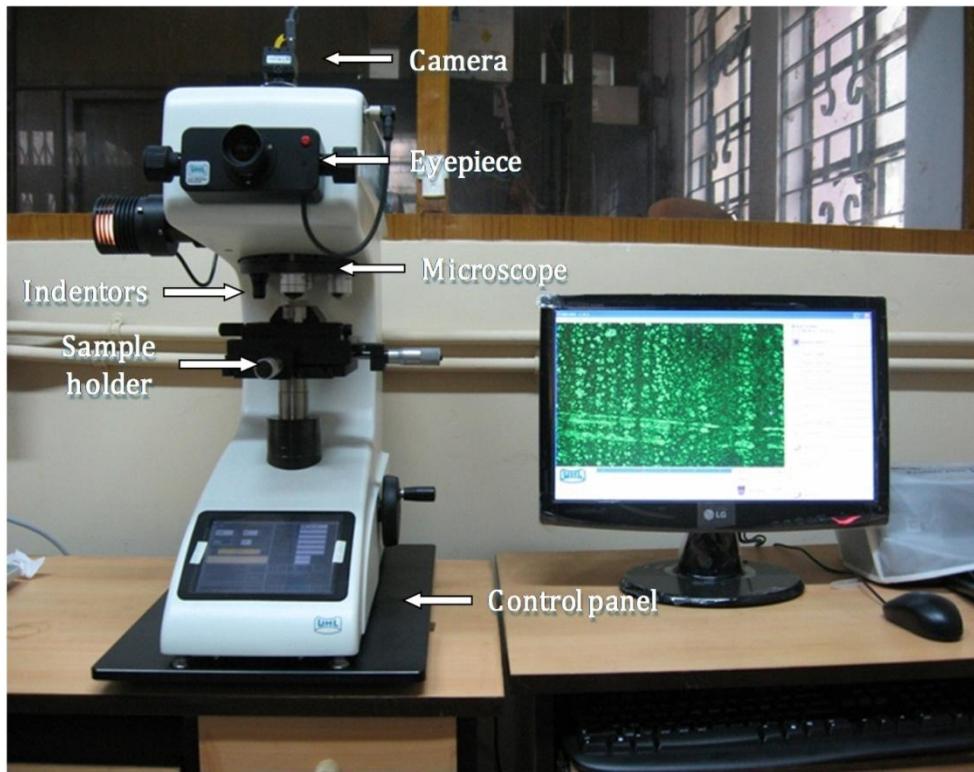
Figure 2.4 Vicker's microhardness tester

Vicker's hardness test

The Vickers hardness test is a commonly used technique due to its wide load range capability. Moreover, the indenter can be used for all materials irrespective of hardness. The method consists of indenting the test material with a diamond indenter, in the form of a pyramid with a square base and an angle of 136 degrees between opposite faces (as in Figure 2.5). The applied force ranges in between 1 gf and 2000 gf. The full load is normally applied for 10 to 15 seconds. The two

diagonals (d_1 and d_2) of the indentation left in the surface of the material after removal of the load are measured using a microscope and their average (d) is calculated. Vickers hardness (HV) is calculated with the following equation.

$$HV = \frac{1.8544\,F}{d^2} \qquad\qquad (2.4)$$

Where load (F) is in Kilogram force and the mean of two diagonals created by the pyramidal indentor (d) is in millimeter. The Vickers hardness should be reported like 700 HV0.5, which means a Vickers hardness of 700, was obtained using a 500 gf test force.
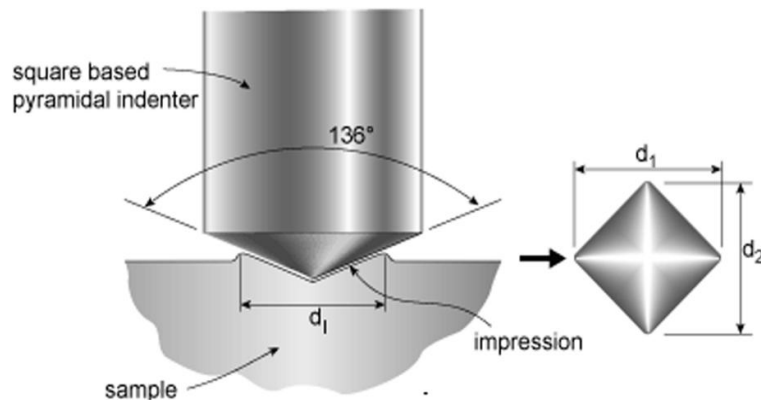
Figure 2.5 Vicker's indentation and diagonals of the impression

The Vickers method is capable of testing the softest and hardest of materials, under varying loads. With modern advances in technology, it is now possible to offer automatic indentation measurement. This has the benefit of eliminating any operator influence over the result, increasing repeatability and reproducibility.

2.3.3 Tensile strength

The tensile tests are conducted on INSTRON 8801, as per ASTM D3039-07 standards test method for tensile properties of composite specimens. This test method determines the in plane tensile properties of polymer and glass epoxy composites with or without aluminium particulate filler. The dimension of the

sample is 150 mm×12 mm×6 mm with a fixed gauge length of 100 mm. Tests are conducted for the samples at normal room temperature (27Deg C) and quasi-static strain-rate of 10E-4/s. At least three numbers of specimens for each composite are used to get the mean value of the tensile strength. INSTRON 8801 with tensile test setup and the test specimens are shown in Figure 2.6.

Figure 2.6 (a) INSTRON 8801, (b) tensile test setup, (c) test samples

2.3.4 Flexural and inter laminar shear strength (ILSS)

The flexural strength of a composite is the maximum tensile stress that it can withstand during bending before reaching the breaking point. The three point bend test is conducted on glass epoxy and aluminium powder filled glass epoxy composite samples using a testing machine INSTRON 8801 as per ASTM D790- 10 standard test method. The dimension of each specimen is 60 mm ×12 mm×6 mm. Span length of 50 mm and a constant cross head-speed of 1.5 mm/min are maintained. The arrangement for the test and the test specimen are shown in

Figure 2.7. For both flexural strength and ILSS, the test is repeated three times for each composite type and the mean value is reported. The flexural strength of the composite specimen is determined using the following equation.

$$\text{Flexural strength} = \frac{3PL}{2bt^2} \qquad (2.5)$$

where, L is the span length of the sample (mm)

P is maximum load (N)

b the width of specimen (mm)

t the thickness of specimen (mm)

The data recorded during the three point bend test is used to evaluate the Inter laminar shear strength (ILSS) also

The ILSS values are calculated as follows:

$$\text{ILSS} = \frac{3P}{4bt} \qquad (2.6)$$
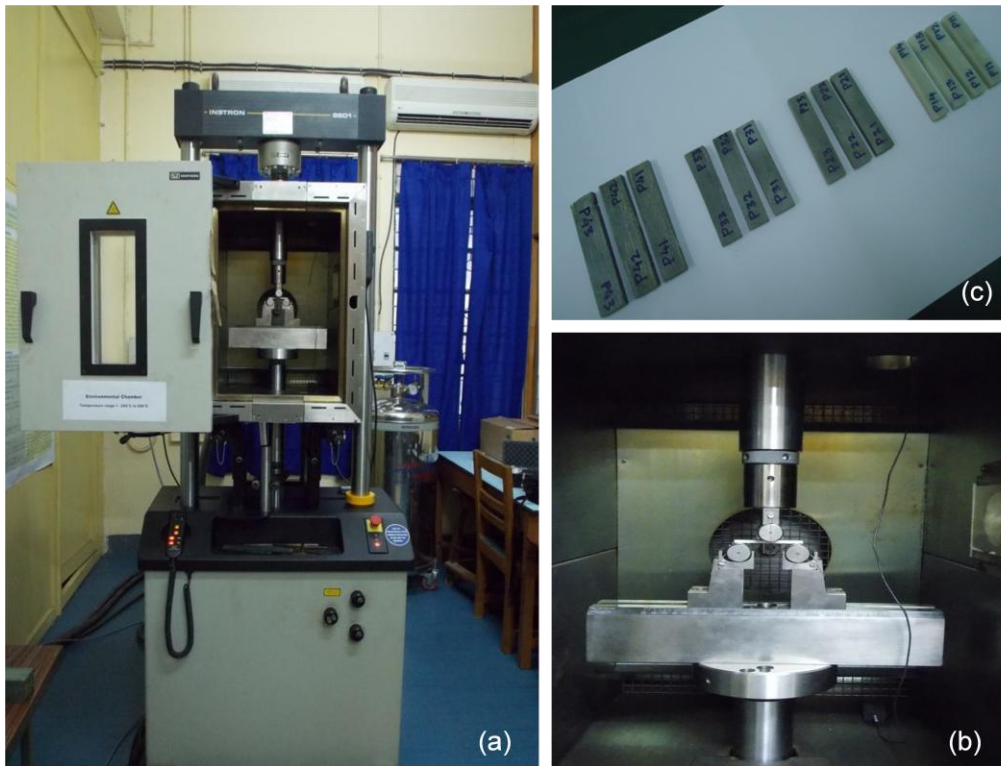
Figure 2.7 (a) INSTRON 8801 with 3-point bending fixture, (b) larger image of the fixture showing the point of loading, (c) test samples

2.4 Tribological testing

The word tribology, derived from the Greek word "tribos" meaning rubbing, is defined as interdisciplinary science and technology related to friction, wear and lubrication. The tribology is concerned with developing and improving materials and surfaces to control friction and prevention of wear of surfaces having relative motion under load. Many different experimental arrangements are used to study sliding friction and wear. These are usually carried out either to examine the process by which friction and wear takes place or to simulate practical situations to generate friction and wear data. Close monitoring and control of all the variables which may influence friction and wear are essential if the test results are to be used for scientific purposes. Moreover, the variables of friction and wear test for laboratory purpose should be selected carefully so that it is consistent with the type of the application. The operating variables of any tribometer are type of motion, applied load, velocity/frequency, ambient temperature, humidity, test duration etc. In the present study, types of motion are simulated: reciprocating motion and sliding motion. Hence two different tribometers are used: reciprocating tribometer and sliding tribometer (pin on disc).

2.4.1 Reciprocating test apparatus

In the reciprocating test, a friction and wear tester, TR-282, (make-DUCOM) is used to determine the friction and wear behavior under dry conditions at different frequencies and normal loads. The machine has a fixed stroke length of 1 (one) mm. The circular samples of 10 mm diameter and 3 mm thickness are prepared from the fabricated composites as per requirements. The fiber orientation of the test face is perpendicular to the reciprocation direction.

Figure 2.8 shows the reciprocating tribotester, TR-282, test sample and the fiber orientation at the test surface. The process parameters which has been taken up under major consideration for this test along with their different levels has been

Table 2.6 Process parameters and their levels

Process parameters	Units	Levels			
		I	II	III	IV
Sliding frequency	Hz	15	30	45	60
Normal load	Kg	0.4	0.6	0.8	1.0
Time	Minute	10	20	30	40
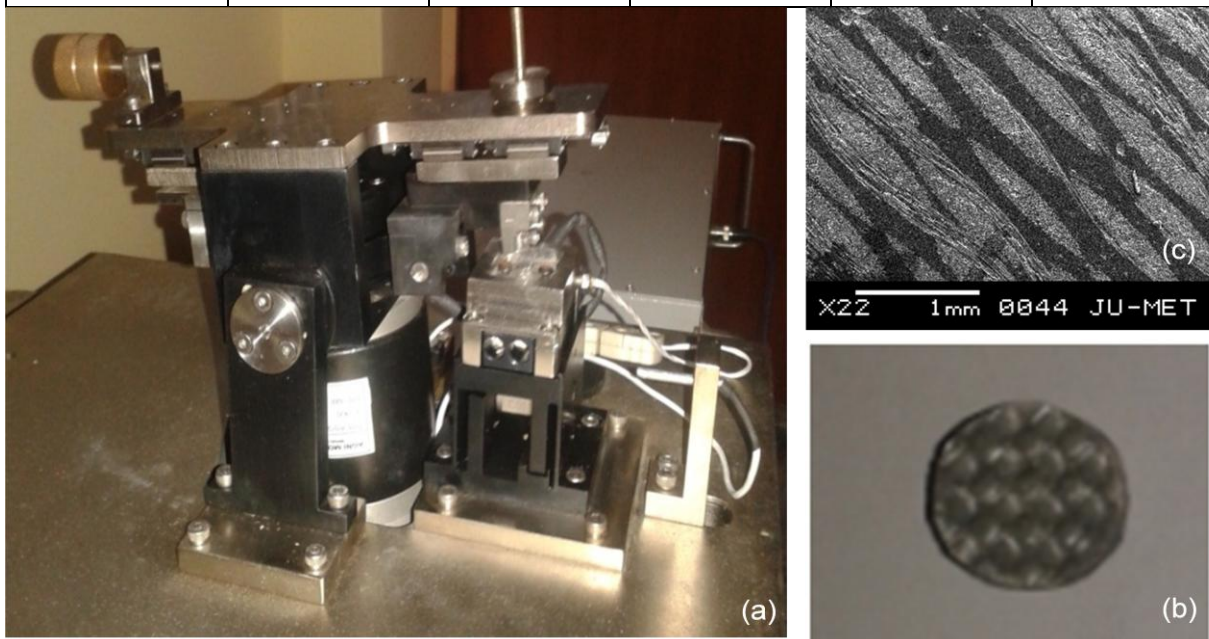
Figure 2.8 (a) Reciprocating tribotester, TR-282; (b) test sample, (c) SEM image of the test surface showing the fiber orientation

indicated in Table 2.6. The tests are conducted for each type of composite by selecting the test duration, normal load, reciprocating frequency and the mode of data accusation. The flat surface of the sample comes in contact with the steel ball as counter face. Prior to testing, the samples are rubbed over a 600 grade SiC paper followed by 1000 grade SiC paper to have smooth surface with similar ave-
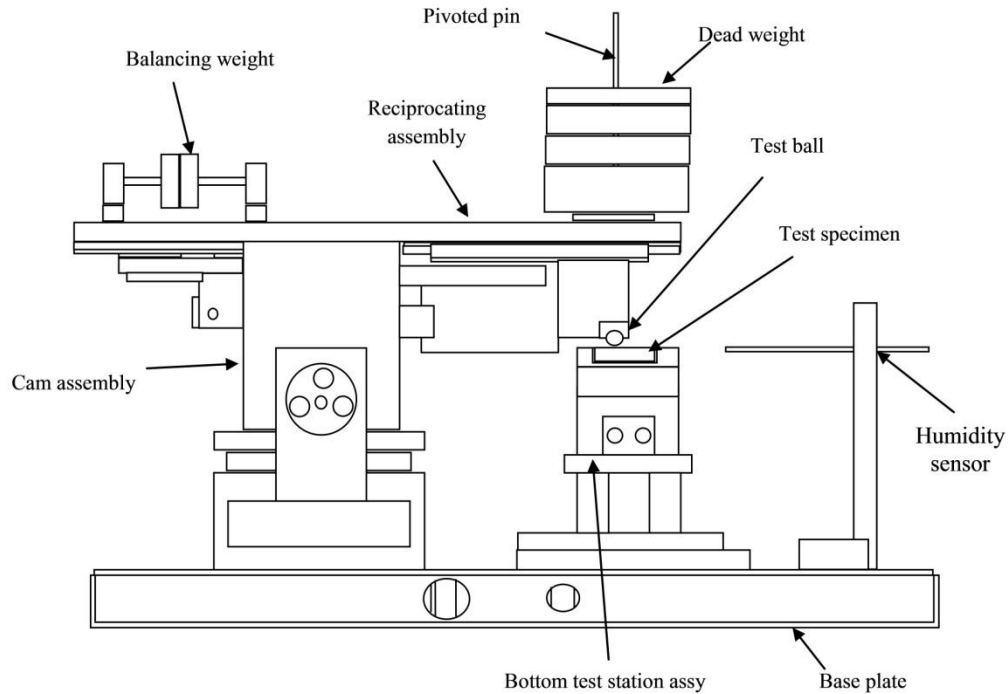
Figure 2.9 Schematic diagram of reciprocating tribotester, TR-282

rage roughness value (R_a) value of 0.8 μm. This is done to ensure proper contact between the counter face and flat surface of the samples. The surfaces of both the sample and the steel ball are cleaned with the soft paper soaked with acetone before the test. The test samples are weighted initially using a afcoset electronic balance (0.1 mg accuracy). The weighted sample and the ball are fixed in their respective positions of the test machine. The normal load to the ball is applied through a pivoted liver. The ball with 6 mm dia, material: AISI E-52100 steel, hardened to 58-66HR$_c$ (nearly 600 HV), R_a<0.05 μm is made to have a point contact with the test surface of the sample.

The schematic diagram of reciprocating tribotester is shown in Figure 2.9. The tests are conducted for a couple of months within the range of humidity between 41-80%. After the pre set time is reached, the test is stopped using the timer mechanism provided with the machine. The weight of the test samples on cleaning with soft paper is measured in the same balance. The difference between the initial and final weight is a measure of reciprocating wear loss for the

specified test duration. A minimum of four trials are conducted to ensure repeatability of test data. The friction force as well as the friction coefficient at the interface of the ball and specimen is recorded in the computer at each second. The steel ball is reciprocated on the fixed sample involving friction in dry condition for all type of composite samples at different normal loads, frequencies and durations. This arrangement decreases the tendency for the topography modification effect caused by polymer transfer, keeping the contact nature of the steel–polymer interface almost unchanged during the whole test.

2.4.2 Pin on disc test apparatus

The sliding contact tests are conducted with the help of a pin on disc tribotester (TR-20LE-CHM-400, DUCOM) according to ASTM D G 99 standard. Figure 2.10 shows the pin on disc type tribotester.
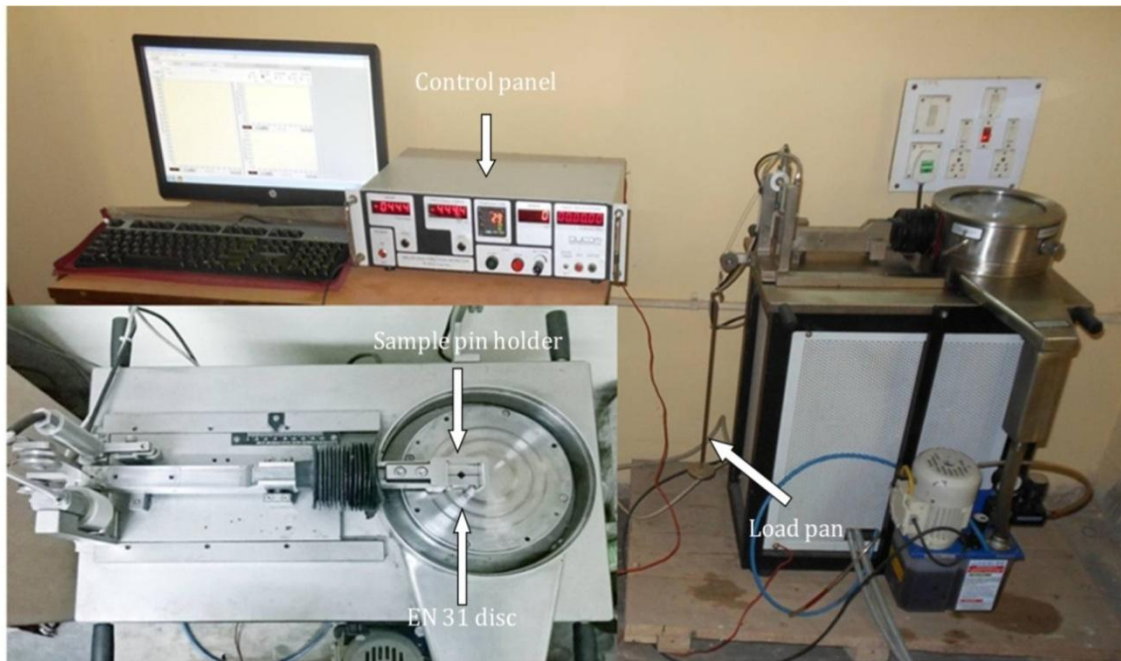
Figure 2.10 Pin on disc type tribotester (TR-20LE-CHM-400, DUCOM)
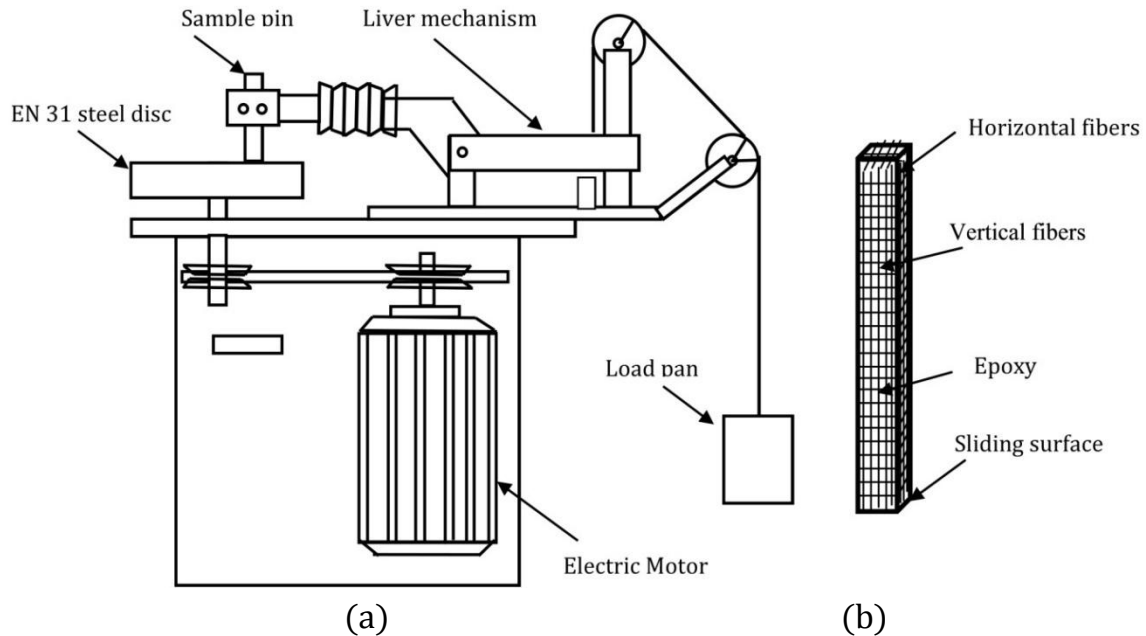
Figure 2.11 (a) Schematic diagram of pin on disc type tribotester and (b) sample pin

In the present case, pin type samples of 3 mm×3 mm cross section and 30 mm height are used. Samples of all the composites are prepared in such a way that the fiber orientation at the test surface (3 mm×3 mm) is perpendicular to the sliding direction. Sample pin makes a surface contact at a selected track diameter with the counter rotating disc. The counter surface disc is made of EN 31 steel hardened to 60 HR_c (nearly 600 HV) having dimensions of 165 mm diameter, 8 mm thick and surface roughness (R_a) of 1.6 μm. Prior to test run, sample test surfaces are rubbed with a 600 and 1000 grade SiC paper to achieve similar Ra value (1.4 μm) to ensure proper contact between the disc and flat test surface of the sample. The sample and the steel disc are cleaned with the soft paper soaked in acetone before test. Initial weight of test samples are measured using afcoset electronic balance of 0.1 mg accuracy. Weighed sample is fixed in the holder of the test machine. The normal load on the sample pin is applied through a pivoted lever with a string and pan assembly. For a certain test condition, each experiment is conducted for four times to find the repeatability of test data. At

least two set of test data of similar nature are averaged and presented for interpretation. At the end of each preset time, test run is stopped automatically using a timer mechanism provided with the machine. Weight of the worn sample on cleaning with soft paper is again measured in the same balance. The difference between the initial and final weight is the amount of sliding wear for the specific test condition. Friction force at the contact surface of the disc and sample is recorded in the computer at each second and corresponding friction coefficient is obtained by dividing the recorded data with normal load.

The schematic diagram of pin on disc type tribotester and sample pin are shown in Figure 2.11. The test parameters for the sliding contact test are selected as sliding duration, normal load, sliding speed and the type of the composite samples at normal atmospheric condition under dry condition. Total 9 (nine) types of composites are tested under different duration, load and speed conditions. Tests are conducted at a fixed track diameter of 115 mm. The range of the test parameters has been selected based on literature. The ranges of the duration and normal load have been fixed between 5-60 minutes and 10-50 N respectively. Sliding speed between 1-5 m/s corresponding to the rotational speed of 116-830 rpm and the range of the sliding distance of 300-3600 m is used. Each test is conducted for the particular combination of selected time, load and speed for a particular composite specimen.

2.5 Scanning electron microscopy (SEM)

The surfaces of the specimens are examined by using a JEOL JSM6300 scanning electron microscope (SEM) as shown in Figure 2.12. Scanning electron microscopy (SEM) is a very important technique to observe the microstructure or the surface morphology of a material in detail. In this method, the surface of a specimen to be examined is scanned with an electron beam, and the reflected (or back-scattered) beam of electrons are collected and then displayed at the same s-

Figure 2.12 Scanning electron microscope (JEOL JSM6300)

canning rate on a LED (light emitting diode) display. There is provision to photograph the image displayed on the screen, which represents the surface features of the specimen. SEM requires the specimen to be electrically conductive. For SEM of non-conductive specimen, a thin coating of a conductive material is generally applied on the specimen.

2.6 Energy dispersive X-ray analysis

Energy dispersive X-ray spectroscopy, abbreviated as EDS, EDX, or EDXA (Energy dispersive X-ray analysis) is an analytical technique used for elemental analysis and chemical characterization of a sample surface. At present, chemical composition of a surface can be characterized using different analysis techniques, which share the same basic principle. A particle beam (electronic, optical or ionic) is directed at the surface of the material under examination which in turn induces the emission of secondary or backscattered particles viz. photons,

electrons or ions etc. These secondary particles can be characterized to get the composition of the surface.

EDX is used in conjunction with SEM as both the techniques use the same source of electrons. EDX verifies and gives the elemental composition and proportion of a sample. It does not give any information regarding the bonding of the atoms to the elements. Furthermore in EDX, the penetration of electrons into a sample is in the range of 0.1 to 1 μm and hence elemental composition can be detected accurately within this range of thickness of the sample.

3. MECHANICAL CHARACTERIZATION

3.1 Introduction

This chapter presents the measured values of the physical and mechanical properties of neat epoxy, aluminium particulate epoxy, glass epoxy and glass epoxy composites filled with aluminium particulate fillers with different concentration. The relative effects of glass fiber loading and aluminium filler concentration on various properties of the composites have also been discussed.

3.2 Density and void fraction

Density is a material property which is of prime importance in several weight sensitive applications. Density of a composite depends on the relative proportion of matrix and the reinforcing materials. There is always a difference between the measured and the theoretical density values of a composite due to the presence of voids and pores. These voids significantly affect some of the mechanical properties and even the performance of composites. Higher void contents usually mean lower fatigue resistance, greater susceptibility to water penetration and weathering (Agarwal et al., 2006). The knowledge of void content is desirable for estimation of the quality of the composites. In the present research work, the

theoretical and measured densities of the different epoxy based composites, along with the corresponding volume fraction of voids is presented in Table 3.1. It is found that the composite density values calculated theoretically from weight fractions using Eq. (2.2) differ from the experimentally measured values, as expected. It is evident from Table 3.1 that the density values for epoxy based composites increase with the incorporation of aluminium powder as well as glass fiber reinforcement. It is further observed that with the incorporation of aluminium powder, the void fractions in aluminium epoxy composites also increase. Similar trends are noticed for the glass-epoxy composites with the incorporation of aluminium powder. But the void fractions in glass epoxy composites decrease with the increase of fiber content.

Table 3.1 Measured and theoretical densities along with the void fractions of the neat epoxy, aluminium epoxy, glass epoxy and glass epoxy filled with aluminium powder composites

Composition			Measured density (gm/cc)	Theoretical Density (gm/cc)	Volume fraction of voids (%)
A	E	Epoxy (100 wt%)	1.21	1.22	.819
B_1	5AlE	Epoxy + 5 wt% Aluminium	1.24	1.26	1.58
B_2	10AlE	Epoxy + 10 wt% Aluminium	1.27	1.30	2.30
B_3	15AlE	Epoxy + 15 wt% Aluminium	1.29	1.33	3.00
C_1	50GE	Epoxy (50 wt%) + Glass Fiber (50 wt%)	1.69	1.72	1.74
C_2	60GE	Epoxy (40 wt%) + Glass Fiber (60 wt%)	1.77	1.79	1.11
C_3	70GE	Epoxy (30 wt%) + Glass Fiber (70 wt%)	1.83	1.85	1.08
D_1	5AlGE	Epoxy (35 wt%) + Glass Fiber (60 wt%) + 5 wt% Aluminium	1.84	1.87	1.60
D_2	10AlGE	Epoxy (30 wt%) +Glass Fiber (60 wt%) + 10 wt% Aluminium	1.91	1.95	2.05
D_3	15AlGE	Epoxy (25 wt%) + Glass Fiber (60 wt%) + 15 wt% Aluminium	1.97	2.03	2.95

3.3 Micro-hardness

Hardness is considered as one of the most important factors that govern the wear resistance of any material. In the present work, micro-hardness values of the aluminium epoxy and glass epoxy composites with different aluminium concentrations have been obtained. The test results (Figure 3.1) show that with the presence of aluminium filler upto 10 wt%, microhardness of the aluminium epoxy composites is improved and with further addition of aluminium upto 15 wt%, hardness decreases. This trend of improvement of hardness with 10 wt% aluminium filler content is also observed in case of the glass-epoxy composites. In both the cases, maximum improvement is observed at 5 wt% aluminium addition. The decrease of hardness with 15 wt% aluminium addition may be attributed as agglomeration of aluminium particles resulting to decrease of material strength and integrity.
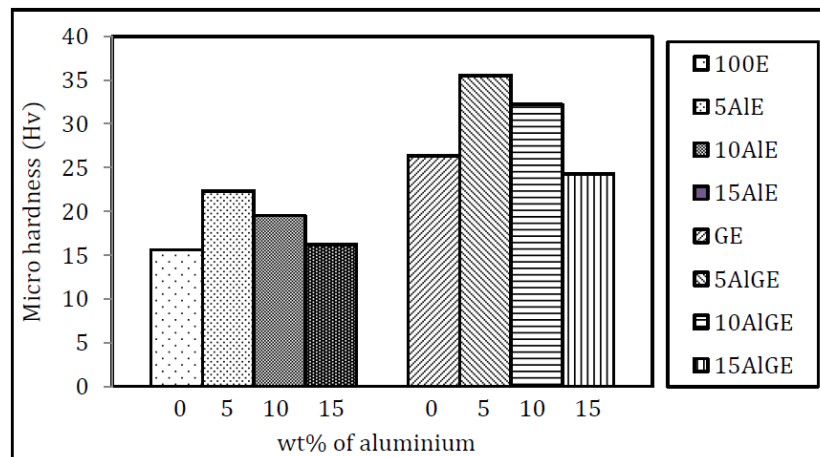
Figure 3.1 Micro-hardness of composites with aluminium concentration

3.4 Tensile properties

The tensile strengths of glass epoxy composites filled with aluminium powder are shown in Figure 3.2. It is found that, there is a gradual drop in tensile strength with increase in aluminium content. The unfilled glass epoxy composite has strength of 347.60 MPa in tension, and this value drops to 306.64 MPa,

278.75MPa and 210.29 MPa with aluminium powder addition of 5 wt%, 10 wt% and 15 wt% respectively. The reduction in tensile strength with filler addition may be due to the chemical bond strength between filler particles and the matrix body is too weak to transfer the tensile load or the sharp corners of irregular shaped filler particles result in stress concentration zones in the matrix body during tensile loading or due to the increase in void percentage in the composites with increase in filler content (Rout and Satapathy, 2012). The variation of tensile modulus with different aluminium concentration in glass-epoxy composites is sh-
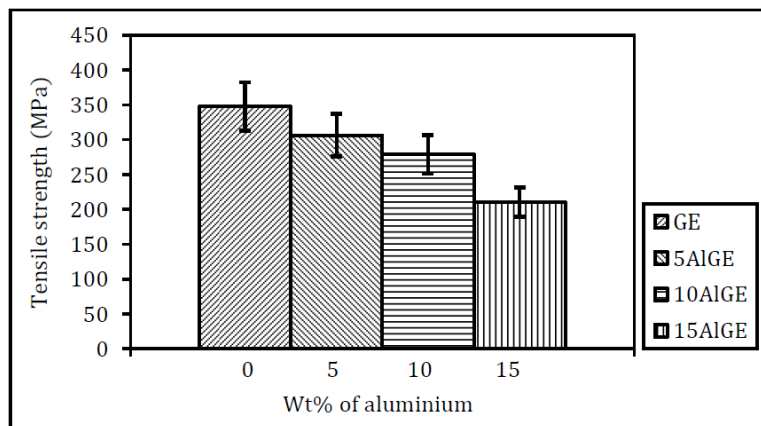
Figure 3.2 Tensile strength of composites with aluminium concentration

own in Figure 3.3. It is observed that the tensile moduli of glass epoxy composites improve significantly with 10 wt% of aluminium powder content (10AlGE). But in case of 5 and 15 wt% aluminium powder filled glass epoxy composites (5AlGE and 10AlGE) decrease with respect to unfilled glass epoxy composite (GE).
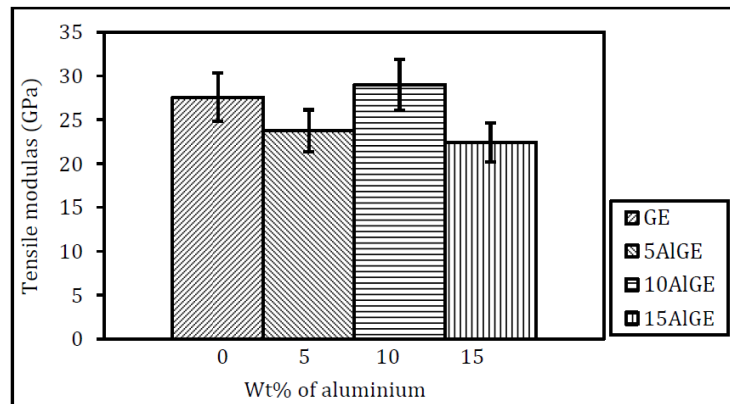
Figure 3.3 Tensile modulus of composites with aluminium concentration.

Previous reports demonstrate that normally the fibers in the composite restrain the deformation of the matrix polymer, reducing the tensile strain (Fu and Lauke, 1998; Thomason et al., 1996). So even if the strength decreases with filler addition, the tensile modulus of the composite is expected to increase for a certain wt% of aluminium powder addition as has been observed in the present investigation.

3.5 Flexural strength

Composite materials used in structures are prone to fail in bending and therefore the development of new composites with improved flexural characteristics is essential. In the present work, the variation of flexural strength of glass-epoxy composites with different wt% of aluminium filler concentration is shown in Figure 3.4. The highest improvement in flexural strength is observed with 5 wt% of aluminium content whereas 15 wt% aluminium filled glass epoxy composite shows the lowest strength. But the composite with 10 wt% of aluminium powder shows the better performance than glass epoxy composite having no filler but inferior to 5 wt% aluminium filled glass epoxy composite. 15 wt% aluminium filled composite shows least strength.
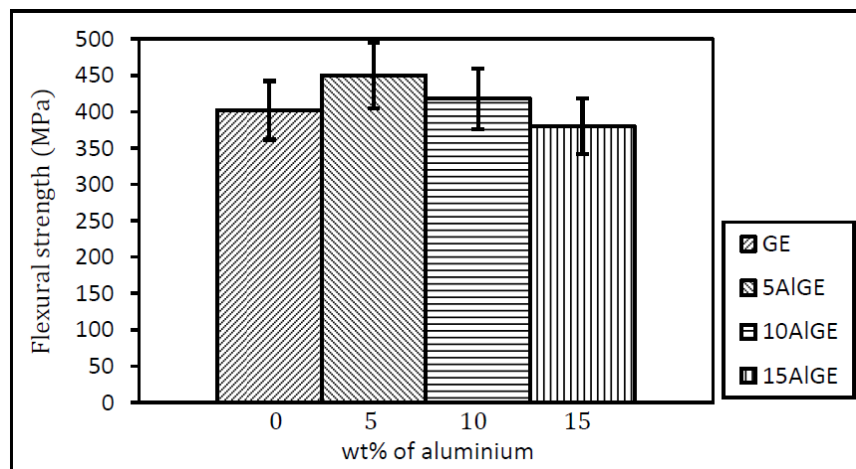
Figure 3.4 Flexural strength of composites with aluminium concentration

unfilled composite. The improvement in the flexural strength of the composites with filler content (upto 10 wt%) is probably caused by good compatibility of the particulates and the epoxy matrix, leading to increase in interfacial bonding. The lower values of flexural properties (as 15AlGE) may also be attributed to fiber to fiber interaction, voids and dispersion problems. However, it also depends on other factors such as the size, and shape of the filler material. Influence of the aluminium filler quantity on the flexural strength is noticed for the fixed wt% of fiber reinforcement glass-epoxy composites. Remarkable improvement in flexural strength is observed in 5 wt% filled glass-epoxy and 10 wt% filled glass-epoxy composites as compared to the unfilled one. It is evident from this study that as far as the flexural strength is concerned, quantity of the aluminium powder as filler material plays a very significant role.

3.6 Inter laminar shear strength (ILSS)

Short beam shear test is carried out on the glass epoxy and aluminium powder filled glass epoxy composites to determine the inter-laminar shear strength (ILSS). The variation of ILSS of glass epoxy and glass epoxy with alumini-
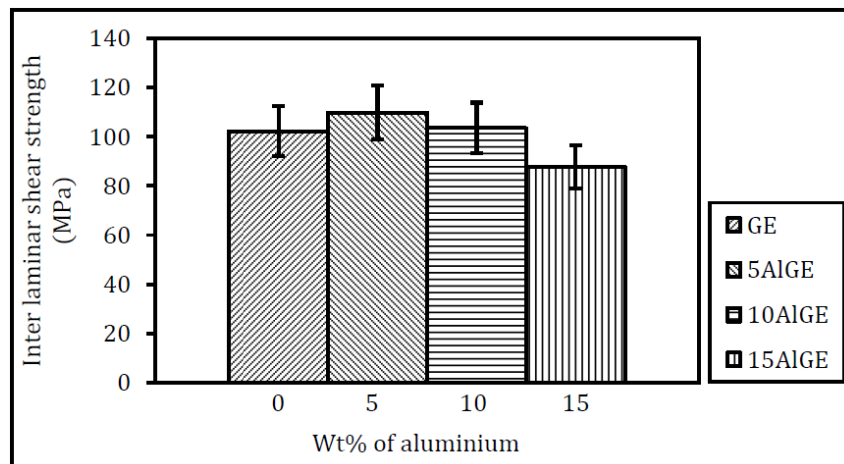
Figure 3.5 Inter-laminar shear strength of composites with aluminium concentration

um filler composites is presented in Figure 3.5. It is observed that with the addition aluminium powder up to the level of 10 wt%, the ILSS of glass epoxy

composites increases in comparison to unfilled glass epoxy composite but starts decreasing on further aluminium addition. This reduction may be due to the formation of voids in the matrix which is generally located at the inter-laminar region of composites or may be because of poor interfacial bond among the constituents of the composites. In the present investigation, the maximum value of ILSS is observed for glass epoxy with 5 wt% aluminium concentration.

4. FRICTION AND WEAR IN RECIPROCATING CONTACT

4.1 Introduction

Friction coefficient and wear depend on number of parameters such as normal load, geometry, relative surface motion, reciprocating frequency, time as well as reciprocating distance, surface roughness of the reciprocating surfaces, type of material, system rigidity, temperature, stick-slip, relative humidity, lubrication etc. Among these factors, this chapter presents the reciprocating friction and wear behavior of glass epoxy and aluminium powder filled glass epoxy composites at different levels of frequency and normal load. Composites used for experimentations are 50GE, 60GE, 70GE, GE (60 wt% glass fiber), 5AlGE, 10AlGE, and 15AlGE. Friction and wear under different combination of frequency and load for the composites are presented with respect to sliding time, frequency (15- 60 Hz), normal load (0.4- 1.0 Kg) and distances (18- 144 m). SEM and EDX analysis are conducted to reveal the mode of wear involved during the sliding process.

4.2 Glass fiber reinforced epoxy composites

Friction and wear behavior of glass epoxy composites with varying wt% of glass fiber reinforcement are studied under the frequency of 15, 30, 45, and 60 Hz and the normal load of 0.4, 0.6, 0.8, and 1.0 Kg for a fixed reciprocating time of 30

(thirty) minutes. Friction coefficient is ploted with respect to time at fixed frequency and load of 15 Hz and 0.4 Kg to study the effect of reciprocating time on friction behavior. The effect of reciprocating frequency, normal load and fiber reinforcement on friction and wear behavior are presented with the help of bar chart at a fixed normal load and frequency of 1.0 Kg and 60 Hz respectively.

4.2.1 Effect of time, frequency, load and reinforcement on friction behavior

A) Effect of reciprocating time
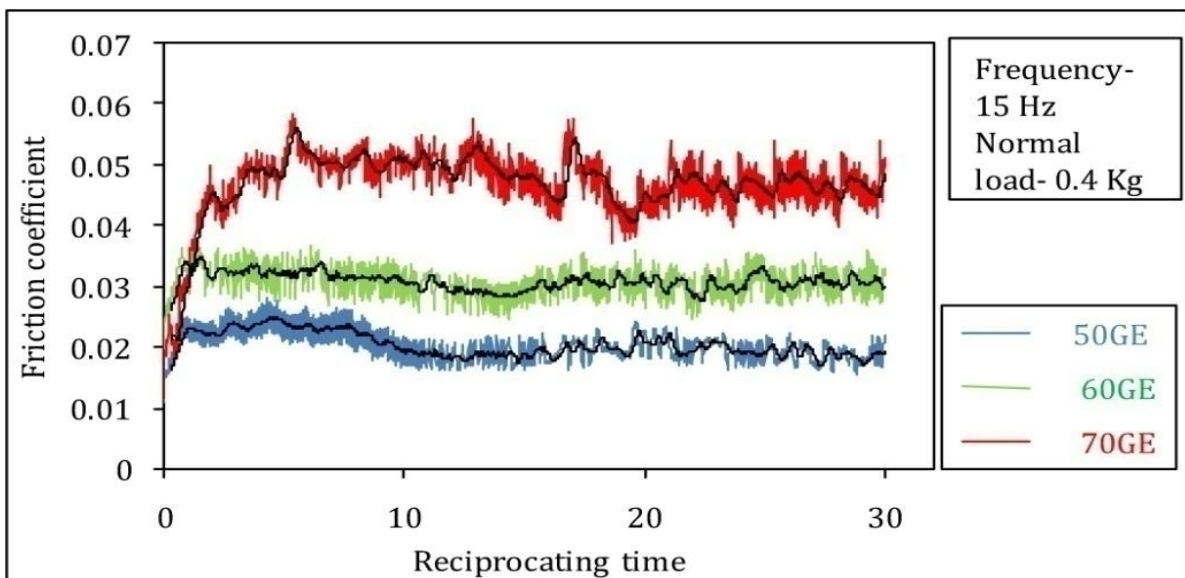
Figure 4.1 Friction coefficient as a function of reciprocating time of 50GE, 60GE and 70GE composites at a fixed frequency and normal load of 15 Hz and 0.4 kg

The variation of friction coefficient with respect to reciprocating time of 50GE, 60GE, and 70GE composites at a fixed frequency and load of 15 Hz and 0.4 Kg is shown in Figure 4.1. The trend of the friction coefficient for all the composites is similar in nature. Graphs are plotted with the data, collected at every second. The black coloured line in the graphs is the 20 period moving average line. It is observed that the friction coefficient is unstable at the initial stage and tends to stabilize after a certain period of time. During the transient period, a number of phenomena occur, such as changes in counterface surface

46

topography and polymer rubbing surface, the development of polymer transfer film on the steel ball surface, and a rise in interface temperature owing to the dissipation of energy in rubbing. When the fiber content is increased from 50 to 60 wt%, the average friction value increases from 0.020 to 0.030 and for 70 wt% of glass fiber loading, the friction coefficient increases to 0.47. The friction coefficient is at its lowest for 50 wt% of fiber reinforcement. This behavior is similar to that reported by Zeng et al. (1987). The friction of the composite material seems to be governed by its shear strength which influences the rupture of adhesive bonds at the interface. The likelihood of fiber-glass disrupting the transfer film, as exhibited during the test by large cyclic fluctuations in friction force is also account for increased friction with the higher proportions of fiber glass (Bahadur and Zheng, 1990).

B) Effect of reciprocating frequency, normal load and fiber reinforcement

In reciprocating contacts, frequency has an important effect on friction and wear of glass fiber reinforced epoxy composite Figure 4.2 shows the variation of friction coefficient with respect to frequency (15-60 Hz) and normal load (0.4-1.0 Kg). Figure 4.2 (a) shows that friction coefficient of 50 and 60 wt% fiber reinforced composites increases with increase of frequency. These findings are in agreement with the findings of Mimaroglu et al. (2007) and Unal, et al. (2004). With the increase in reciprocating frequency, the temperature rises at the contact zone is mainly due to the reduced cooling time per stroke of the steel ball. Heat generated at the contact surface may decrease the strength of the specimen materials and resulting more or increased adhesion with ball (Mimaroglu et al., 2007; Bhushan, 2013) leading to increase of friction coefficient. Additionally, increase in friction coefficient may be due to easy detachment of softened epoxy from the reinforcement and subsequent breakage of reinforced glass fibers with the increase in frequency. These findings are in agreement with the findings of

Mimaroglu et al. (2007) and Suresha et al. (2006). However for 70GE, no such variation of friction is observed, friction remains nearly constant for varying reciprocating frequency.

Figure 4.2 (b) shows that friction coefficient of 60GE decreases with the increase in normal load. This may be the reason of formation of thin film which acts as lubricating agent due to the plastic deformation of the matrix as an effect
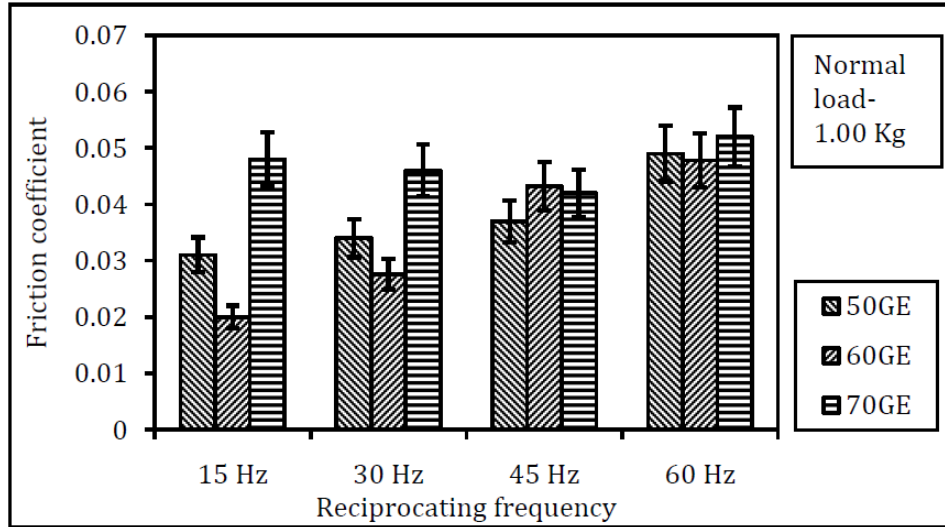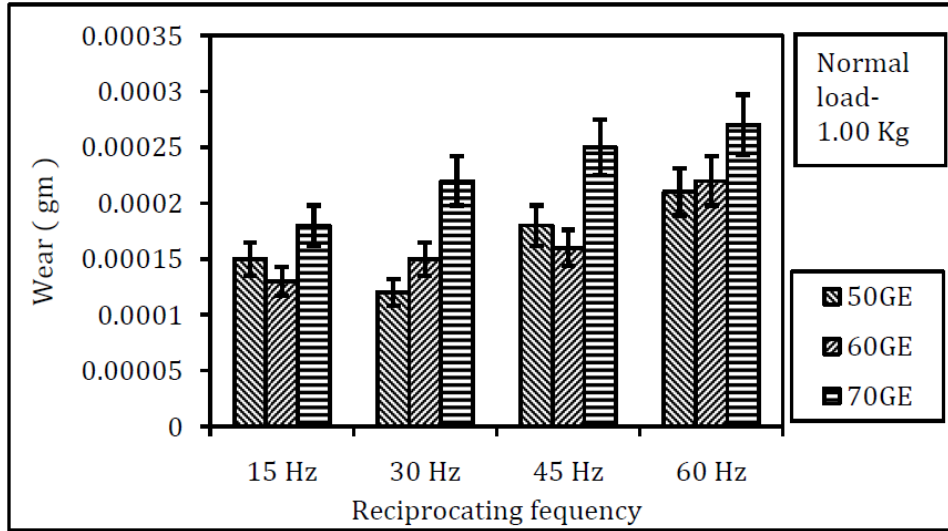

(a)
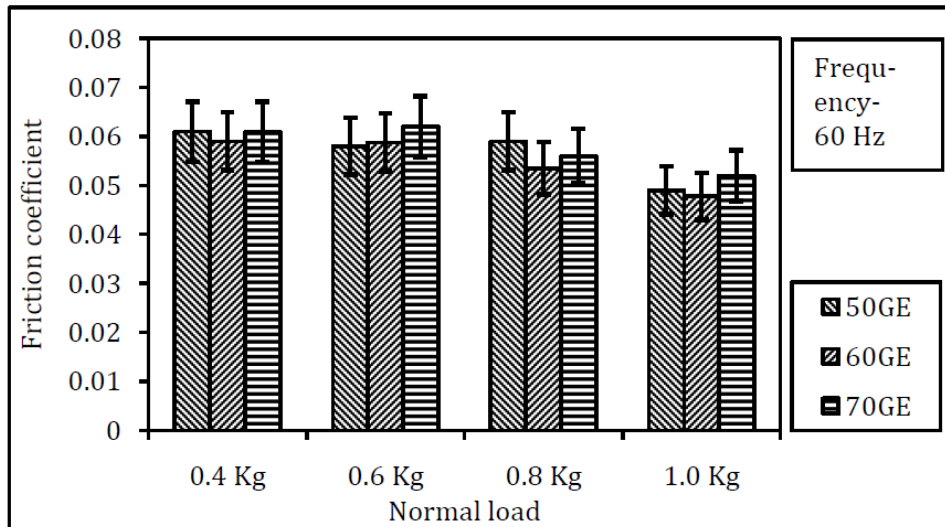
(b)

Figure 4.2 Friction data of 50GE, 60GE, and 70GE samples with respect to (a) reciprocating frequency of 15-60 Hz at a normal load of 1.0 Kg, (b) normal load of 0.4- 1.0 Kg at a frequency of 60 Hz

of heat generation with the increase of normal load (Vasconcelos et al., 2006). It is also observed in Figure 4.2 (b) that the friction of 50GE, 70GE composites with respect to load does not maintain any particular trend, rather, it is fluctuating, this is probably because of the imbalance proportion of constituents in composites. In case of when fiber reinforcement is less than 60 wt%, i.e for 50GE composite, friction coefficient for the increase of load from 0.4 to 0.6 Kg decreases but with further increase of load to 0.8 kg, friction increases and finally decreases at 1.0 kg normal load. The increase of friction at 0.8 Kg of normal load may be attributed due to the increase of adhesion at the contact zone due to resin enrichment. For 70GE composite when the reinforcement is higher than 60 wt%, friction coefficient increases with the increase of load from 0.4 to 0.6 Kg but with further increase of load friction coefficient decreases. At the initial stage, increase of friction may be because of the fiber enrichment which disrupt for the formation of lubricating film at contact.

From Figures 4.2 (a and b), it is also observed that among the three composites, 50GE, 60GE, and 70GE, composite 60GE shows the lowest friction for almost all the experimental conditions whereas 70GE records the highest and friction coefficient 0f 50GE is higher than 60GE but less than 70GE composite. Hence, it may be concluded that 60 wt% is the optimum level of reinforcement, below or above which friction coefficient increases. This behavior is similar to that reported by Zeng et al. (1987). With the addition of more than 60 wt% fiber reinforcement, i.e., for 70GE composite, the likelihood of fiber-glass disrupting the transfer film, as exhibited during the test by large cyclic fluctuations in friction force, could also account for increased friction with the higher proportions of fiber-glass.

4.2.2 Effect of frequency, normal load and reinforcement on wear behavior

Wear variation with respect to reciprocating frequency and normal load of 50GE 60GE, and 70GE composites is shown in Figure 4.3. Figure 4.3 (a) shows the wear variation with frequency (15-60 Hz) for a fixed normal load of 1.0 Kg. The general trend of wear is that it increases with increase in frequency for all three composites except for 50GE composite at 30 Hz frequency where wear decreases with respect to increase of frequency from 15 to 30 Hz. With the increase of freq-

(a)
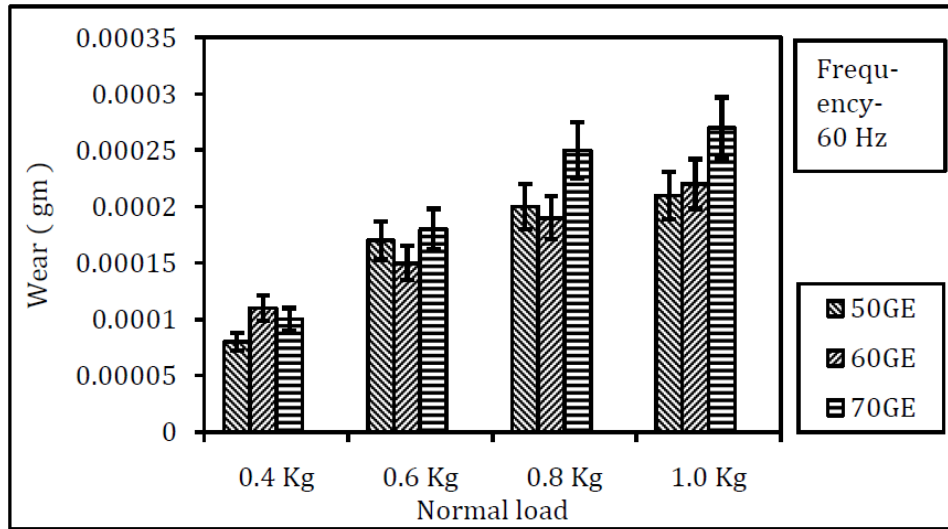
(b)

Figure 4.3 Wear data of 50GE, 60GE, and 70GE samples with respect to (a) reciprocating frequency of 15-60 Hz at a normal load of 1.0 Kg, (b) normal load of 0.4-1.0 Kg at a frequency of 60 Hz

uency, axial trust increases at the contact surface which ultimately leads for the increase of wear. The similar observations has been reported by others (Voss and Friedrich, 1987; Lhymn and Light, 1987). Wear variation with normal load (0.4-1.0 Kg) at a fixed frequency of 60 Hz is shown in Figure 4.3. This figure indicates that wear increases with the increase in normal loads for all the glass epoxy composites. The shear force and frictional thrust are increased with the increase in applied normal load and leads to accelerate the wear.

In Figure 4.3 (a and b), it is also observed that among the composites, sample 70GE, except for lower load of 0.4 Kg and highest frequency of 60 Hz combination reports the highest wear. Wear of 50GE composite is lower than 70GE composite for all the test conditions but in most of the conditions, it is even higher than 60GE composite. The variation of wear with glass fiber reinforcement is similar to that of the coefficient of friction (Figure 4.2) discussed earlier. For fiber proportions higher/lower than the optimum reinforcement is responsible for increase of wear.

4.3 Aluminium powder filled glass epoxy composites

The friction and wear behavior of glass epoxy and aluminium powder filled (5-15 wt%) glass epoxy composites under dry and reciprocating contacts condition has been studied. The woven glass fiber reinforcement is maintained fixed at 60 wt% for all the composites in these cases. The tests are conducted on the samples of GE, 5AlGE, 10AlGE and 15AlGE composites under reciprocating frequency of 15, 30, 45, 60 Hz and normal load of 0.4, 0.6, 0.8, 1.0 Kg for a fixed run time. The effect of frequency, normal load and aluminium concentration on friction and wear behavior of composites has been discussed in details.

The effect of sliding distance on friction and wear behavior of all the composites has been considered separately. Experiments are conducted at a fixed frequency of 30 Hz and at a fixed normal load of 1.0 Kg with a variation of time from 5-40

minutes. The observations of SEM and EDX analysis of samples are presented and discussed.

## 4.3.1 Effect of frequency, load and aluminium powder on friction behavior

A) Effect of reciprocating frequency and normal load on friction behavior

Variation of friction coefficient with respect to frequency and normal load of GE, 5AlGE, 10AlGE, and 15AlGE composites is presented in Figure 4.4. At a fixed normal load of 0.6 Kg, friction variation with respect to reciprocating frequency (15-60 Hz) is shown in Figure 4.4 (a). The general trend of friction of all the composites is that it increases with increase of reciprocating frequency. With the increase in frequency, more heat is generated at the contact surface resulting in more adhesion with the reciprocating ball. Also increase in frequency may lead to an increase in interface temperature due to reduced cooling time per stoke of the ball resulting in subsequent increase in adhesion of composite surface with the reciprocating ball (Nuruzzaman et al., 2012; Mimaroglu et al., 2007; Bhushan, 2013).

Figure 4.4 (b) shows the friction variation with respect to normal load (0.4- 1.0 Kg) at a fixed reciprocating frequency of 30 Hz. The general trend of friction is that it decreases with increase of normal load for GE, 5AlGE and 10AlGE composites whereas for 15AlGE composite, it increases with respect to load from
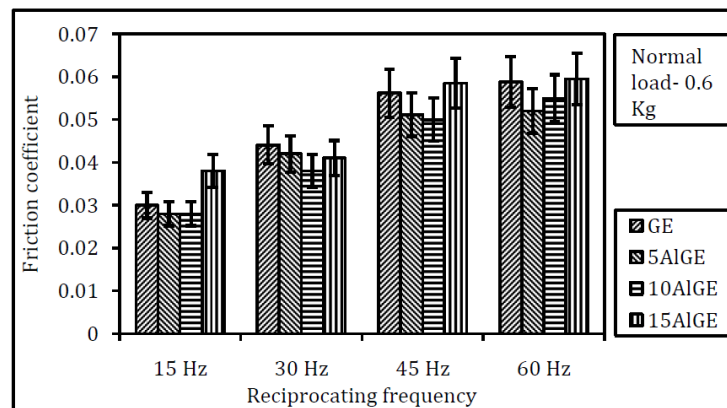
(a)
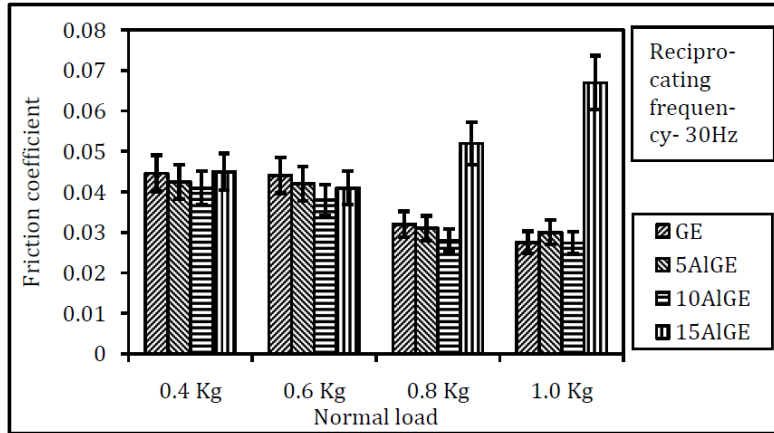
(b)

Figure 4.4 Friction data of GE, 5AlGE, 10AlGE, and 15AlGE samples with respect to (a) reciprocating frequency of 15-60 Hz at a normal load of 0.6 Kg, (b) normal load of 0.4- 1.0 Kg at a frequency of 30 Hz

0.8 Kg load onwards. For all the composites, except 15AlGE, friction coefficient decreases with increase of normal load. Increase in normal load leads to an increase in temperature at the contact interface, which in turn, causes thermal degradation of polymer since polymers become soft with rise in temperature. This results in weaker adhesive bonding between fibers/fillers and matrix yielding in formation of thin film transfer and smooth shearing of fiber or filler. As a result friction reduces at higher normal load. For 15AlGE composite, temperature at the sliding interface increases with increase in normal load causing thermal penetration which results in weakness in the bonds at the interfaces between fiber, matrix and particles. Consequently, the fibers/particles or both become loose in the matrix and aluminium particles protruded out and converted to hard oxide particles which acts as a third body at the contact and for a limited stroke length, the wear debris containing aluminium/oxide/glass particles remain at the reciprocating track. As a result, friction coefficient increases for 15AlGE composite at 0.8 Kg normal load onwards.

## B) Effect of aluminium powder in glass epoxy system on friction behavior

In Figure 4.4 (a), it is also observed that at all levels of frequency (15-60 Hz), friction coefficient is reduced for 5AlGE and 10AlGE composites compared to GE sample which implies that incorporation aluminium particles upto 10 wt% reduces friction. This may be attributed to poor heat conductivity of GE samples. At a particular frequency and load condition, for GE samples, heat generated at the contact interface is mostly used to soften the epoxy matrix, resulting in more or increased adhesion with ball counter face leading to high frictional value. With incorporation of aluminium particles, as in case of 5AlGE and 10AlGE samples, heat conductivity of the resulting composite increases. This essentially helps in conducting away the heat from the contact interface and results in reduced adhesion with the counterface ball. This in turn yields low friction coefficient. But with higher concentration of aluminium (as in case of 15AlGE samples) friction coefficient reports the highest value at all the frequency levels. This may be because of the oxidization of protruded aluminium particles which act as a third body at the contact interface.

In Figure 4.4 (b), it is also observed that for a fixed reciprocating frequency and for all normal load conditions considered, friction coefficient of composite 10AlGE shows the minimum value and it increases with higher concentration of aluminium particles (as in 15AlGE composite). In fact at higher normal loads (0.8–1.0 kg), friction coefficient for 15AlGE composite becomes comparable to GE composite. The probable explanation for this has already been provided. It is important to note here that for reduction of friction, aluminium particles may be incorporated in the composite but higher concentration of aluminium will spoil the purpose. Accordingly, the amount of aluminium particles to be incorporated needs to be controlled accurately.

4.3.2 Effect of frequency, load and aluminium powder on wear behavior

A) Effect of reciprocating frequency and normal load on wear behavior

The wear behavior of GE and 5AlGE, 10AlGE, 15AlGE composites with respect to reciprocating frequency and normal load are shown in Figure 4.5. Figure 4.5 (a) shows that the wear of all the composites increases with increase of frequency at a fixed normal load of 0.6 Kg. During sliding, both normal and tangential loads are transmitted through the asperity contact points by adhesive and ploughing actions. Both adhesive and ploughing actions cause frictional thrust. The glass fibers present in the matrix resin on exposure to the counter surface break because of the frictional thrust. With increasing frequency, it has already been observed that the magnitude of the frictional thrust increases and this results in increase in wear of the composites. Woven roving glass epoxy composite (GE) is a poor thermal conductive material; as a result heat generated at the contact zone remains entrapped there and is used for thermal penetration and results in softening of the matrix. This weakens the bond between the reinforcing glass fibers and causes debonding of fibers. The debonded glass fibers
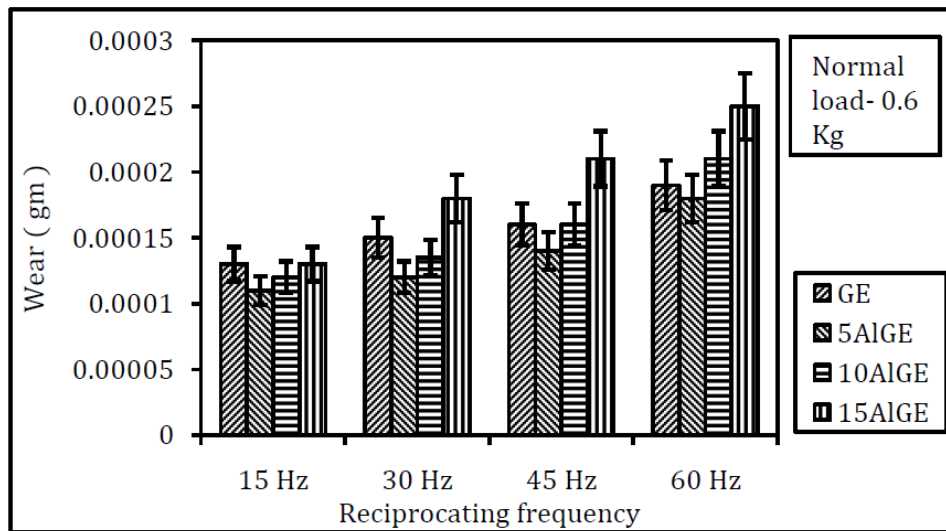
(a)
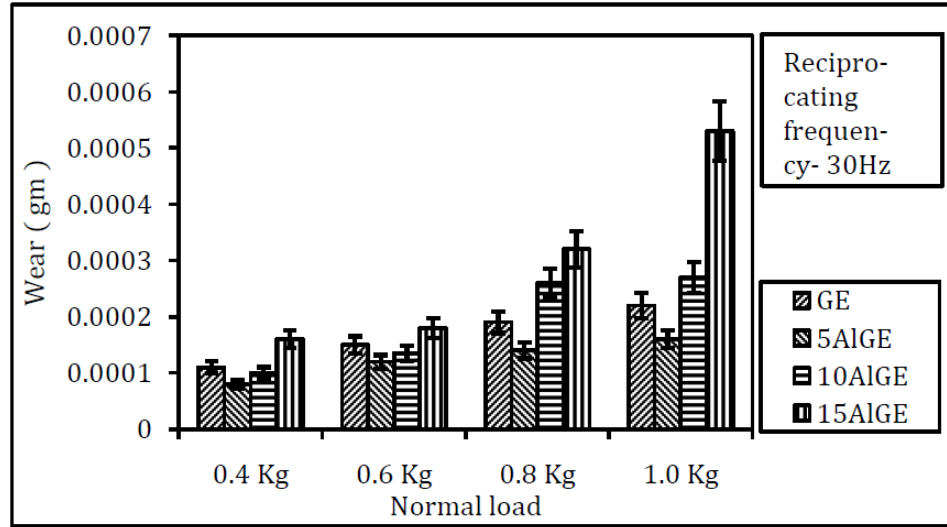
(b)

Figure 4.5 Wear data of GE, 5AlGE, 10AlGE and 15AlGE samples with respect to (a) reciprocating frequency of 15-60 Hz at a normal load of 0.6 Kg, (b) normal load of 0.4- 1.0 Kg at a frequency of 30 Hz

for its brittle nature fracture owing to the repeated loading. The frictional heat, on the other hand, results in charring of the matrix resin at the contact zone. The combined effect of thermal softening and charring of epoxy matrix results in debonding of the glass fibers and loss of structural integrity of the composite (Mimaroglu et al., 2007; Suresha et al., 2006).For aluminium particulate glass epoxy composites (5AlGE, 10AlGE, 15AlGE), contact surface of the sample contains epoxy, aluminium particles, and glass fibers. The presence of aluminium particles increases with the increase of aluminium wt% in composites. The soft matrix asperities are easily deformed and sheared under repeated loading action. Simultaneously, hard ball asperities or the presence of hard aluminium oxide particles between the sliding surfaces plough and micro-cut the soft surface resulting in the change of surface characteristics. As a result, the aluminium particles present in the matrix resin on exposure to the ball surface tends to protrude out followed by the breakage of glass fibers depending on the stiffness and strength of composites. On increase of frequency, the magnitude of the

frictional thrust increases, this results in increase in wear of the aluminium particulate glass epoxy composites.

Variation of wear with normal load (0.4–1.0 Kg) at a fixed frequency of 30 Hz is shown in Figure 4.5 (b). It is seen that wear increases with increase of normal loads for all the composites. Increase in normal load leads to an increase in temperature at the contact interface, which in turn, causes thermal degradation of polymer since polymers become soft with rise in temperature. Also higher load leads to higher penetration of the hard asperity peaks of the counter surface into the matrix of the composite. As a result wear increases with increase in load.

B) Effect of aluminium powder in glass epoxy system on wear behavior

In Figure 4.5 (a), it is also observed that in glass epoxy system, with the incorporation of aluminium powder, 5AlGE shows the lowest wear and the value is lower than the glass epoxy (GE) composite at all combination of load and frequency. Wear of 10AlGE composite also lower than GE sample upto 45 Hz frequency level and further increase of frequency wear increases than GE sample. Among the composites, wear of the 15AlGE composite is the highest even more than the GE composite at all the experimental frequency levels.

Due to incorporation of aluminium particles, heat conductivity of the composite increases. As a result, thermal penetration and subsequent softening of the matrix is reduced leading to reduction in wear. Thus 5AlGE and 10AlGE yield lesser wear compared to GE composite. However, further increase in aluminium concentration (as in 15AlGE) in the composite, these particles help in breakage of fibers and debonding of fibers from matrix as well leading to increase in wear.

In Figure 4.5 (b), it is also observed that at all the normal load conditions, wear of 5AlGE composite bears the lowest value in comparison to GE and other aluminium particulate glass epoxy composites. Wear of 10AlGE composite is higher than 5AlGE but at the lower load conditions (0.4-0.6 Kg), it is also less than

GE composite. Wear of 15AlGE composite holds the wear value higher than GE sample and it has the highest value at all experimental conditions. Limited incorporation of aluminium particle in glass epoxy composite systems increases the material stiffness and thermal conductivity. This leads to improved wear resistance With the increase of aluminium content, thermal conductivity increases but at the same time for higher content of aluminium particles, material stiffness decreases leading to increase in wear (Suresha et al., 2006; Zhou, 2011). In case of 15AlGE composite, the amount of aluminium particles present may be high enough to form agglomeration resulting in poor interfacial bond and easy pull out of aluminium particles from the composite during the reciprocating action. The protruded aluminium particles along with fractured glass fibers add to rapid and severe wear due to existence of a mixed abrasive and adhesive wear condition (Archard, 1953; Friedrich, 2012).

4.3.3 Effect of sliding distance on friction characteristics

Figure 4.6 shows the friction coefficient variation with respect to the reciprocating distance for the composites. Detailed numerical values of friction data are provided in Table 4.1. Unfilled (GE) and 5 wt% aluminium filled (5AlGE) samples maintained almost similar nature with a little fluctuation at the initial stage. The overall friction as well as friction value for each distance run is higher for unfilled (GE) than the 5AlGE, 10AlGE composite samples. For GE composite sample, friction coefficient starts at a value of 0.098 at 18 m run and maintains higher frictional trend to 0.127 at reciprocating distance of 36 m, then goes down and maintains almost stable trend. This may be explained with the help of Figure 4.7. As the asperities of hard counterpart come in contact with the composite system (GE), the comparatively soft epoxy matrix due to the repeated action of shear force breaks easily prior to the breakage of vertical/horizontal fibers (Friedrich and Reinicke, 1998). Due to this feature, roughness of the

reciprocating surface increases than the initial roughness leading to the increase of friction coefficient. The SEM micrographs (shown in Figure 4.8) duly support this phenomena. The fiber part of the composite is extended out of the level of the matrix system as seen in Figure 4.8 (a). Figure 4.8 (b) represents the sample surface with the highest friction level at 36m distance of run. The asperity in contact with the surface breaks to the powdery particles of metal elements result-
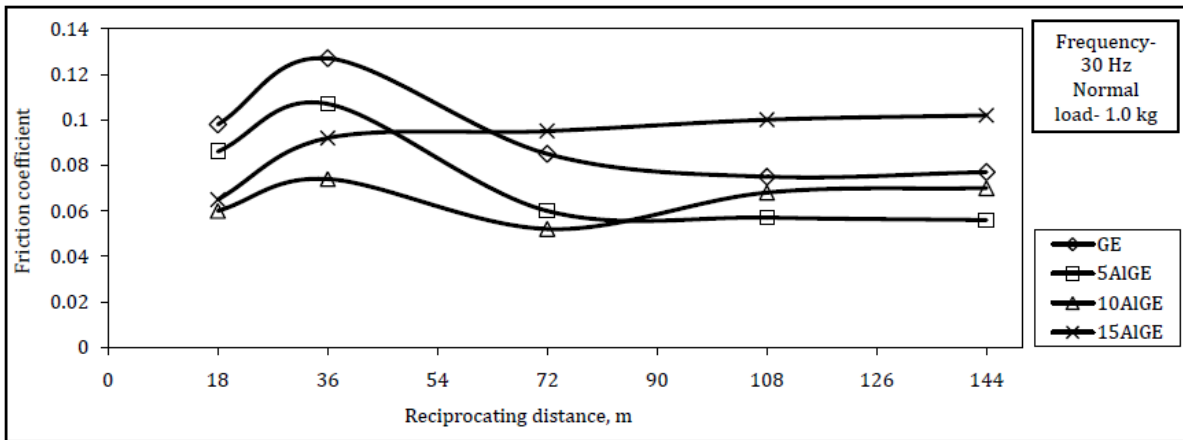

Figure 4.6 Friction coefficient as function of reciprocating distance for glass epoxy composites

ing in the erosion of the steel ball, and this causes decrease of friction coefficient. The shear deformed epoxy matrix, powdery particles of the metal elements and the pulverized glass particles together constitute the wear debris. The debris thus
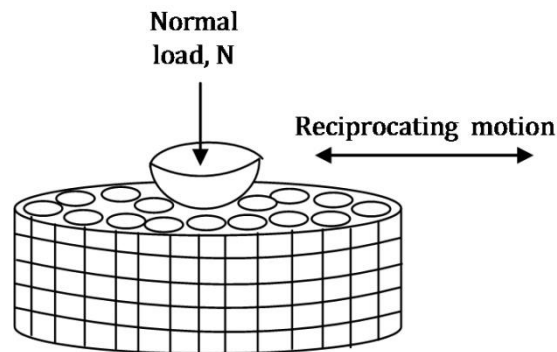
Figure 4.7 Tribological system with metal asperity vs composite with woven fiber orientation

formed may remain at the contact zone, may be displaced to both sides of the track due to the ploughing action or may be agglomerated at the dead end positions of the reciprocating stroke. The friction behavior depends on the constituents of the wear debris more precisely the type of particles remaining at the real contact zone. With further increase of distance, temperature at the contact surface increases due to heat generation which softens the matrix and ultimate formation of a thin film that helps to maintain a stable friction coefficient for the rest of the experimental distance. Addition of aluminium powder to the epoxy system improves the material stiffness and thermal conductivity. The better thermal conductivity contributes to a more efficient dissipation of the heat

Table 4.1 Friction coefficient of composites at different distance run

Reciprocating distance (m)	Friction coefficient			
	GE	5AlGE	10AlGE	15AlGE
18	0.098	0.086	0.060	0.065
36	0.127	0.107	0.074	0.092
72	0.085	0.060	0.052	0.095
108	0.075	0.057	0.068	0.100
144	0.077	0.056	0.070	0.102

generated on the contact area. For 5AlGE composite, at the beginning of the reciprocating motion, the sample surface consists of glass fiber, epoxy matrix and aluminium particles which are in contact with the steel counter surface. As the motion starts, shear forces are applied, less amount of matrix gets deformed, aluminium particles do not protrude out from the composite for high stiffness of the composite resulting from better interfacial bonding of the constituents. This causes reduction in friction coefficient at starting. But the roughness of the surface increases latter due to the exposed aluminium particle and fiber. This leads to the increase of friction coefficient to 0.107 for the reciprocating distance of 36 m. On subsequent reciprocation, the surface of the specimen gets smoothened. This reduces the friction coefficient from a value of 0.107 to 0.060. Heat dissipation from the contact surface increases with the increase of

aluminium quantity and particle size (Zhou, 2011). Heat generated at the contact area softens the matrix and for mation of thin lubricating film at the contact serfa-
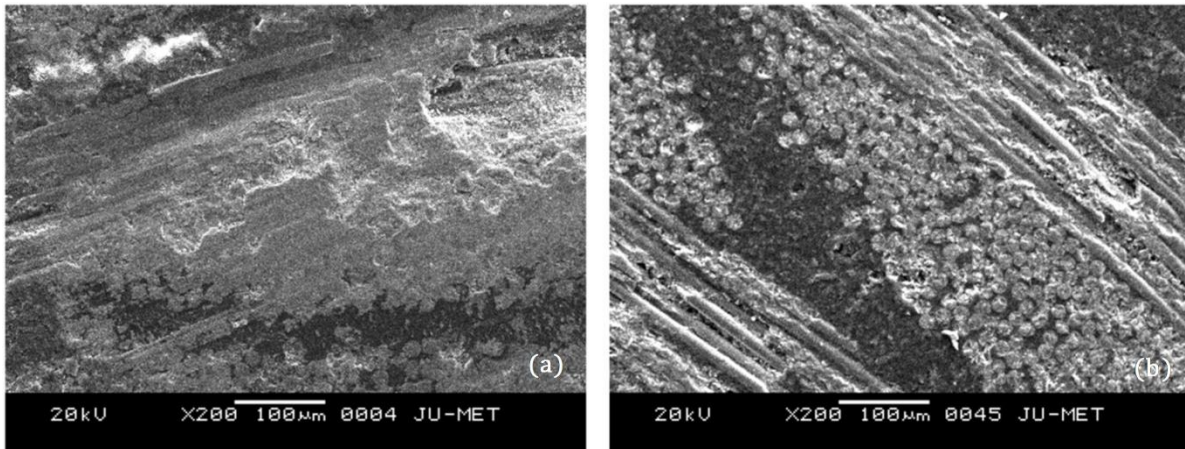

Figure 4.8 SEM images for the unfilled glass epoxy composite showing the surface roughness for (a) 18 m distance run and (b) 36 m distance run

ce keeps the friction coefficient all most constant. For 10AlGE samples, all most similar trend is maintained for the same reason as unfilled GE and 5AlGE composites up to the reciprocating distance of 72 m and at this distance heat generated at the contact surface can be conducted to the other part of the composite sample as the aluminium particle with good concentration behaves as a good conductor of heat. So the temperature of the contact surface does not rise much. Easy pull out of the aluminium particles and its subsequent formation of harder oxide particles and its action as a third body particle along with the glass particles further increases the friction up to the distance of 108 m. At this higher friction range, the heat generated probably cannot be conducted away at the same rate resulting in increase in temperature and helps in softening the epoxy matrix and deformation of the oxide particles and finally forms a very thin lubricating film as a result of which friction coefficient maintains constant trend for the rest of the experimentation time. For 15AlGE composite samples, friction coefficient increases from 0.065 to 0.092 with the corresponding distance of 18 and 36 m respectively, then maintains a slow but steady increase to 0.095 for 72

m distance and finally maintains the steady condition. The increase of friction coefficient for the corresponding distance from 18 to 36 m may be attributed to the easy pull out of aluminium particles from the composite and its presence along with the glass particles at the contact zone. Further increase of the reciprocating distance leads to thin film formation at the contact surface resulting in constant friction.

4.3.4 Effect of sliding distance on wear characteristics

In glass epoxy composites the process of material removal in dry sliding condition is dominated by four wear mechanisms, viz., matrix wear, fiber sliding wear, fiber fracture and interfacial debonding. The matrix wear occurs due to plastic deformation and fiber sliding wear occurs due to fiber rubbing, fiber rupture, fiber cracking, and fiber pulverizing. In Figure 4.9, wear loss in respect of reciprocating distance for unfilled and 5, 10, and 15 wt% aluminium powder filled glass epoxy composites at a constant normal load 1.0 Kg and frequency 30 Hz has been shown. In both unfilled and filled cases trend shows that the wear
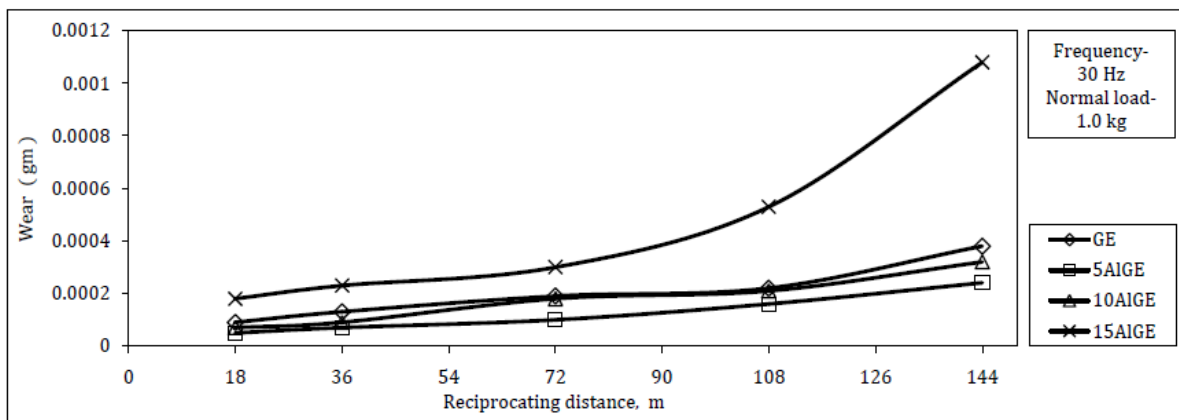

Figure 4.9 Wear as a function of reciprocating distance for glass epoxy composites

increases with the increase of reciprocating distance. To explain the relative wear for different distances, results are presented in the form of a bar diagram in Figure 4.10. From the graph and bar chart, it is observed that among the tested

composites, aluminium filled glass epoxy composites; 5AlGE exhibits the least wear where as 15AlGE composite shows the highest. The wear for
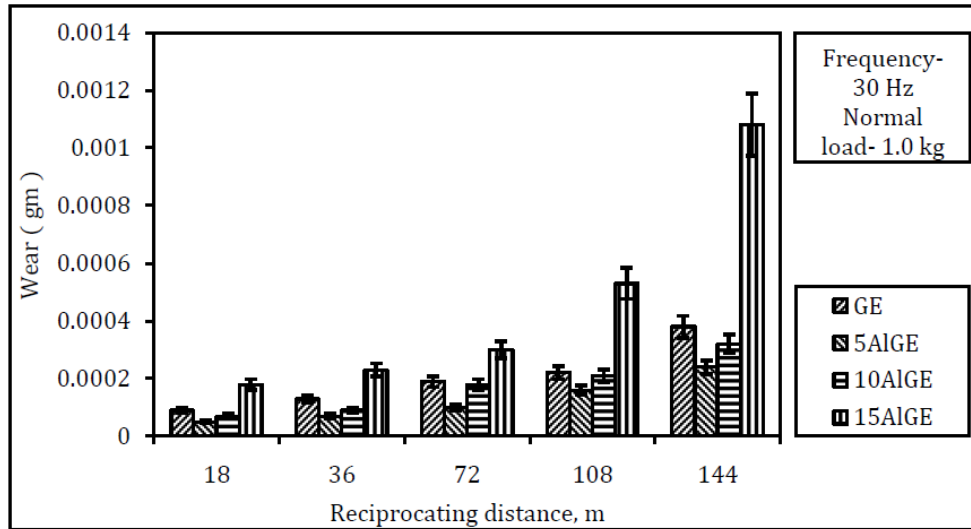

Figure 4.10 Wear data of GE, 5AlGE, 10AlGE, and 15AlGE composites with respect to reciprocating distance at a frequency and normal load of 30 Hz and 1.0 Kg

10AlGE composite is higher than 5AlGE but it is always less than the unfilled glass epoxy, GE samples. Detailed numerical data for wear is shown in Table 4.2. The

Table 4.2 Wear of composites at different distance run

Reciprocating Distance (m)	Wear (gm)			
	GE	5AlGE	10AlGE	15AlGE
18	0.00009	0.00005	0.00007	0.00018
36	0.00013	0.00007	0.00009	0.00023
72	0.00019	0.00010	0.00018	0.00030
108	0.00022	0.00016	0.00021	0.00053
144	0.00038	0.00024	0.00032	0.00108

limited presence of aluminium powder upto 10 wt%, composites show less wear loss than the unfilled glass epoxy composite, and above 10 wt% aluminium addition increases the wear considerably and it is higher than the GE composite. The performance of the glass epoxy composite is primarily determined by the properties of glass fibers and its orientation relative to the reciprocating direction. During the reciprocating motion the hard asperity tips of the steel ball are in continuous interaction with the various components of the composite

(Figure 4.7). This leads to variation in the wear mechanism of the composite material. Figure 4.11 systematically illustrates the possible sequence of the wear steps acting between steel ball and unfilled or aluminium powder filled glass epoxy composites. Usually for GE samples, the softer epoxy matrix between the much harder fibers is removed first and then cracking of the much harder fiber pieces occurs, which finally leads to the repetition of the wear cycles (Friedrich and Reinicke, 1998). In respect to fiber orientation, this particular phenomenon may be explained (El-Sayed et al., 1995) as shown in Figure 4.12. In woven glass fiber orientation, the asperities of the steel ball may come in contact in two possible ways. When fibers are oriented normal to the reciprocating surface, debonding will occur at the surface and will propagate down along the length of the fiber to a finite distance; the stronger the fiber the longer the resulting debo-
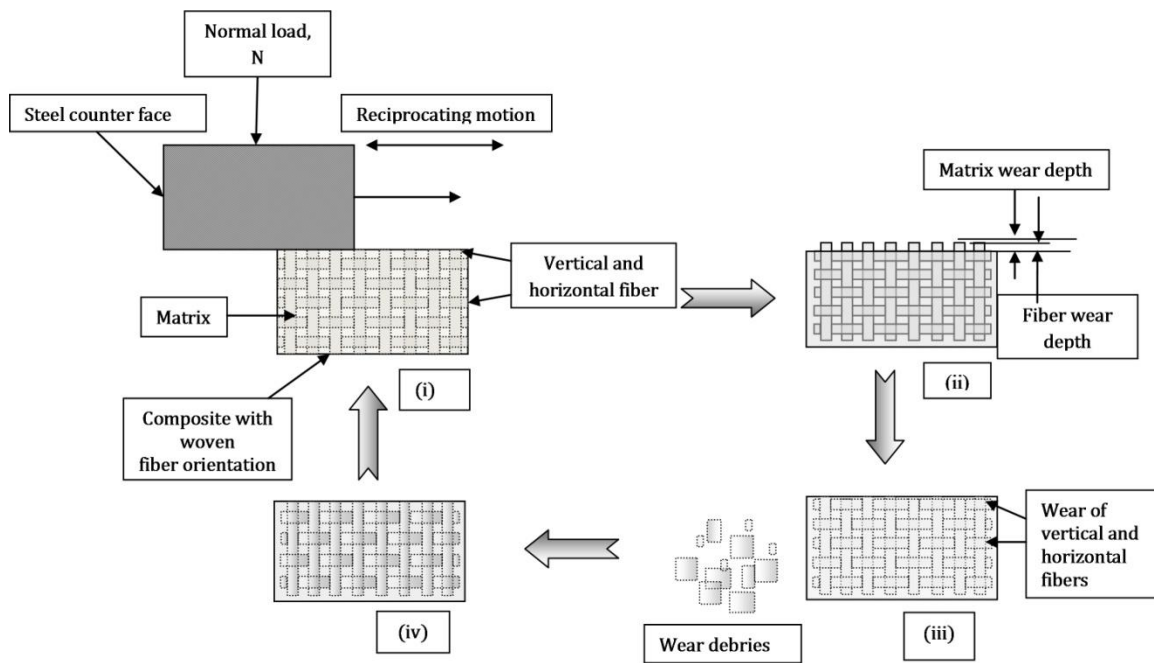
Figure 4.11 Possible sequence of wear steps at the surface of the composite

nding distance but not exceeding to the next parallel fibers in transverse or longitudinal orientation. For weaker vertical fibers, the fiber breakage occurs before debonding propagation. Wear of these fibers occurs because of the shear

force component (F_s). When fibers are oriented parallel to the reciprocating surface as in transverse or longitudinal orientation, initiation of the debonding occurs at the fiber resin interface at a finite depth from the surface. Initiation of cracks may also occur at surface or fiber resin interface, where the tensile stress component perpendicular to the surface is maximum (Ward, 1970). The cracks and the debonding length of fiber will increase owing to continuous loading. By this process fiber failure resulting in freely protruding bulk parts can occur which leads to increase in wear rate. This may apply with no appreciable difference between transverse and longitudinal orientation. At the junction of vertical and parallel fiber, debonding depends on both the shear (F_s) and tensile force components (F_t). It is expected that when fiber wt fraction increases, the force carried by each fiber decreases, which means that the two components of this force decrease leading to a decrease in wear. The basic aim to incorporate aluminium powder in glass epoxy composite system is to increase the material st-
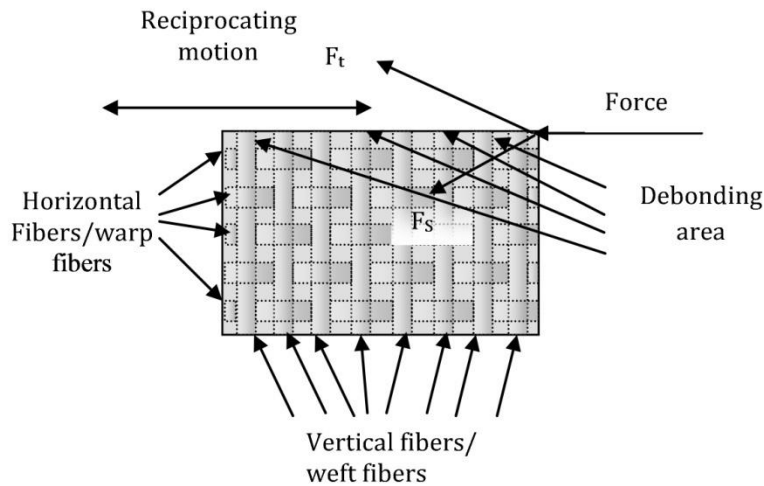

Figure 4.12 Schematic representation of failure mode of woven fiber reinforced aluminium powder unfilled/filled composites

iffness and thermal conductivity. The better thermal conductivity contributes to a more efficient dissipation of the heat generated on the contact area and ultimately reduces the plastic deformation of the soft matrix resulting to the

reduction of matrix wear. This may be attributed as 5AlGE and 10AlGE samples, aluminium powder dispersed in the matrix covers the packets of plain weave woven glass fabric reduces the void fractions, provides the better inter facial bond strength due to increase surface area and exhibits additional strength and hardness to the composite. This ultimately leads to reduce wear loss than unfilled glass epoxy composite. For the addition of 15 wt% aluminium to the composite, the quantity of aluminium particle present is high enough to form the agglomeration, resulting poor interfacial bond and easy pull out of aluminium particle from the composite. The protruded aluminium particle converts to hard oxide particles which act as a third body along with the pulverized glass particles resulting in rapid wear for the rest of the experimentation time. This severe wear is due to the existence of a mixed abrasive/adhesive contact condition (Archard, 1953; Friedrich, 1986).

4.3.5 Surface morphology and energy dispersive X-Ray spectroscopy

4.3.5.1 Aluminium powder distribution in composites

The surface morphologies of selected unfilled and aluminium powder filled glass epoxy composite specimens under different conditions and respective surface elements are characterized. Figures 4.13, 4.14, 4.15, 4.16 show the distribution of constituent elements present in the unfilled and filled composites in the reciprocating area/worn surface. Figure 4.13 shows the fiber and matrix present in GE sample whereas Figure 4.16 shows the maximum aluminium particle present in 15AlGE sample.
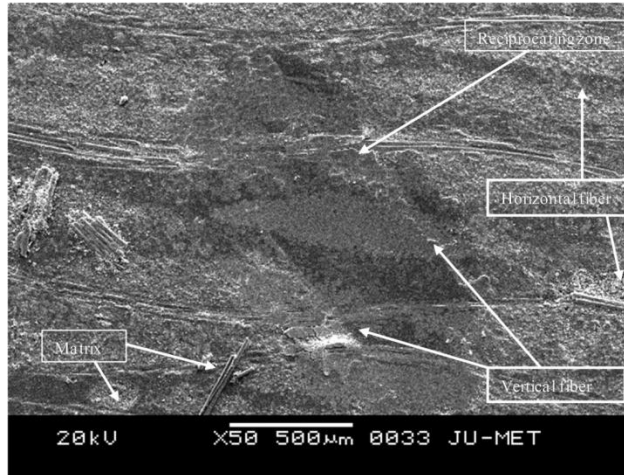
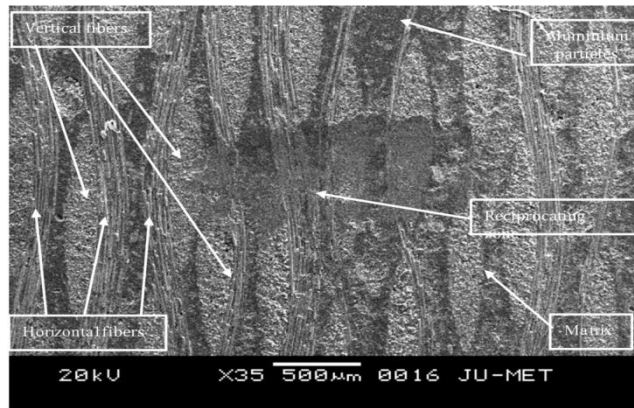Figure 4.13 Worn surfaces of composites: unfilled, GE composite

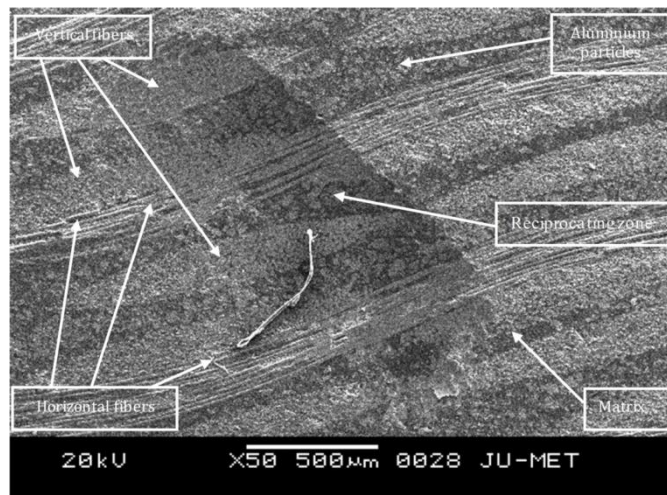Figure 4.14 Worn surfaces of composites: 5 wt% aluminium powder filled, 5AlGE composite

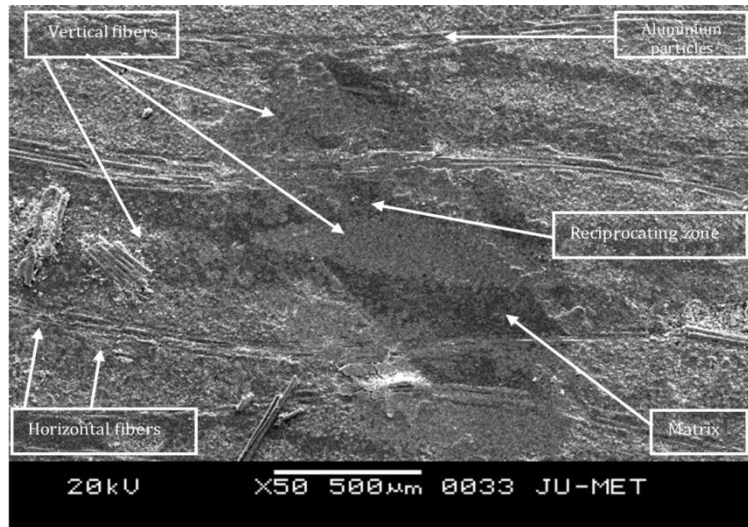Figure 4.15 Worn surfaces of composites: 10 wt% aluminium powder filled, 10AlGE composite

Figure 4.16 Worn surfaces of composites: 15 wt% aluminium powder filled, 15AlGE composite

4.3.5.2 Effect of sliding distance on surface features of composites

Figure 4.17 shows the SEM micrograph of worn surfaces of unfilled glass epoxy composites at different distances of run. It is observed in Figure 4.17(a) that the height of the fibers are more than the matrix system resulting in increase of the surface roughness leading to the increase of friction coefficient as in Figure 4.6. The exposed horizontal fibers are completely separated from the matrix. Very few breakages of fiber and small amount of wear debris are also noticed. Figure 4.17(b) is a SEM micrograph at 144 m distance run. It shows the presence of a significant iron concentration at the light grey region. The steel sphere suffers wear and incorporates iron particles in the interfacial layer. SEM image shows multiple parallel micro-cracks, approximately perpendicular to the reciprocating direction (vertical direction), indicating the presence of a fatigue mechanism (Suh, 1986). SEM micrograph of the worn surface for 5AlGE composite sample has been shown in Figure 4.18 viewed at different distances of run. Figure 4.18(a) shows the exposure of aluminium particles which increases the roughness of the contact surface. These aluminium particles definitely get oxidized (light grey) and
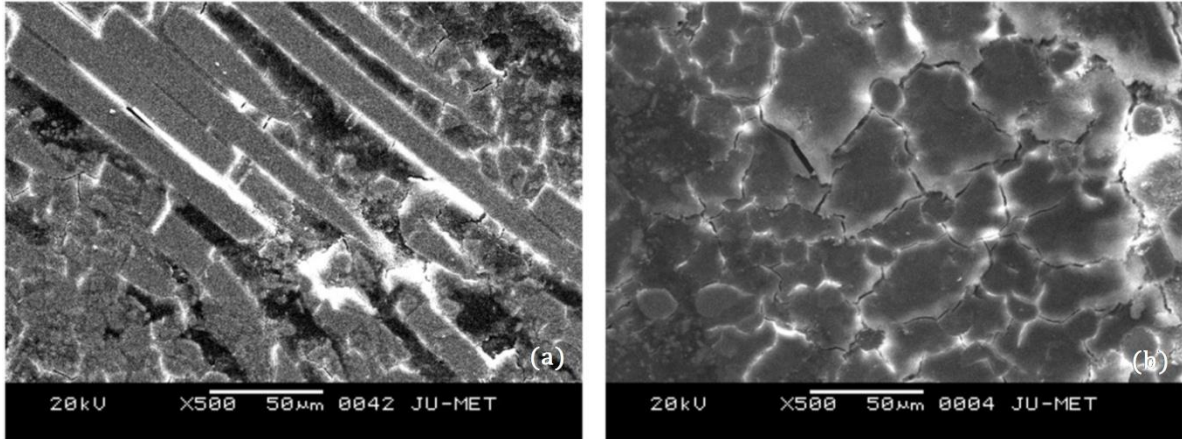
68

Figure 4.17. SEM images of unfilled glass epoxy composite at a) 36 m distance run showing the exposed horizontal and vertical fibers and wear debris, b) 144 m distance run with light grey contours that surround the micro cracks reveal the existence of iron
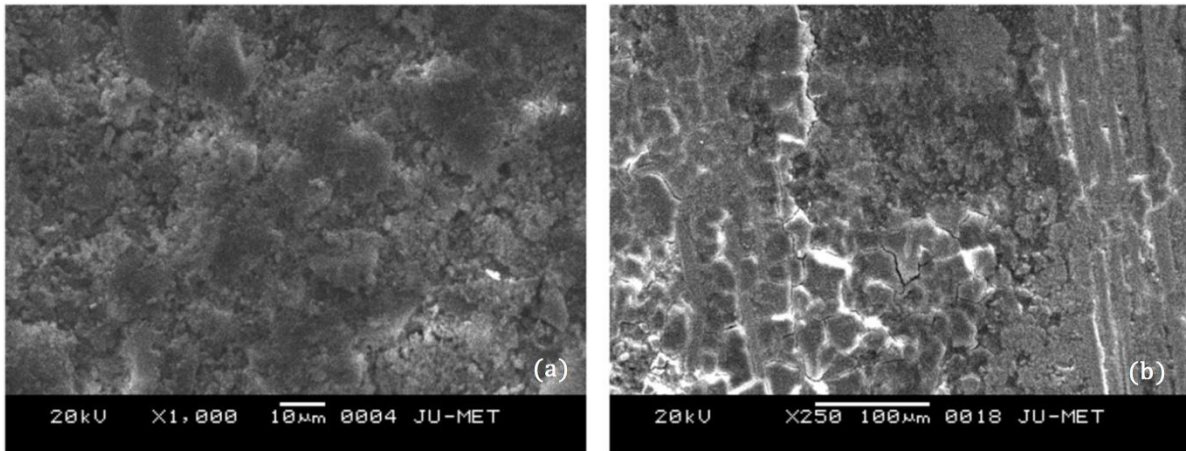

Figure 4.18 SEM images of 5 wt% aluminium filled glass-epoxy composite at a) 18 m reciprocating distance showing the much harder aluminium particles, b) 144 m reciprocating distance showing the agglomeration of wear debris at the dead end position

make the surface harder. During this period, very less quantity of epoxy matrix wears out from the sample. Figure 4.18(b) represents the dead end surface condition of the forward stroke of the reciprocating motion. It indicates that there is an agglomeration of large quantity of wear debris at the dead end position and further crack propagation beyond the contact surface is clearly observed. For 10AlGE samples SEM micrograph for the worn surfaces has been shown in Figure 4.19. Figure 4.19(a) indicates that at the end of 72 m distance run there is clear

indication of exposed vertical and horizontal fiber erosion and it makes the contact surface further rough as a result of which for the distance run from 72 m to 108 m, friction coefficient increases and it validates the result as shown in Figure 4.6. It also corroborates the findings of the wear loss shown in Figure 4.9. It shows the agglomeration of wear debris at the dead end position of the stroke. Figure 4.19(b) shows the position of the horizontal fibers at a distance of 144m. It clearly shows the breakage of fibers and further initiation of cracks at the middle of the contact surface, wear debris are also observed. Figure 4.19(c) shows the plastically deformed aluminium particles with the initiation of micro cracks at a
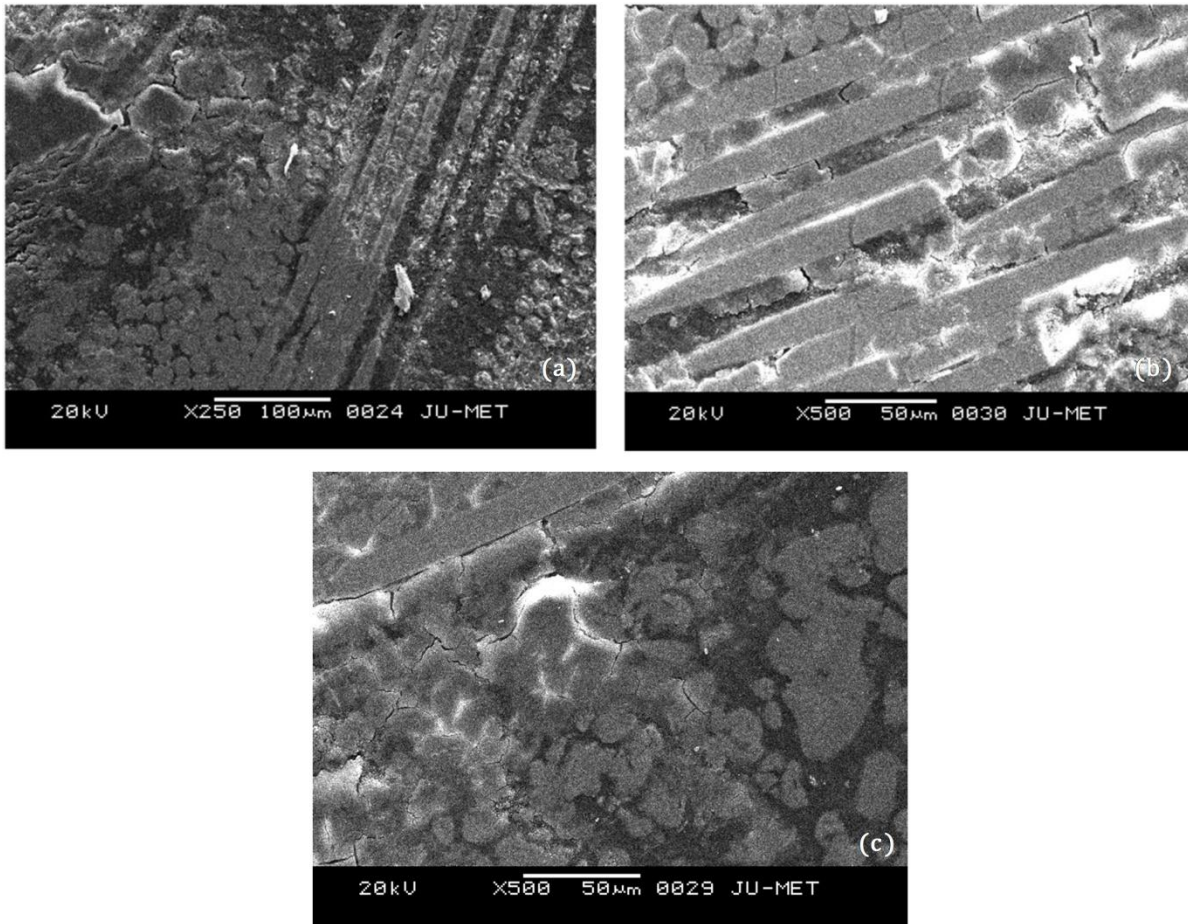

Figure 4.19 SEM images of 10 wt% Al filled glass-epoxy composite at (a) 72 m reciprocating distance with the erosion of horizontal and vertical fibers, (b) 144 m reciprocating distance with breakage of horizontal fibers and wear debris, (c) 144 m reciprocating distance with plastically deformed aluminium particles.

distance of 144 m run for 10AlGE sample. SEM micrograph for 15AlGE samples at a run distance of 144 m has been shown in Figure 4.20. It shows the presence of micro cracks contributing to the easy pull out of aluminium particles and glass fiber resulting to highest wear.
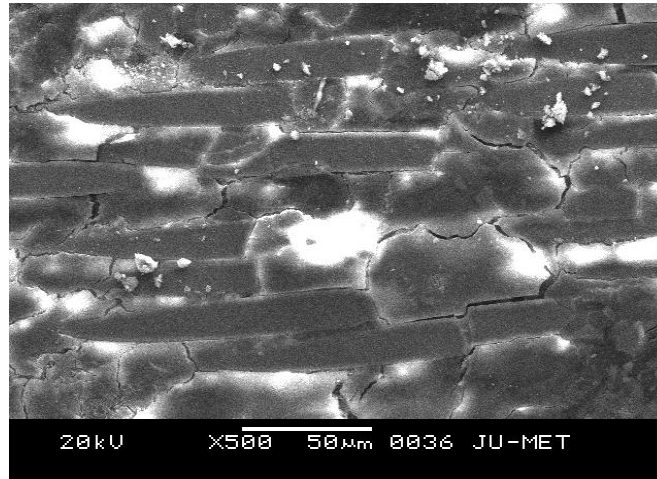

Figure 4.20 SEM image of 15 wt% aluminium filled glass-epoxy composite at 144 m reciprocating distance with micro cracks contributing to the aluminium particles and fiber debonding

4.3.5.3 Energy dispersive X-ray spectroscopy (EDX) analysis

The EDX analysis is done to find the composition of elements present on the surface of specimens. The chemical composition of 5AlGE sample is shown in Table 4.3 and Figure 4.21. The same for 15AlGE sample is shown in Table 4.4
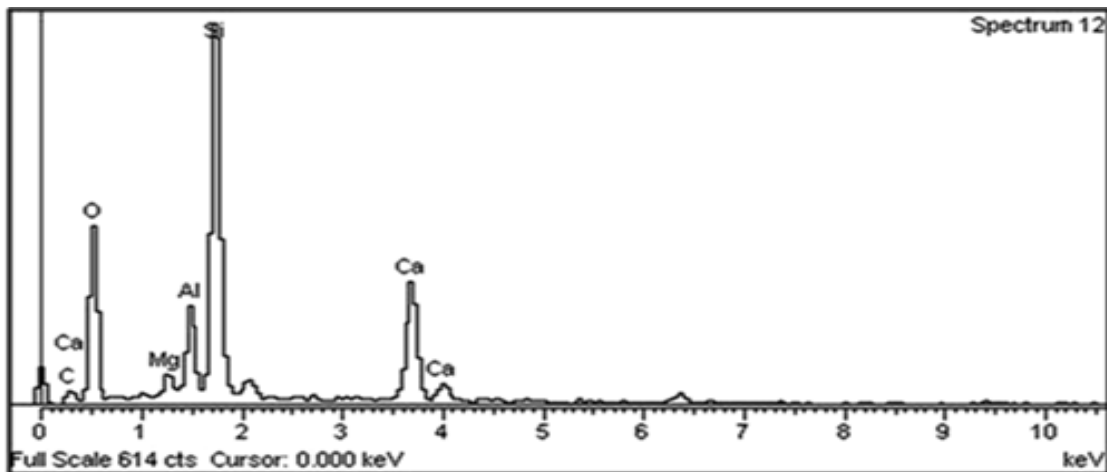

Figure 4.21 EDX spectra for elemental composition of polished surface of 5 wt% aluminium filled glass epoxy composite, 5AlGE sample

Table 4.3 Chemical composition of polished surface of 5 wt% filled glass epoxy composite, 5ALGE sample

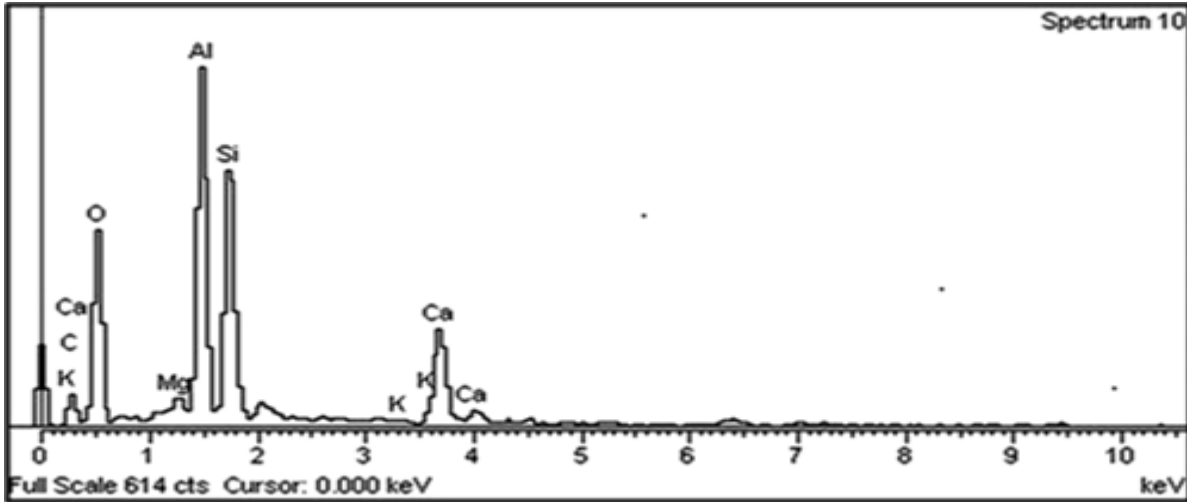| Elements	C	O	Mg	Al	Si	Ca	Total
Weight%	7.51	51.15	1.42	5.17	23.76	10.97	100.00

Figure 4.22 EDX spectra for elemental composition of polished surface of 15 wt% aluminium filled glass epoxy composite, 15ALGE sample

Table 4.4 Chemical composition of polished surface of 15 wt% filled glass epoxy Composite, 15ALGE sample

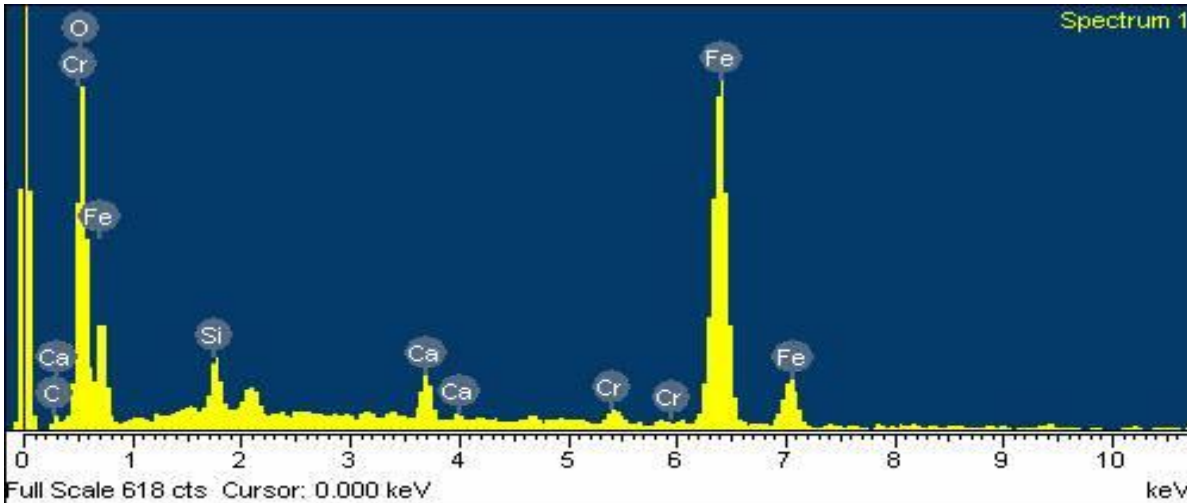| Elements	C	O	Mg	Al	Si	K	Ca	Total
Weight%	15.72	45.98	1.03	15.67	14.24	0.35	7.02	100.00

Figure 4.23 EDX spectra of elemental composition of worn surface of unfilled glass epoxy Composite, GE sample at 72 m distance run

Table 4.5 Chemical composition of unfilled glass epoxy composite at 72 m distance run

Elements	C	O	Si	Ca	Cr	Fe	Total
Weight %	4.45	32.79	3.02	2.62	1.62	55.51	100.00

and Figure 4.22 respectively. From these, it is clearly seen that the wt% of aluminium presence is 5.17 and 15.67 along with the other elements. The presence of aluminium particle is slightly higher than the respective wt% of 5 and 15 respectively. This excess quantity may be due to the contribution of aluminium present in the glass fiber. The result is at par with Figure 4.14 and Figure 4.16 based on the quantity of aluminium powder added during fabrication rather it quantitatively validates the fabrication process. Figure 4.23 and Table 4.5 show the EDS analysis for unfilled glass epoxy composites at 72 m distance run. Elements present on the surface clearly indicate the erosion of steel ball which in turn agree with the result as shown in Figure 4.17.

5. FRICTION AND WEAR IN SLIDING CONTACT

5.1 Introduction

This chapter presents the friction and wear results of glass epoxy, aluminium epoxy and aluminium powder filled glass epoxy composites, sliding against a stainless steel counterface, EN31 in dry and normal atmospheric condition. Friction and wear results are reported in different conditions of speed, load and time. The ranges of speed and load are selected as 1-5 m/s and 10- 40 N respectively whereas sliding distance is maintained between 300-3600 m, corresponding to sliding time of 5-40 minutes. The glass fiber orientation has been maintained perpendicular to the sliding direction. The surface morphology of the composites are studied using a scanning electron microscope (SEM) and elemental composition is characterized by EDX analysis.

5.2 Glass fiber reinforced epoxy composites

The sliding friction and wear of glass epoxy composites with varying wt% of glass fiber reinforcement has been studied under sliding speed of 1-4 m/s and normal load of 10-40 N and for a fixed sliding duration of 10 (ten) minutes. The friction and wear results are presented with respect to sliding speed and normal load. The effect of glass fiber reinforcement has been compared with respect to neat epoxy.

5.2.1 Effect of sliding time and fiber reinforcement on friction behavior

The variation of friction coefficient with respect to sliding time of neat epoxy and glass epoxy composites for a fixed combination of speed and load has been shown in Figure 5.1. The frictional force is captured in every second during the experiment and these values are divided by the normal load to get coefficient of friction value. All the materials show similar frictional behavior. The friction coef-
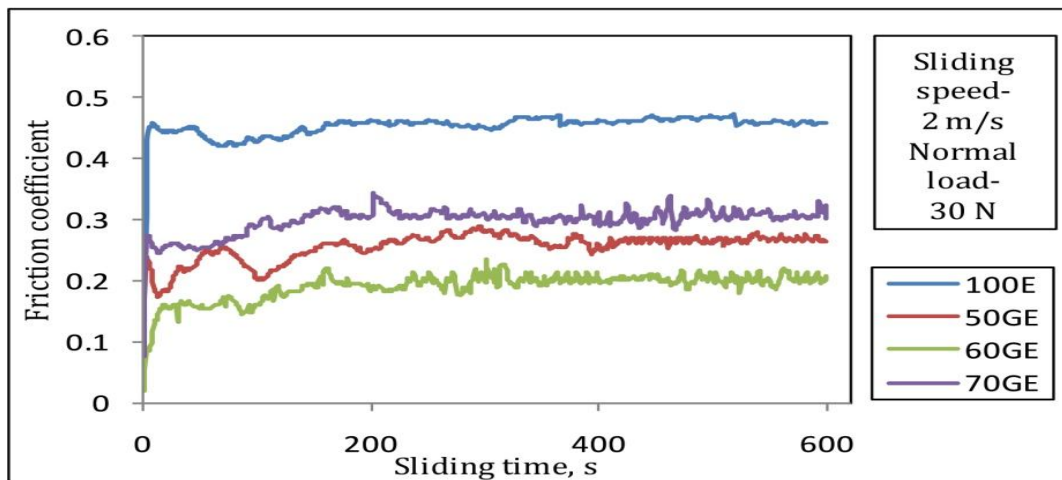

Figure 5.1 Friction coefficient as a function of sliding time of 100E, 50GE, 60GE, and 70GE composites at a fixed sliding speed of 2 m/s and normal load of 30 N

ficient is unstable at the start of sliding (running-in) and then reaches a steady state after a sliding time of approximately 3 (three) minutes. This behavior is common in both neat epoxy and glass epoxy composites irrespective to the fiber reinforcement, since there is a high shear force in the contact zone in the first

stage of the adoption process between the asperities in contact. After this stage, a steady state friction coefficient is achieved if there is no change in the contacted surfaces. For the stability of the friction coefficient, similar findings are reported in studies of carbon-epoxy by Zhou et al. (2009); glass or a carbon-aramid hybrid weave-epoxy and three-dimensional braided carbon fiber epoxy by Wan et al. (2006). The instability of the friction coefficient of glass epoxy composites is mainly due to the modifications that occur on the track surface of the counterface (Yousif, 2013). After the running in period, formation of thin lubricating film at the contact surface helps to maintain the friction coefficient steady for the rest of the experimental time.

In Figure 5.1, it is also observed that among the materials, neat epoxy shows the maximum friction coefficient and 60GE composite shows the minimum friction coefficient. The friction coefficients of 50GE and 70GE composites are in between 100E and 60GE. In between 50GE and 70GE. The latter bears the higher value with lot of fluctuations. Neat epoxy, 100E shows the highest friction coefficient because of the presence of adhesion at the contact surfaces owing to the easy plastic deformation of epoxy. Among the glass epoxy composites, 70GE records the highest friction coefficient, this is because of higher fiber concentration at the contact surface. This behavior is similar to that reported by Bahadur and Zheng (1990) where it is concluded that friction of the composite material seems to be governed by its shear strength which influences the rupture of adhesive bonds at the interface. The likelihood of fiber-glass disrupting the transfer film, as exhibited during the test by large cyclic fluctuations in friction force, could also account for increased friction with the higher proportions of glass fiber. Among 50GE and 60GE, composite 50GE shows higher friction than 60GE, it may be due to higher adhesion at the contact surfaces for lesser fiber concentration. The friction coefficient of 60GE is less and stable among the materials because of the balanced proportion of reinforcement and matrix.

5.2.2 Effect of speed, load and fiber reinforcement on friction behavior

The influence of the sliding speed and normal load on the friction coefficient of neat epoxy and glass epoxy composites is shown in Figure 5.2. The average value of the friction coefficient for a sliding duration of 10 (ten) minutes is presented for a fixed combination of normal load and sliding speed of 20 N and 2 m/s. The variation of friction coefficient with respect to sliding speed at a fixed normal load of 20 N is presented in Figure 5.2 (a). The general trend of friction of the materials is to increase with increase of sliding speed. With the increase in sliding speed, more heat is generated at the contact surface resulting in higher adhesion with disc. Also increase in sliding speed may lead to an increase in inter-
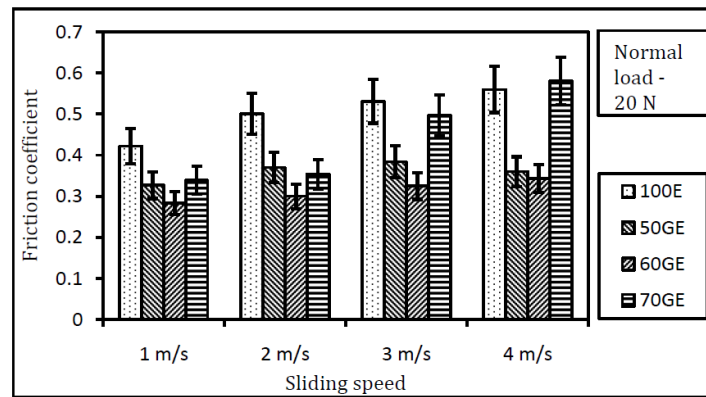
(a)
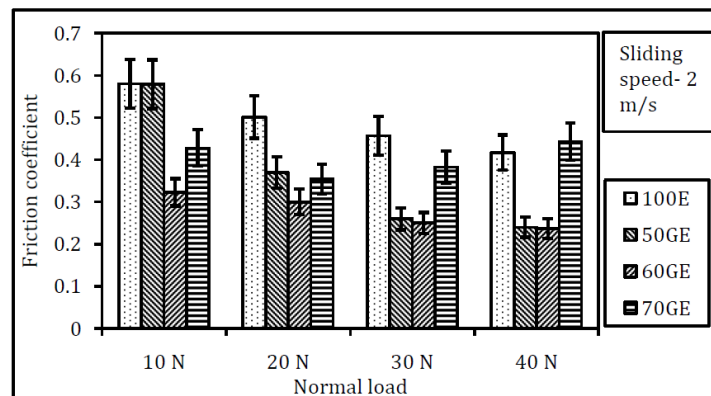
(b)

Figure 5.2 Friction data of 100E, 50GE, 60GE, and 70GE samples with respect to (a) sliding speed of 1-4 m/s at a normal load of 20 N, (b) normal load of 10-40 N at a sliding speed of 2 m/s

face temperature due to reduced cooling time per revolution of the disc resulting in subsequent increase in adhesion of composite surface with the disc (Nuruzzaman et al., 2012; Mimaroglu et al., 2007)

In Figure 5.2 (a), it is also observed that among the neat epoxy and composites, 60GE composite bears the lowest friction at all the speed range (1-4 m/s) under the fixed normal load of 20 N. It may be attributed as the presence of balanced proportion of reinforcement and matrix in 60GE composite. The friction coefficient of 100E and 50GE is higher may be because of the increased adhesion acting between the contact surfaces. 70GE composite holds the higher friction because of the higher concentration of glass fibers at the contact surface leading to higher frictional trust.

Variation of friction coefficient with normal load (10– 40 N) for all the samples at a sliding speed of 2 m/s is shown in Figure 5.2 (b). It is seen that friction coefficient decreases with increase of normal load for all the samples. Increase in normal load leads to an increase in temperature at the contact interface, which in turn, causes thermal degradation of polymer since polymers become soft with rise in temperature. This results in weaker adhesive bonding and formation of thin transfer film and smooth shearing of epoxy or fiber. As a result, decreasing trend of friction coefficient is observed with the increase of normal load for 100E, 50GE, 60GE samples. Friction coefficient of 70GE composite first to decrease with increase of load from 10- 20 N but further increase of load, friction increases reporting a mismatch from the frictional behavior of other samples.

In Figure 5.2 (b), it is also observed that for a fixed sliding speed and for all normal load conditions considered, friction coefficient for neat epoxy (100E) and 50GE, 70GE composites is higher than the 60 wt% glass fiber reinforced epoxy composite. The possible reason of this has already been provided. It is here, important to note that for reduction of friction, the amount glass fiber reinforcement needs to be maintained accurately.

5.2.3 Effect of speed, load and fiber reinforcement on wear behavior

Wear variation with respect to sliding speed at a fixed normal load of 20 N for neat epoxy and 50, 60, and 70 wt% glass fiber reinforced epoxy composites is shown in Figure 5.3 (a) whereas Figure 5.3 (b) shows the wear variation with re-
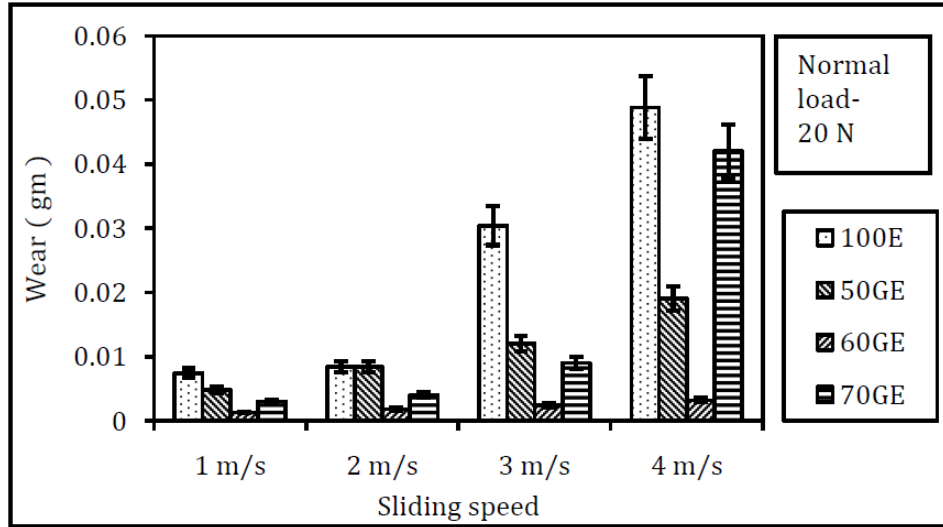
(a)
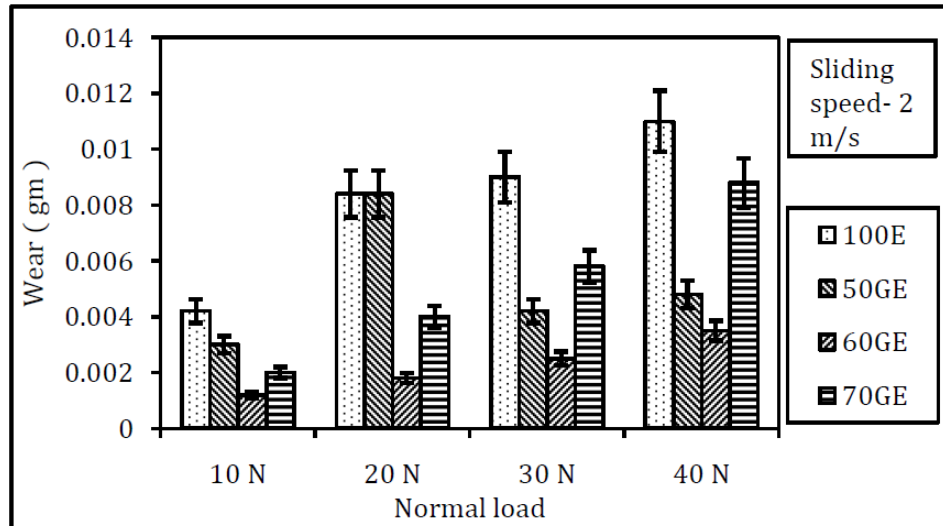
(b)

Figure 5.3 Wear data of 100E, 50GE, 60GE, and 70GE samples with respect to (a) sliding speed of 1-4 m/s at a normal load of 20 N, (b) normal load of 10-40 N at a sliding speed of 2 m/s

spect to normal load at a fixed sliding speed of 2 m/s for neat epoxy and 50, 60, and 70 wt% glass fiber reinforced epoxy composites. In both the Figures, it is seen that wear increases with increase of sliding speed and normal load for all combination of load and speed for all the materials. In glass epoxy composite, during sliding, both normal and tangential loads are transmitted through the asperity contact points by adhesive and ploughing actions. The soft asperities are easily deformed and sheared under repeated loading action. Simultaneously, hard counter face asperities or the presence of any hard particles between the sliding surfaces change the surface characteristics. Both adhesive and ploughing actions cause ploughing and micro-cut the soft surface, resulting in frictional thrust and it increases with the increase of sliding speed and normal load and ultimately increase the wear. The wear increases with increasing sliding velocity and the same has been reported by others (Voss and Friedrich, 1987; Lhymn and Light, 1987) as well.

In Figure 5.3, it is also observed that among the materials, wear of 60GE composite is the lowest than the other materials. Neat epoxy reports the maximum wear with respect to speed and load at any combination. With the addition of 50 wt% of glass fiber to the epoxy, the wear reduces. This result is similar to that observed by Voss and Friedrich (1985) for polyethersulfone reinforced with glass fibers. The wear increases with increasing glass fiber content with the values in excess of 60 wt%, for all sliding speeds and loads. The lowest wear is found for 60 wt% of fiber glass. Such a minimum in wear with fiber proportion has been reported for other composites as well (Friedrich, 1986; Voss and Friedrich, 1985; 1987). The variation of wear with glass fiber proportion is similar to that of the coefficient of friction (Figure 5.2) already discussed. For fiber proportions lower or higher than the optimum wt% is responsible for increased wear. Hence, 60 wt% fiber reinforcement is reported as optimum reinforcement for better friction and wear performance.

5.3 Aluminium particulate epoxy composites

The sliding friction and wear of aluminium epoxy composites with various wt% of aluminium concentration has been studied. The results of friction and wear are presented with respect to sliding speed (1-4 m/s) and normal load (10-40 N) at a fixed combination of load and speed of 20 N and 2 m/s. The effect of aluminium concentration has been compared in reference to neat epoxy.

5.3.1 Effect of speed, load and aluminium powder on friction behavior

Figure 5.4 presents the variation of friction coefficient with respect to sliding speed (1-4 m/s) and normal load (10-40 N) for neat epoxy and aluminium particulate epoxy composites. At a fixed normal load of 20 N, variation of friction coefficient with respect to sliding speed of 1-4 m/s is shown in Figure 5.4 (a) whereas Figure 5.4 (b) presents the variation with respect to normal load of 10-40 N at a fixed sliding speed of 2 m/s. In Figure 5.4 (a), the general trend of friction for neat epoxy (100E) and upto 10 wt% aluminium epoxy composites is that it increases with the speed because of the much enhanced adhesion in between sample and disc counterface. For 15AlE composite, trend is just reverse, i.e it decreases with the increase of sliding speed. It is also observed that among 100E, 5AlE, 10AlE and 15AlE materials at all the sliding speeds, neat epoxy (100E) shows the highest frictional value and 10AlE and 15AlE record the lowest value for lower (1-2 m/s) and higher (3-4 m/s) sliding speeds respectively. This behavior of the composites is because of the addition of aluminium powder which increases the thermal conductivity and effects the material stiffness (Vasconcelos et al., 2006).

In Figure 5.4 (b), the trend of friction coefficient for 100E, 5AlE, and 10AlE composites is that it decreases with increase of normal load. Increase in normal load leads to an increase in temperature at the contact interface, which in turn, causes thermal degradation of matrix since epoxy becomes soft with rise in temp-
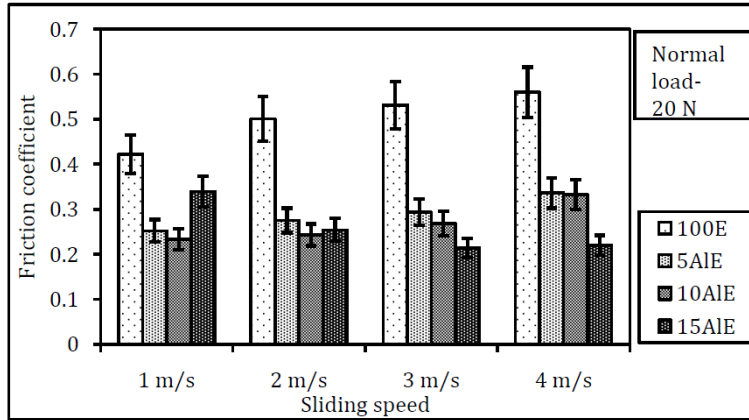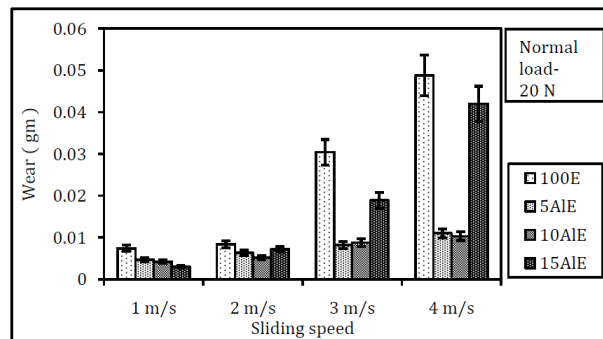
(a)
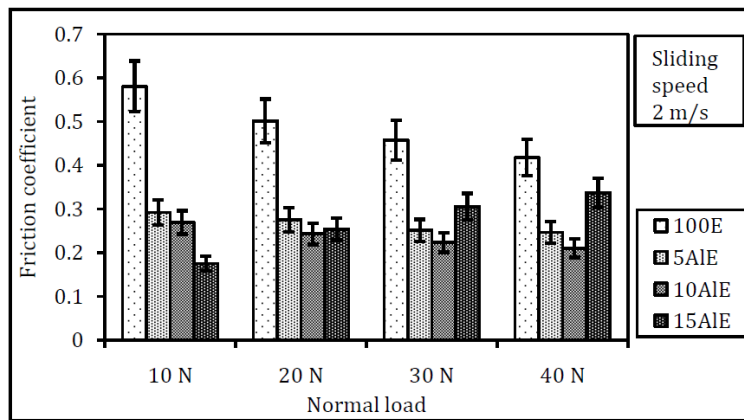
(b)

Figure 5.4 Friction data of 100E, 5AlE, 10AlE, and 15AlE samples with respect to (a) sliding speed of 1-4 m/s at a normal load of 20 N, (b) normal load of 10-40 N at a sliding speed of 2 m/s

erature. This results in weaker adhesive bonding between aluminium particles and epoxy matrix yielding in formation of thin film transfer and smooth shearing of filler. As a result friction reduces at higher normal load. For 15AlE, the reverse trend of friction is observed, i.e friction increases with increase of normal load. This is because of the presence of protruded out aluminium/oxide particles at the contact surfaces. It is also observed that friction coefficient for 10AlE is the lowest for 20- 40 N normal load conditions. The decrease of friction coefficient with respect to normal load is also very marginal. This may be due to the balanced proportion of aluminium particles in epoxy system leading to improved material stiffness and thermal conductivity.

5.3.2 Effect of speed, load and aluminium powder on wear behavior

Wear variation with respect to sliding speed (1-4 m/s) and normal load (10-40 N) of neat epoxy and aluminium epoxy composites is shown in Figure 5.5. Figure 5.5 (a) presents the wear variation with sliding speed at a constant normal load of 20 N. The wear trend of all the materials is that it increases with increase of sliding speed. This is because of the increase in axial trust with the increase of sliding speed. It is also observed that among the materials, 100E shows the highest wear at all the sliding speeds. Wear performance of 5AlE and 10AlE composites is better for 2-4 m/s speed conditions whereas 15AlE performs better at 1 m/s sliding speed than other materials.

Figure 5.5 (b) presents the wear variation with respect to normal load (10-40 N) at a fixed sliding speed of 2 m/s. The trend of wear of all the materials is that it

(a)
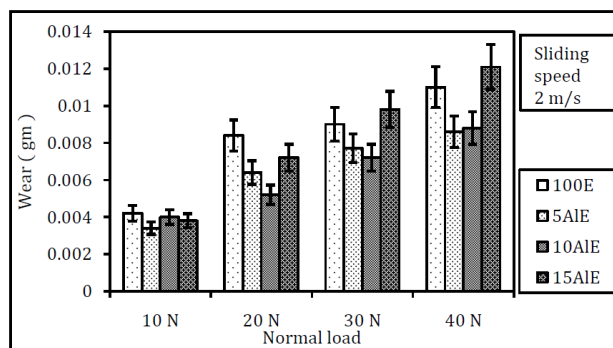
(b)

Figure 5.5 Wear data of 100E, 5AlE, 10AlE, and 15AlE composite samples with respect to (a) sliding speed of 1-4 m/s at a normal load of 20 N, (b) normal load of 10-40 N at a sliding speed of 2 m/s

increases with increase of normal load. This is because of the increase of axial trust with increase of normal load. It is also observed that the wear of the materials at each normal load is different. Lowest wear is recorded by 5AlE corresponding to 10 and 40 N loads. 10AlE records lowest at 20 and 30 N loads. Wear of 15AlE is highest at higher loads (30 and 40 N).

5.4 Aluminium powder filled glass epoxy composites

Friction and wear characteristics of glass epoxy and aluminium powder filled glass epoxy composites are presented with respect to sliding speed (1-5 m/s), normal load (10-40 N) and sliding distances (300-3600 m) at different combinations of load and speed. Glass fiber reinforcement is maintained fixed at 60 wt% and only aluminium powder concentration in glass epoxy system is varied from 0- 15 wt%.

5.4.1 Effect of speed, load and aluminium powder on friction behavior

Friction coefficient for glass epoxy composite (GE) and aluminium particulate glass epoxy composites (5AlGE, 10AlGE, and 15AlGE) for varying sliding speeds and normal loads are presented in Figure 5.6. The variation of friction coefficient with sliding speed for all four composite samples at a fixed normal load of 20 N is shown in Figure 5.6 (a). The general trend of variation of friction for samples GE, 5AlGE, and 10AlGE is that friction increases with increase in sliding speed whereas friction coefficient for 15AlGE sample decreases with increase in sliding speed. With the increase in sliding speed, more heat is generated at the contact surface resulting in more or increased adhesion with disc. Also increase in sliding speed may lead to an increase in interface temperature due to reduced cooling time per revolution of the disc resulting in subsequent increase in adhesion of composite surface with the disc (Nuruzzaman et al., 2012; Mimaroglu et al., 2007; Bhushan, 2013). Hence friction increases with sliding speed for GE, 5AlGE, and

10AlGE samples. For the sample 15AlGE, the general trend is just reverse; here friction coefficient decreases with increase in sliding speed. For this higher wt% of aluminium concentration, temperature at the sliding interface increases with increase in sliding speed causing thermal penetration to occur which results in weakness in the bonds at the interfaces between fiber, matrix and particles (Vishwanath et al., 1993). Consequently, the fibers/particles or both become loose in the matrix and help in sliding to continue at ease. As a result, friction coefficient decreases. In Figure 5.6 (a), it is also observed that at low range of sliding speeds (1–3 m/s), friction coefficient is reduced for 5AlGE compared to GE samples implying that incorporation aluminium particles reduces friction. However for higher concentration of aluminium particle incorporation, friction increases. It is clearly observed that friction for 10AlGE composite samples is higher than 5AlGE sample and for 15AlGE sample it is even higher. This may be
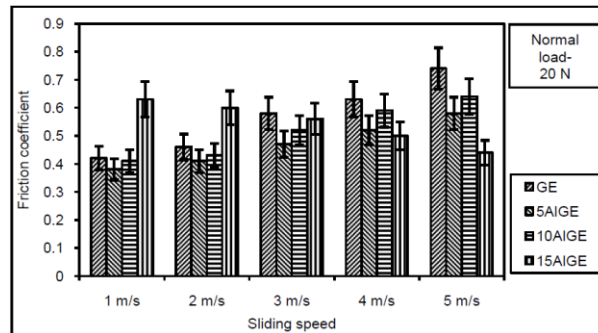
(a)
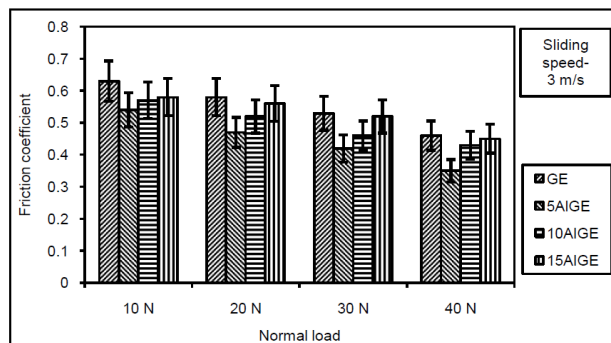
(b)

Figure 5.6 Friction data of GE, 5AlGE, 10AlGE, and 15AlGE samples with respect to (a) sliding speed of 1-5 m/s at a normal load of 20 N, (b) normal load of 10-40 N at a sliding speed of 3 m/s

attributed to poor heat conductivity of GE samples. At a particular speed and load condition, for GE samples, heat generated at the contact interface is mostly used to soften the epoxy matrix, resulting in more or increased adhesion with disc leading to high frictional value. With incorporation of aluminium particles, as in case of 5AlGE samples, heat conductivity of the resulting composite increases. This essentially helps in conducting away the heat from the contact interface and results in reduced adhesion with the counterface disc. This in turn yields low friction coefficient. This trend continues for higher aluminium concentration as well (10AlGE and 15AlGE samples) at low range of sliding speeds. But at higher sliding speeds (4–5 m/s), friction coefficient decreases initially for incorporation of aluminium particles (as in case of 5AlGE and 10AlGE samples), but with higher concentration of aluminium (as in case of 15AlGE samples) friction reduces due to weakening of the bonds at the interfaces between fiber, matrix and particles leading to reduced resistance to sliding. Variation of friction coefficient with normal load (10–40 N) for all the composite samples at a sliding speed of 3 m/s is shown in Figure 5.6 (b). It is seen that friction coefficient decreases with increase of normal load for all the samples. Increase in normal load leads to an increase in temperature at the contact interface, which in turn, causes thermal degradation of polymer since polymers become soft with rise in temperature. This results in weaker adhesive bonding between fibers/fillers and polymers yielding in formation of thin film transfer and smooth shearing of fiber or filler. As a result friction reduces at higher normal load.

In Figure 5.6 (b), it is also observed that for a fixed sliding speed and for all normal load conditions considered, friction coefficient for glass epoxy (GE) composite is higher than the aluminium particulate (5, 10 and 15 wt%) glass epoxy composites. Composite 5AlGE shows the minimum friction coefficient and it increases with higher concentration of aluminium particles (as in 10AlGE and 15AlGE composites). In fact at higher loads (30–40 N), friction coefficient for

15AlGE composite becomes comparable to GE composite. The probable explanation for this has already been provided. It is here important to note that for reduction of friction, aluminium particles may be incorporated in the composite but higher concentration of aluminium will spoil the purpose. Accordingly, the amount of aluminium particles to be incorporated needs to be controlled accurately.

5.4.2 Effect of sliding distance on friction behavior

The variation of friction coefficient with sliding distance for glass epoxy and aluminium particulate glass epoxy composites (category D) at a constant sliding speed of 1 m/s and normal load of 30N is shown in Figure 5.7 and Table 5.1. The general trend of friction coefficient of all the samples is unstable at the initial stage and it tends to be stable after a certain sliding distances. During the transient period, a number of phenomena occur, such as changes in topography of composite sliding surface and counter surface in contact, rise in interface temperature due to the dissipation of energy in sliding, and development of
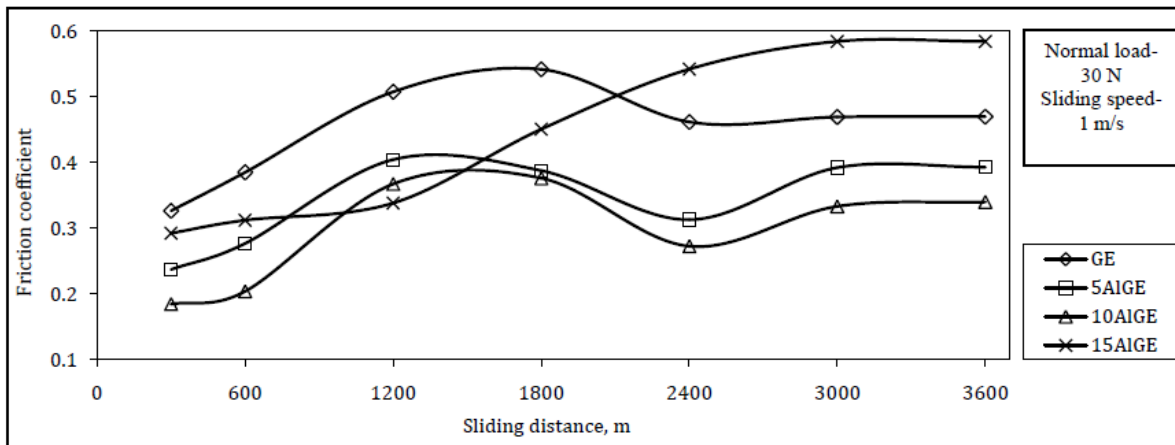

Figure 5.7 Friction coefficient as function of sliding distance for different glass epoxy composites at a constant load and speed of 30 N and I m/s.

polymer transfer film on the steel disc surface which ultimately leads for the constant friction coefficient. The overall as well as friction value at each distance run of GE composite is higher than aluminium filled, 5AlGE and 10AlGE

composites. 10AlGE composite with lowest experimental value maintains almost similar nature with 5AlGE composite. Curve for GE sample starts with a friction value of 0.3265 at 300 m sliding and goes on increasing upto its maximum value of 0.5418 at 1800 m distance. Friction coefficient then decreases from 0.5418 to 0.4618 du ring the sliding from 1800 m to next 600 m, leading to stable friction coefficient from about 2400 m for the rest of the experimental distance. This may

Table 5.1 Friction coefficient of composites at different sliding distances

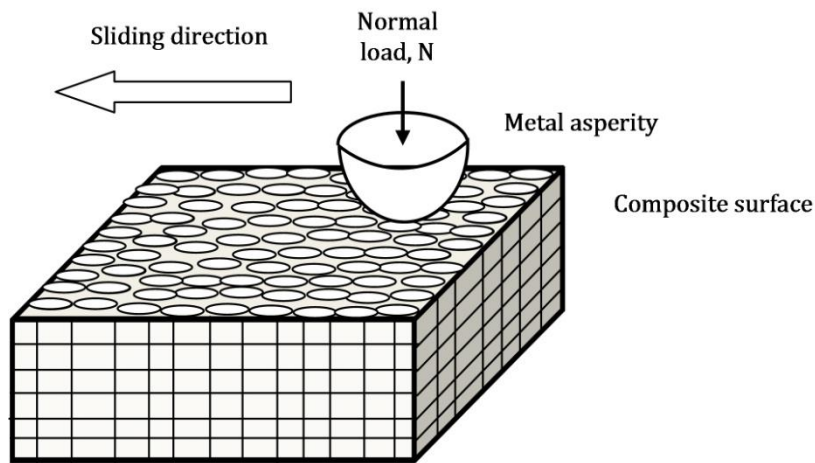| Sliding distance, m	Friction coefficient			
	GE	5AlGE	10AlGE	15AlGE
300	0.3265	0.2371	0.1843	0.2922
600	0.3849	0.2768	0.204	0.3121
1200	0.5075	0.4043	0.3673	0.3383
1800	0.5418	0.3877	0.376	0.4507
2400	0.4618	0.313	0.2723	0.54212
3000	0.4692	0.3921	0.3333	0.58432
3600	0.4698	0.3928	0.34	0.58436

Figure 5.8 Tribological system with metal asperity vs composite with woven fiber orientation

be explained with the help of Figure 5.8. EN 31 steel disc (hardness, nearly 600 HV) is used as counter part material. As the hard disc asperities come in contact with the glass epoxy composite surface, the comparatively soft epoxy matrix due

to repeated action of shear force breaks easily prior to the breakage of vertical/horizontal fibers (Friedrich and Reinicke, 1998). Due to this feature, roughness of the sample surface increases than the initial roughness leading to the increase of friction coefficient to maximum value of 0.5418. At this distance of sliding, contact is mainly in between the fibers and the disc asperities. Due to repeated loading, the asperity of the steel disc breaks to the powdery particles of metal elements and fibers to glass particles resulting in the erosion of disc and smoothing of sample contact surface, and this causes decrease of friction coefficient. Wear debris containing particles of epoxy matrix, metal elements, and the pulverized glass is thus formed which may remain at the contact zone, or may be displaced fully or partially from the contact zone. In general prior to the thermal softening of epoxy matrix as well as formation of lubricating film, debris particles are expected to be away from the contact zone due to the centrifugal action. The friction behavior precisely depends on the type of wear particles remain at the real contact zone. With further increase of distance, temperature at the contact surface increases due to heat generation which softens the matrix and ultimate formation of a thin film helps to maintain stable friction for the rest of the experimental distance.

As filler material, aluminium powder addition to the glass epoxy system improves material stiffness and thermal conductivity which increases with the increase of aluminium quantity and particle size (Zhou, 2011). The better thermal conductivity contributes to a more efficient dissipation of heat generated on the contact area. Also aluminium has high oxygen index, easily reacts with the oxygen to form oxides in normal atmospheric condition. Increase of aluminium concentration in composites, thermal conductivity and the possibility of oxide formation at the outer surfaces increases but more than optimum use of aluminium reduces the material stiffness. For 5AlGE sample, at starting, friction coefficient is 0.2271 and it increases to 0.4043 at 1200 m and gradually goes

down to 0.313 at 2400 m of sliding. From 2400 to 3000 m of sliding distance, friction coefficient further increases to 0.3921 at 3000 m and maintains this stable friction value for the rest experimental period. For 5AlGE composite, at the beginning of the sliding motion, the sample surface consists of glass fiber, epoxy matrix and aluminium with its less amount of oxide particles which are in contact with the disc counter surface. As the motion starts, shear forces are applied, less amount of oxide and matrix get deformed, aluminium particles do not protrude out for high stiffness of the composite resulting from better interfacial bonding of the constituents. This causes reduce friction coefficient at starting. But the roughness of the surface increases latter due to the exposed aluminium particle and fiber. This leads to the increase of friction coefficient to 0.4043 corresponding to the sliding distance of 1200 m. On subsequent sliding, the surface of the specimen and disc get smoothened and reduces the friction coefficient from 0.4043 to 0.313 at sliding distance of 2400 m. At this distance, heat generated at the contact area softens the matrix and results more adhesion in between smooth and soft sample surface and the disc counter face. This causes further increase of friction coefficient from 0.313 to 0.3921 at 3000 m of sliding distance and ultimately formation of thin lubricating film at the contact surface keeps the friction coefficient all most constant for the rest experimental distance. For 10AlGE sample, more oxide particles are formed at the test surface and when this soft brittle sub layer comes on contact with the hard disc asperities breaks easily as a result of which at 300 m of sliding friction coefficient starts with a lower value of 0.1843, on further increase of sliding distance by 300 m friction coefficient slowly increases to 0.204.This may be the reason as gradual shifting of contact to the actual composite surface. Sliding distance from 600 to 1800 m friction coefficient increases from 0.204 to 0.3673, the peak value for 10AlGE sample, the reason is same as explained for 5AlGE composite. The peak frictional value for 10AlGE is achieved at higher sliding distance than 5AlGE sample may be

because of prior oxidization effect and higher heat conductivity of 10AlGE sample. For rest of the sliding distances 10AlGE composite sample follows the similar curve and reason of which is same as explained for 5AlGE composite. For 15AlGE composite sample, friction coefficient starts with a value of about 0.2922 and slowly increases to 0.3383 corresponding to the sliding distance of 1200 m. It further increases from 0.3383 to 0.5843 with the corresponding distance of 1200
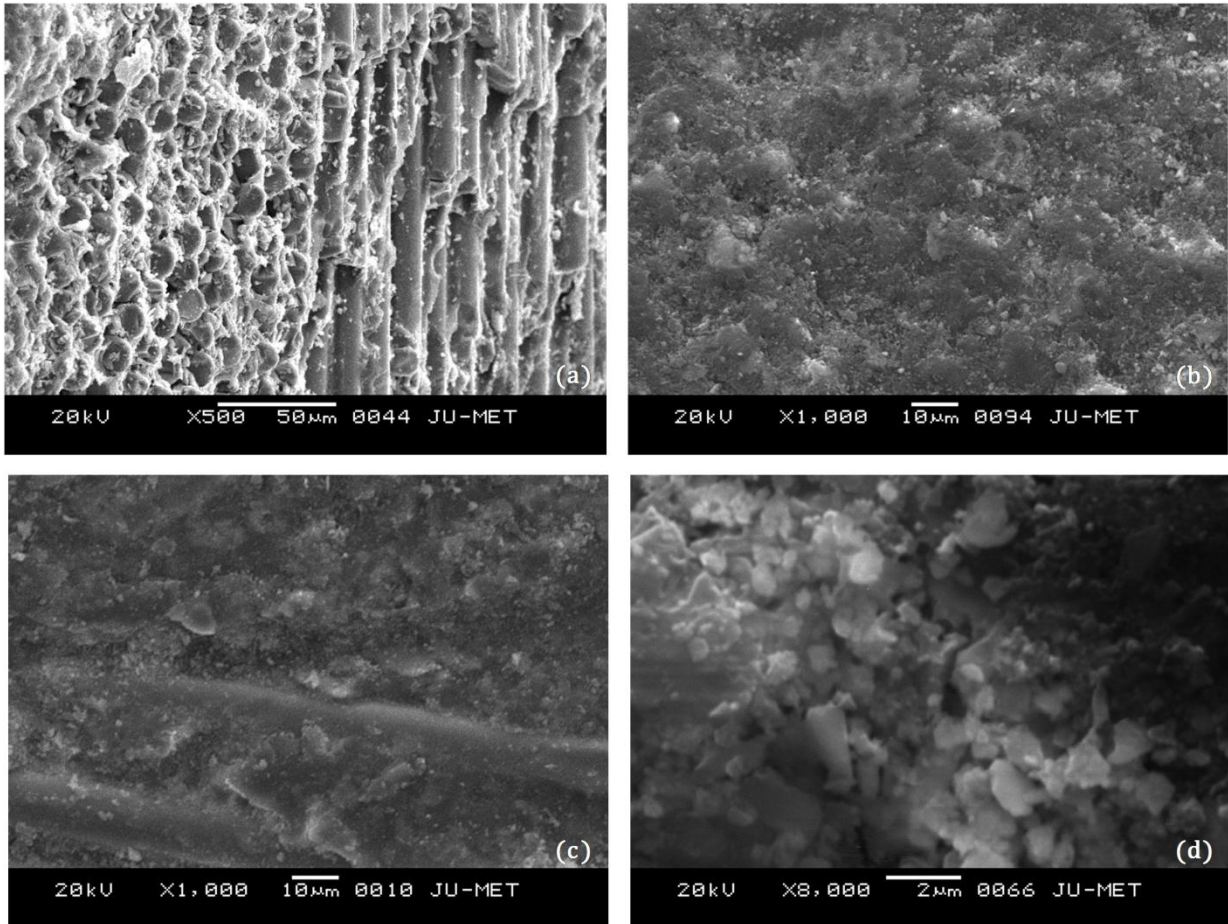
Figure 5.9 SEM micrograph for 300 m distance run showing the surface roughness at normal load 30 N, sliding speed 1 m/s for the samples (a) GE, (b) 5AlGE, (c) 10AlGE, and (d) 15AlGE.

m to 3000 m respectively and on further increase of sliding distance friction coefficient remains steady. At the contact surface, 15AlGE composite sample contains highest exposed aluminium particles most of these particles are very negligible area of contact for the possible agglomeration. At normal atmospheric condition, particles almost converted to aluminium oxide particles which are

hard than the aluminium particles. These hard oxide particles when come in contact with the disc makes the friction coefficient high than the other aluminium particulate samples. From 300 m to 1200 m distance, friction coefficient slowly increases because of the breakage of superficial oxide layer and subsequently shifting of contact to actual composite layer. The increase of friction coefficient for the corresponding distance from 1200 to 3000 m may be attributed to the easy pull out of aluminium particles from the composite and possible formation of much harder oxide particles and its presence along with the glass particles at the contact zone. Further increase of the sliding distance, contact surface temperature increases leading to thin film formation at the contact surface resulting in constant friction.

It is also observed that at the initial stage of sliding i.e at a distance of 300 m run, different composite samples report different friction value with out maintaining any particular trend. Friction coefficient decreases than GE sample with the addition of aluminium powder (0-10 wt%) but for 15AlGE composite, its starts with a value of 0.2922 in between GE and 5AlGE composites. Prior oxidization of aluminium particulate sample surface may be the possible reason for this behavior which may be best explained with the SEM micrographs as shown in Figure 5.9. Figure 5.9 (a) represents the GE sample surface which is free from oxidization effect. Matrix as soft part at the contact zone starts to remove increasing the surface roughness than the initial sample surface. Figure 5.9 (b) is for 5AlGE sample, less oxidization effect results the exposure of hard aluminium particles attached within the matrix. At this stage of sliding, surface roughness is seen Figure 5.9 (b) than Figure 5.9 (a). Prior surface oxidization effect is clearly observed in Figure 5.9 (c) for 10AlGE sample. Contact is still in between porous and brittle oxide layer and disc. In Figure 5.9 (d) prior oxidization effect is much more prominent. Only a part of the artificial layer is removed. Hard aluminium oxide particles are clearly seen leading to the increase friction value at starting

than 5AlGE and 10AlGE samples. It can also be noted that prior oxidization effect persists depending on the artificial layer thickness which in turn is a factor of aluminium concentration in composites. Frictional results show that sample GE has no oxidization effect whereas composite 15AlGE has the maximum effect upto 1200 m distance run. Samples 5AlGE and 10AlGE has the similar effect for 300 and 600 m distance run respectively.

5.4.3 Effect of speed, load and aluminium powder on wear behavior

Wear process of particulate fiber epoxy composites under dry sliding condition is dominated by four wear mechanisms, viz., matrix wear, fiber/particle sliding wear, fiber fracture and fiber/particle matrix interfacial debonding. The matrix wear occurs due to plastic deformation; fiber sliding wear occurs due to fiber rubbing; fiber fractures occurs due to fiber rupture, fiber cracking, and fiber pulverizing while fiber/particle matrix debonding occurs due to the initiation of micro level cracks and its subsequent propagation around the particle. Wear performance of glass epoxy composite is primarily determined by the properties of glass fiber and its orientation relative to the sliding direction whereas for aluminium particulate glass epoxy composites, apart from the fiber and its orientation, particle properties and its quantity to the composite system has a significant effect in controlling wear characteristics.

Variation of wear with sliding speed (1–5 m/s) at a fixed normal load of 20 N is shown in Figure 5.10 (a). It shows that wear increases with increase in sliding speed at for all composite samples. During sliding, both normal and tangential loads are transmitted through the asperity contact points by adhesive and ploughing actions. The soft asperities are easily deformed and sheared under re-
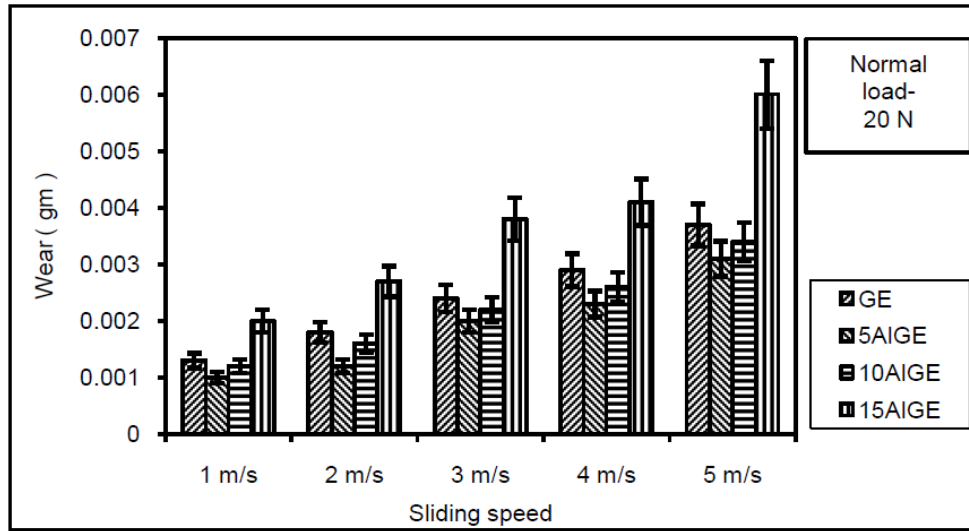
(a)
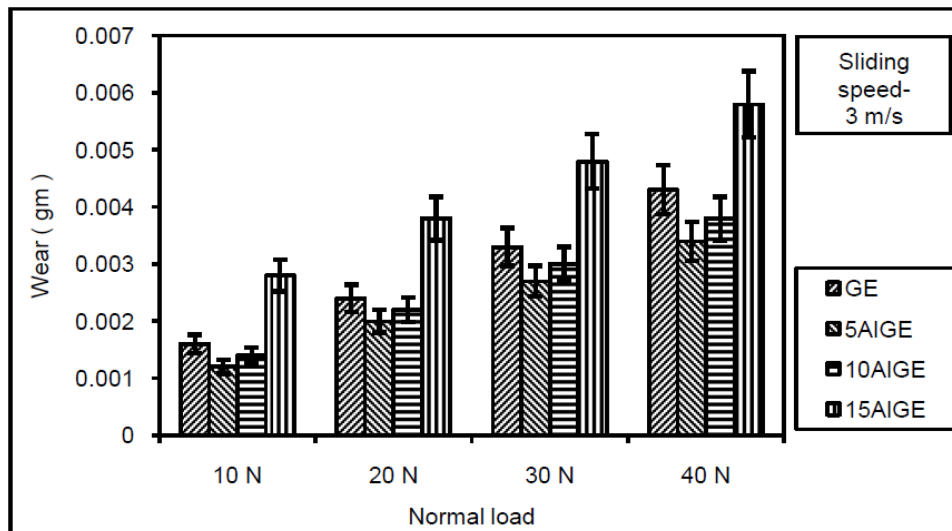
(b)

Figure 5.10 Wear data of GE, 5AlGE, 10AlGE, and 15AlGE composite samples with respect to (a) sliding speed of 1-5 m/s at a normal load of 20 N, (b) normal load of 10-40 N at a sliding speed of 3 m/s

peated loading action. Simultaneously, hard counter face asperities or thepresence of any hard particles between the sliding surfaces plough and micro-cut the soft surface resulting in the change of surface characteristics. Both adhesive and ploughing actions cause frictional thrust. The glass fibers present in the matrix resin on exposure to the counter surface break because of the frictional thrust. With increasing sliding speed, it has already been observed that

the magnitude of the frictional thrust increases and this results in increase in wear of the composites. Moreover, the temperature at the contact surface increases owing to the frictional dissipation during the sliding action. The interface temperature is further increased with the increase of sliding speed mainly due to the reduction in cooling time per revolution of the disc. Woven roving glass epoxy composite (GE) is a poor thermal conductive material; as a result heat generated at the contact zone remains entrapped there and is used for thermal penetration and results in softening of the matrix. This weakens the bond between the reinforcing glass fibers and causes debonding of fibers. The debonded glass fibers for its brittle nature fracture owing to the repeated loading. The frictional heat, on the other hand, results in charring of the matrix resin at the contact zone. The combined effect of thermal softening and charring of epoxy matrix results in debonding of the glass fibers and loss of structural integrity of the composite (Mimaroglu et al., 2007; Suresha et al., 2006).

For aluminium particulate glass epoxy composites (5AlGE, 10AlGE, 15AlGE), contact surface of the sample contains epoxy, aluminium particles, and glass fibers. The presence of aluminium particles increases with the increase of aluminium wt% in composites. The soft matrix asperities are easily deformed and sheared under repeated loading action. Simultaneously, hard disc asperities or the presence of hard aluminium oxide particles between the sliding surfaces plough and micro-cut the soft surface resulting in the change of surface characteristics. As a result, the aluminium particles present in the matrix resin on exposure to the disc surface tends to protrude out followed by the break age of glass fibers depending on the stiffness and strength of composites. On increase of sliding speed, the magnitude of the frictional thrust increases, this results in increase in wear of the aluminium particulate glass epoxy composites. Due to incorporation of aluminium particles, heat conductivity of the composite increases. As a result, thermal penetration and subsequent softening of the matrix

is reduced leading to reduction of wear. Thus 5AlGE yields lesser wear compared to GE composites. However, with increase in aluminium concentration in the composite, these particles help in breakage of fibers and debonding of fibers from matrix as well leading to increase in wear. Hence composite 10AlGE shows higher wear compared to 5AlGE and it is further higher for 15AlGE composite.

Variation of wear with normal load (10–40 N) at a fixed sliding speed of 3 m/s is shown in Figure 5.10 (b). It is seen that wear increases with increase of normal loads for all the composites. Increase in normal load leads to an increase in temperature at the contact interface, which in turn, causes thermal degradation of polymer since polymers become soft with rise in temperature. As a result wear increases with increase in load. Also higher load leads to higher penetration of the hard asperity peaks of the counter surface into the matrix of the composite resulting in higher wear. Limited incorporation of aluminium particulate in glass epoxy composite systems increases the material stiffness and thermal conductivity. This leads to improved wear resistance With the increase of aluminium content, thermal conductivity increases but at the same time for higher content of aluminium particulate, material stiffness decreases leading to increase in wear (Suresha et al., 2006; Zhou, 2011). In case of 15AlGE composite, the amount of aluminium particles present may be high enough to form agglomeration resulting in poor interfacial bond and easy pull out of aluminium particles from the composite during sliding action. The protruded aluminium particles along with fractured glass fibers add to rapid and severe wear due to existence of a mixed abrasive and adhesive wear conditions (Archard, 1953; Friedrich, 2012).

5.4.4 Effect of sliding distance on wear behavior

Wear in respect of sliding distance for unfilled and 5, 10, and 15 wt% aluminium powder filled glass epoxy composites at a constant normal load 30 N

and sliding speed 1 m/s is shown in Figure 5.11. As in friction coefficient, wear also reaches to steady state in certain sliding distances which may be assumed as the distance run needed to build-up of transfer film on the mating steel surface, and for which, temperature is also to rise to an equilibrium state along with other effects. Prior to stable trend of wear, for both unfilled and filled composites, wear increases non linierly with the increase of sliding distance. In sliding, both normal and tangential loads are transmitted through the contact points by adhesive and ploughing actions. The soft asperities are easily deformed and sheared under the repeated loading action. Simultaneously, the hard asperities of the counterface or the hard particles between the sliding surfaces plough and micro-cut the soft surfaces. Thus both adhesive and ploughing actions cause frictional thrust. The glass fibers present in the matrix resin break on exposure to the rubbing surface,
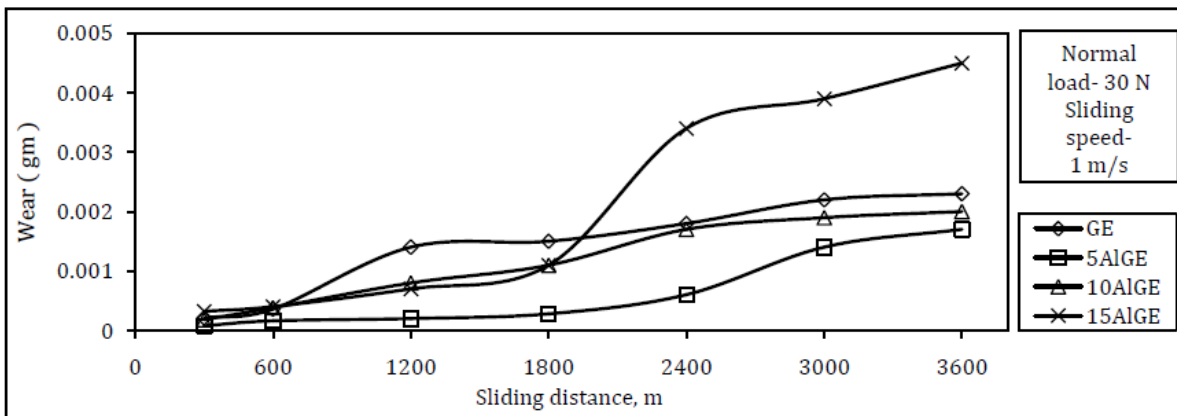
Figure 5.11 Wear vs sliding distance for glass epoxy/aluminium particulate glass epoxy composites

Owing to frictional thrust, and change the surface characteristics. This results in a non linear increase in wear of the composites. The over all wear and sliding distance run needed for the steady state condition are different for composite materials under the same test condition. To explain the relative wear at different distances, results are presented in the form of a bar diagram in Figure 5.12. From the graph and bar chart, it is observed that among the tested composites, 5AlGE exhibits the least wear at all sliding distances where as 15AlGE shows the highest

wear at 2400, 3000, and 3600 m of sliding distances. The wear for 10AlGE composite is higher than 5AlGE but it is always less than GE composite.

In unfilled or filled glass epoxy composites under dry and sliding condition, the matrix wear occurs due to plastic deformation and fiber sliding wear occurs due to fiber rubbing, fiber rupture, fiber cracking, and fiber pulverizing and particle matrix debonding occurs due to the initiation of micro level cracks and its subsequent propagation around the particle at the inter face. Usually for GE samples, the softer epoxy matrix between the much harder fibers is removed first and then cracking of the much harder fiber pieces occurs, which finally leads to
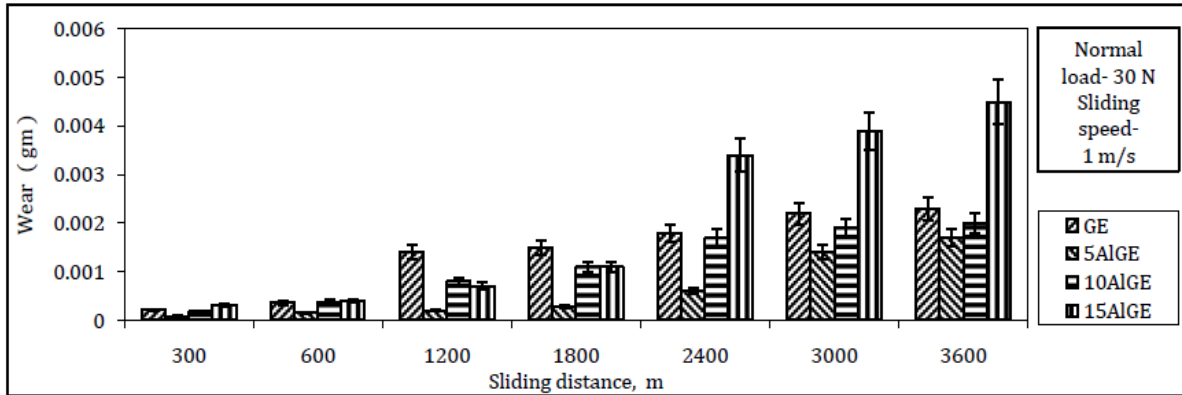
Figure 5.12 Wear data for glass epoxy and aluminium particulate glass epoxy composites at different sliding distances at a constant speed and load of 1 m/s and 30 N

the repetition of the wear cycles (Friedrich and Reinicke, 1998). In respect to fiber orientation, this particular phenomenon (El-Sayed et al., 1995) may be explained with the help of Figure 5.13. In woven glass fiber orientation, the asperities of the steel disc may come in contact in three possible ways. When fibers are oriented normal to the sliding surface and the sliding direction is normal to the warp/horizontal fibers, debonding will occur at the surface and will propagate down along the length of the weft fibers to a finite distance; the stronger the fiber the longer the resulting debonding distance but not exceeding to the next warp fibers in transverse orientation for the fibers which are above the warp fibers at interlacing relative to the sliding direction. Weft fibers which

are below the warp fibers at interlacing, debonding may propagate to the next interlacing point which leads for the higher wear loss. For weaker weft fibers, the fiber breakage occurs before debonding propagation.

When sliding direction is parallel to the warp fibers and the weft fibers are in contact with the rotating disc, the force exerted by the hard asperity tips at the interface is mostly carried by the vertical fibers if the warping fibers are below from the interface. The weft fibers debonding length is maximum upto the next warping surface. This phenomena leads to the less wear than the earlier case as more debonding length normally responsible for the higher wear. At the interlac-
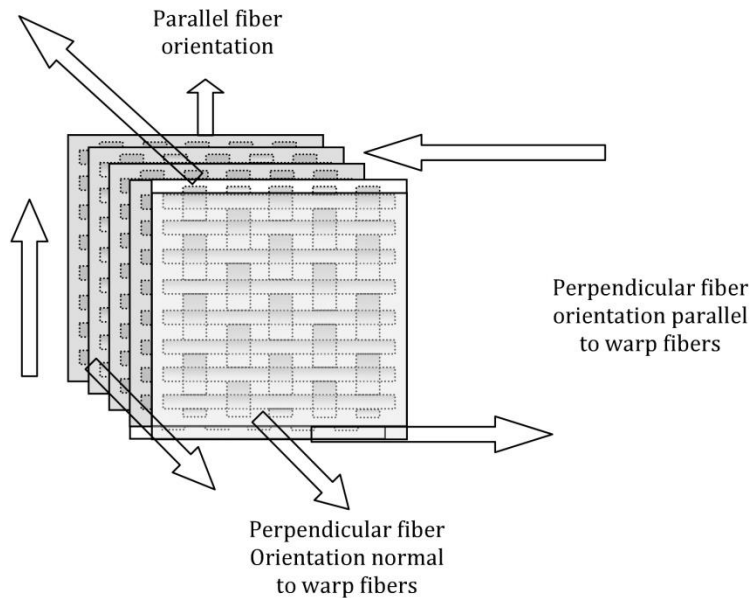
Figure 5.13 Fiber orientation of composite with respect to sliding direction

ing of vertical and parallel fiber, debonding depends on both the shear (F_s) and tensile force components (F_t). It is expected that when fiber wt fraction increases, the force carried by each fiber decreases, which means that the two components of this force decrease leading to a decrease in wear.

When fibers are oriented parallel to the sliding surface as in transverse or longitudinal orientation, initiation of the debonding occurs at the fiber resin interface at a finite depth from the surface. Initiation of cracks may also occur at surface or fiber resin interface, where the tensile stress component perpendicular

to the surface is maximum (Ward, 1970). The cracks and the debonding length of fiber will increase owing to continuous loading. By this process fiber failure resulting in freely protruding bulk parts can occur which leads to increase in wear loss. This may apply with no appreciable difference between transverse and longitudinal orientation. In any tribological situation, the temperature at the contact surface is increased owing to the dissipation of energy during the sliding action and it plays a vital role on the wear process. Woven roving glass epoxy composite is a poor thermal conductive material, as a result heat generated at the contact zone remains there and used for the thermal softening of the matrix. Glass fiber for its brittle nature breaks in powderly forms and stick with the matrix at the contact surface leading to GE sample as the second highest wear material.

As filler material, aluminium powder in glass epoxy composite increases the material stiffness and thermal conductivity. With the increase of aluminium concentration in GE composite thermal conductivity increases but material stiffness decreases for more than its optimum use. Better thermal conductivity contributes to a more efficient dissipation of heat generated at the contact area and ultimately reduces the plastic deformation of the soft matrix resulting to the reduction of matrix wear. This may be attributed as 5AlGE and 10AlGE samples, aluminium powder dispersed in the matrix covers the packets of plain weave woven glass fabric reduces the void fractions, provides the better inter facial bond strength due to increase surface area and exhibits additional strength and hardness to the composite. Increased hardness and better conductivity together ultimately lead to reduce wear loss than GE composite. In between 5AlGE and 10AlGE composites, inspite of more thermal conductivity, 10AlGE composite shows higher wear loss may be due to the decrease in hardness for more than optimum use of aluminium powder in composite.

For 15AlGE composite, the quantity of aluminium particle present high enough to form the agglomeration, resulting poor interfacial bond and easy pull out of

aluminium particle from the composite during sliding action but also easily forms the oxide layer at the test surface. For the distance from 600 to 1800 m of sliding, slow increase of wear loss is observed because of the presence of oxide layer and easy dissipation of heat from the contact surface. For 1800 m onward sliding, thermal softening of matrix starts resulting easy pull out of aluminium particles from the composite. The protruded aluminium particle converts to hard oxide particles which act as a third body along with the pulverized glass particles resulting in rapid wear after 1800 m of distance run for the rest of the experimentation time. This severe wear is due to the existence of a mixed abrasive/adhesive contact condition (Archard, 1953; Friedrich, 1986).

Wear coupled with the surface oxidization effect is highest for 15AlGE composite. Up to the sliding distance of 1800 m, wear practically is within the domain of artificial sub layer. This layer is porous and very light weight because it contains oxide and matrix particles, aluminium particles itself is light weight. Glass particles may have a very little contribution at the surface of the sample. As a result wear volume loss may be more but weight loss is not much more significant up to 1800 m sliding distance. And 1800 m onward sliding, actual sample surface comes in contact with the disc. For 10AlGE and 5AlGE samples surface oxidization effect on wear is limited to 600 m and 300 m of sliding distances respectively.

5.5 Surface morphology

5.5.1 Effect of speed, load and aluminium on surfaces of the composites

In order to observe the effect of sliding speed and normal load on the wear behavior of glass epoxy composite (GE), scanning electron microscopy (SEM) studies are conducted on the worn surfaces of the samples tested at four combination of sliding speeds and normal loads. Figure 5.14(a) shows SEM micrograph of worn surface at sliding speed of 2 m/s and normal load of 20 N.

Similarly, Figure 5.14 (b–d) show SEM micrographs for 5 m/s and 20 N; 3 m/s and 10 N; 3 m/s and 40 N respectively. Figure 5.14 (a) reveals exposed fibers, vertical fibers are out of the matrix level and most of the fibers are fractured, crack formation along the transverse direction of horizontal fibers is initiated. Wear debris particles are clearly noticed. Keeping load constant (20 N), and increasing the sliding speed to 5 m/s, i.e., for the combination of 5 m/s and 20 N, Figure 5.14 (b) shows the erosion of exposed horizontal fibers. Few horizontal fibers are seen as fragmented. The matrix erosion is more than the fibers; the fib-
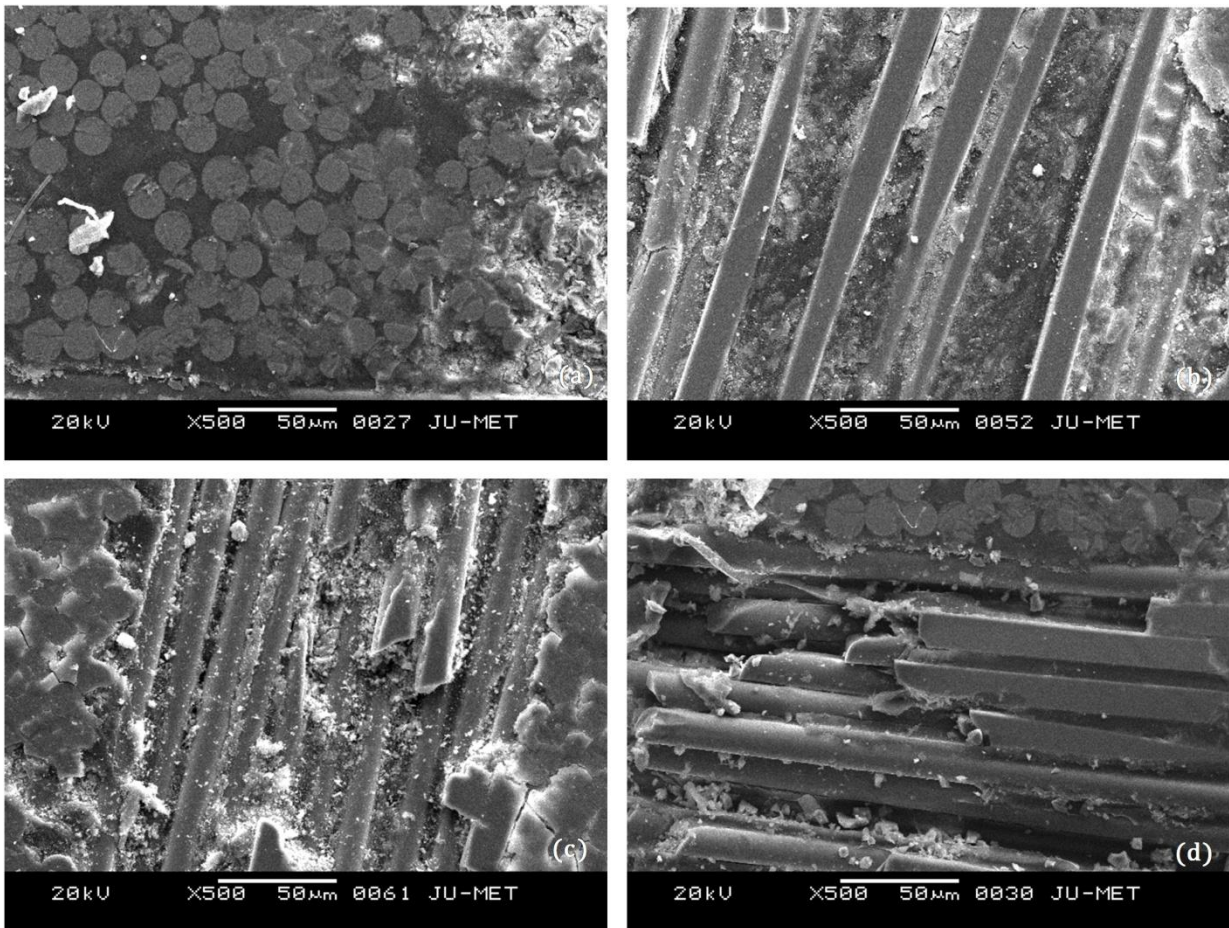

Figure 5.14 SEM micrographs of worn GE samples at varying speed and load combinations (a) 2 m/s and 20 N, (b) 5 m/s and 20 N, (c) 3 m/s and 10 N, (d) 3 m/s and 40 N

ers get out of the matrix level which signifies the existence of adhesive wear. To observe the effect of normal load, the combinations of 3 m/s with 10 N, and 3 m/s

with 40 N on GE worn surfaces are considered. Figure 5.14 (c) shows the SEM features for 3 m/s and 10 N combination. It shows fragmented horizontal fibers and well spread out of debris. In some parts, matrix is still adhered with the fibers. Keeping the sliding speed same at 3 m/s and increasing the load to 40 N yields a sample with deboned fragmented horizontal fibers. Fibers directly in contact with disc, i.e., at upper part fibers are eroded which indicates the delamination of matrix and presence of fatigue mechanism as seen in Figure 5.14 (d). The effect of aluminium powder in glass epoxy system on the wear behavior, SEM studies are conducted at a fixed combination of speed and load of (3 m/s, 20 N) for all four types of composite samples; GE, 5AlGE, 10AlGE and 15AlGE. The SEM micrographs are shown in Figure 5.15 (a-d) respectively. For GE composite, Figure 5.15 (a) shows crack for mation at the fiber matrix interface almost perpendicular to the sliding direction which indicates the presence of fatigue wear process. SEM micrograph of worn surface for 5AlGE composite is shown in Figure 5.15 (b). It shows crack formation and its propagation at the matrix region, the matrix material remains adhered with the fibers. SEM features for 10AlGE composite sample under the same speed and load condition is shown in Figure 5.15 (c). Full exposure of vertical and horizontal fibers is clearly visible. Few aluminium particles are also seen to be deformed during sliding. For 15AlGE sample under similar condition, worn surface feature is shown in Figure 5.15 (d). Fiber erosion and fiber breakage are well spread along with the agglomeration of aluminium particles. Fibers are loosely fitted with the matrix.

The SEM observations are consistent with the experimental wear data presented in Figure 5.10. Wear increases with the increase of sliding speed and normal load for glass epoxy composite (GE). Figure 5.14 (a-b) and (c–d) supplement the result with respect to increase in sliding speed and normal load respectively. For GE composite, with the increase of speed and load, SEM surface feature changes from partial or full removal of matrix part, fiber erosion, fiber matrix interface

crack formation, delamination of fibers, fiber fracture and fiber fragmentation leading to higher wear. Wear decreases with addition of aluminium powder up to 10 wt% in comparison to glass epoxy composite (GE) has been reported in Figure 5.10 which corroborates the present observations. To explain the reduced wear in 5AlGE and 10AlGE samples than GE sample, the abilities of aluminium particles to form a strong inter molecular bond among the constituents and lower frictional force can be invoked as shown in Figure 5.9. In 15AlGE sample, more than 10 wt% aluminium concentrations is high enough to form the weak in-
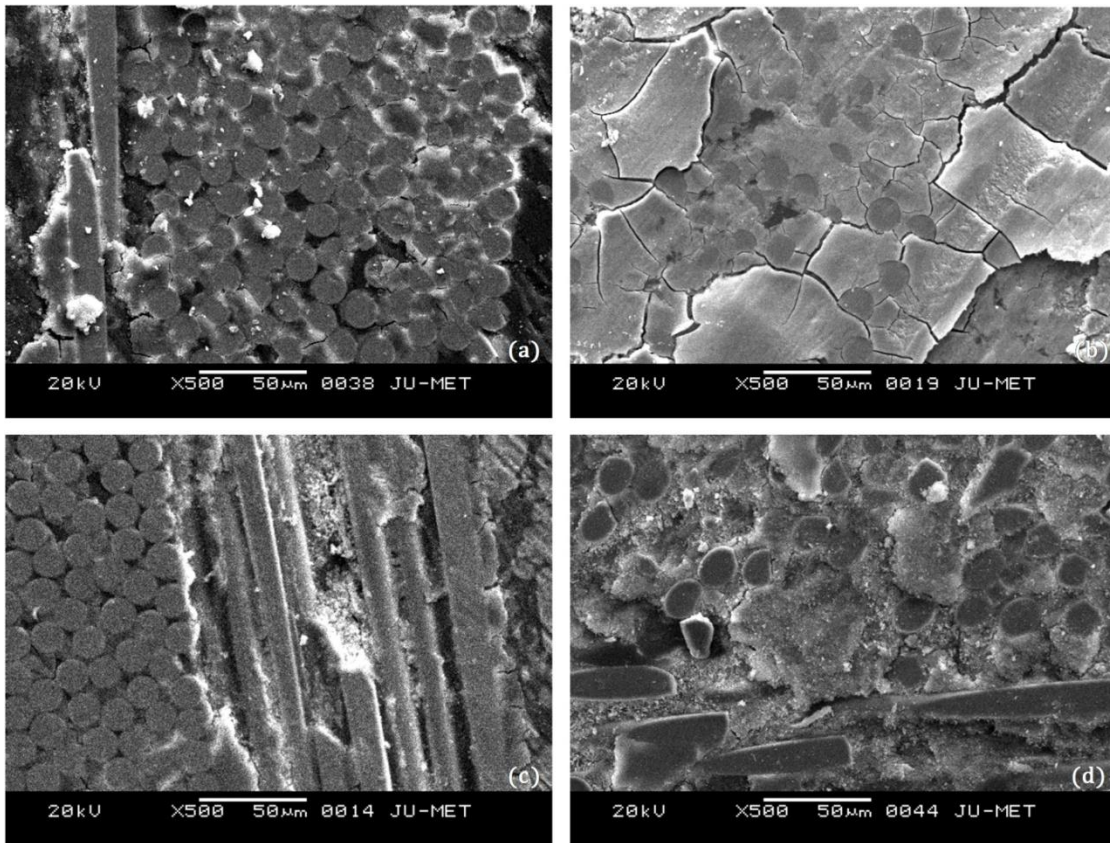
Figure 5.15 SEM micrographs of worn composite samples at sliding speed of 3 m/s and normal load of 20 N, (a) GE, (b) 5AlGE, (c) 10AlGE, (d) 15AlGE

ter molecular bond resulting in easy pull out of aluminium particles and its agglomeration during sliding action (Figure 5.15 d). Among 5AlGE and 10AlGE samples, sample 10AlGE contains more amount of aluminium powder than 5AlGE sample and experimental result shows that incorporation of aluminium above 5 wt% increases the wear loss as well as friction coefficient. From SEM

observation, it is found that aluminium particles get oxidized during the sliding operation and forms much harder oxide particles (Figure 5.15 d). Due to the presence of these abrasive particles, friction coefficient as well as the wear loss is high for 10AlGE sample compared to 5AlGE composite sample. In the present study, for normal load of 20 N, the friction coefficient values increase steadily with sliding speed for GE, 5AlGE, and 10AlGE composites whereas it decreases for the 15AlGE sample. It simply implies that the material integrity level gets reduced leading to loss in its capacity to resist sliding.

5.5.2 Effect of exposed aluminium powder on surfaces

The SEM image of aluminium powder is shown in Figure 2.2. It shows that most of the particle size is less than the 40 micron meter. Only few aluminium particles are higher dimension but not exceeding 80 micron meter. This dimension is considered as the dimension of pure aluminium particles. When it exposed to normal atmosphere, the size is increased by way of oxide formation as aluminium is highly reactive with oxygen. Figure 5.16 (a) and Figure 5.16 (b-d) represent the surface feature of glass epoxy and aluminium filled glass epoxy composite samples prior to the testing.

Figure 5.16 (a) shows the prepared GE sample test surface. Most of the particles appear in the SEM micrograph is very small even less than 10 micron meter. These are combination of glass and epoxy particles. Particles retain on the sample face even after the soft cleaning on final finished sample. Surface oxidization for GE sample is not considered.

For aluminium powder filled glass epoxy composites, samples like 5AlGE, 10AlGE, and 15AlGE, presence of aluminium particles at the test surface is obvious and it increases with the increase of the aluminium concentration. Increase in aluminium particles in surface, decreases the presence of glass/matrix particles. Test surface for 5AlGE composite sample is shown in Figure 5.16 (b). Lesser

amount of aluminium particles present in surface in contact with the oxygen in open atmospheric condition, get oxidized and form the larger aluminium oxide particles. Oxide particles in combination with glass/epoxy particles forms a very thin artificial layer. Moreover, composite with less aluminium concentration, very negligible surface area of aluminium particles are exposed. In Figure 5.16 (b) white gray colour oxide particles are clearly seen. As the quantity of exposed aluminium particles are to increase with the increase of aluminium concentration in composites, the possibility of more oxide formation on the sample surface increases. As a result of which artificial layer thickness becomes very thin, Figure 5.16 (b) to thin shown in Figure 5.16 (c). In 15AlGE sample, the aluminium conc-
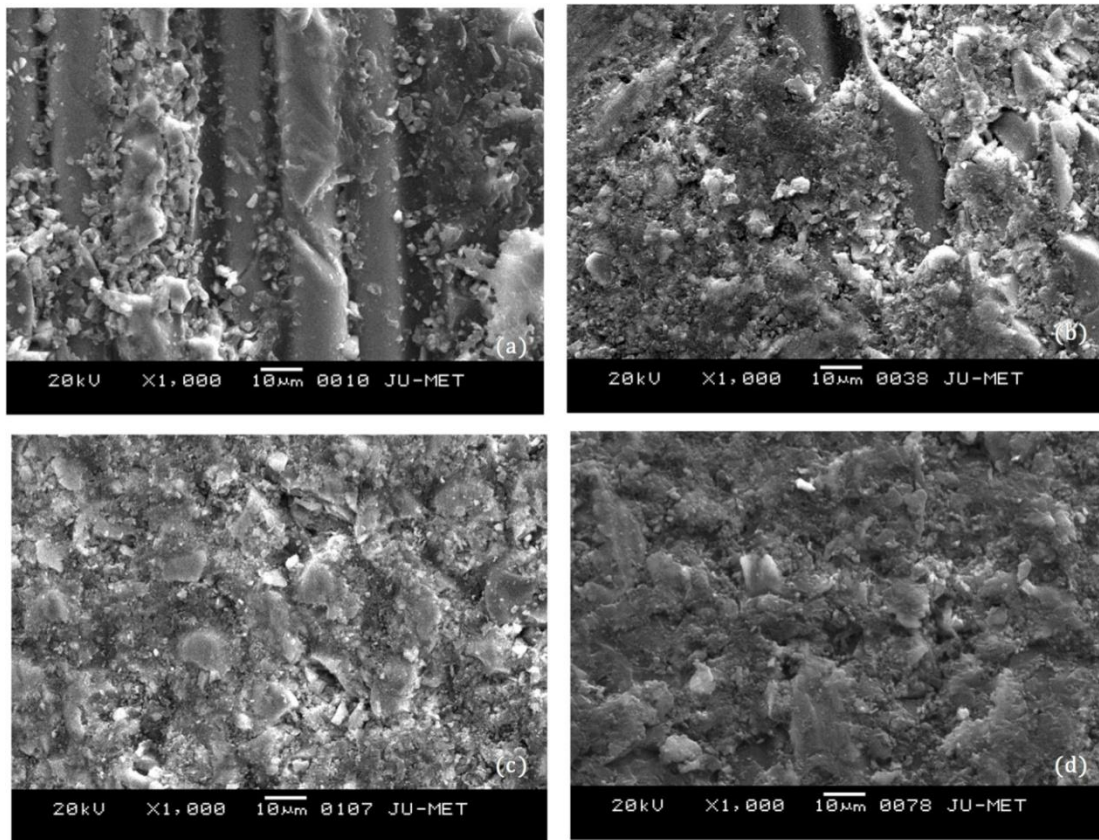

Figure 5.16 SEM images of unworn composite surfaces (a) GE sample surface showing the matrix/glass particles and fibers, (b) 5AlGE sample surface showing the matrix, glass, aluminium and oxide (grey colour) particles, (c) 10AlGE sample surface showing the artificial oxide layers, (d) 15AlGE sample surface showing the oxide layer along with aluminium particle agglomeration.

centration is highest and due to agglomeration of aluminium particles in composite, in the test face, most of the surface area of the particles are exposed to atmosphere. As a result of which test face of 15AlGE sample contains thick artificial layer of oxide and glass/matrix particles as shown in Figure 5.16 (d). The artificial layer thus forms is very brittle in nature because of its high porosity and light weight as aluminium is very light metal particles.

5.5.3 Effect of sliding distance on surfaces

Figure 5.17 shows the SEM micrographs of worn surfaces of unfilled glass epoxy composite at different distances of run. For 600 m distance run, Figure 5.17 (a) shows the exposure of both horizontal and vertical fiber because of the wear out of the soft matrix material in contact of the hard asperities. On increase of the sliding distance further, surface feature at 1800 m distance run is shown in Figure 5.17 (b). It shows that height of the fibers are more than the matrix system resulting in increase of the surface roughness leading to the increase of friction coefficient as in Figure 5.7. The exposed horizontal fibers are completely separated from the matrix. Fiber breakages and wear debris formation are also noticed. Figure 5.17 (c) is a SEM micrograph at 2400 m distance run. It shows the presence of a significant iron concentration at the light grey region. The steel disc suffers wear and incorporates iron particles in the interfacial layer. Fiber erosion and fiber breakage are also noticed. At a distance of 3600 m sliding, Figure 5.17 (d) shows the formation of a thin lubricating film because of the equilibrium state among the tribological factors. SEM image also shows multiple parallel micro-cracks, approximately perpendicular to the sliding direction (vertical direction), indicating the presence of a fatigue mechanism (Suh, 1986).

SEM micrographs of the worn surface for 5AlGE composite sample has been shown in Figure 5.18 viewed at different distances of run. Figure 5.18 (a) shows the exposure of fibers. With further increase of sliding distances more exposure

of fibers are noticed (Figure 5.18 b) which increases the roughness of the contact surface. Matrix part is well spread but still attached with the material. During this period, very less quantity of epoxy matrix wears out from the sample. Figure 5.18 (c) represents the surface feature of 2400 m distance run. It shows the presence

Figure 5.17 SEM images of worn GE sample surface under normal load of 30 N and sliding speed of 1 m/s for different sliding distances of (a) 600 m, (b) 1800 m, (c) 2400 m, (d) 3600 m.

of a significant iron concentration at the light grey region. The steel disc suffers wear and incorporates iron particles in the interfacial layer. In contact of both smooth surfaces, adhesive force at contact increases resulting to the increase of friction further as shown in Figure 5.7. SEM image also shows multiple parallel micro-cracks, approximately perpendicular to the sliding direction, indicating the presence of a fatigue mechanism (Suh, 1986). SEM micrograph for 3000 m

distance run is shown in Figure 5.18 (d). Increase of friction coefficient generates more heat as a result of which It shows plastically deformed aluminium particles and most of the particles are eroded conditions. For 10AlGE samples SEM micrograph for the worn surfaces has been shown in Figure 5.19. Figure 5.19 (a)
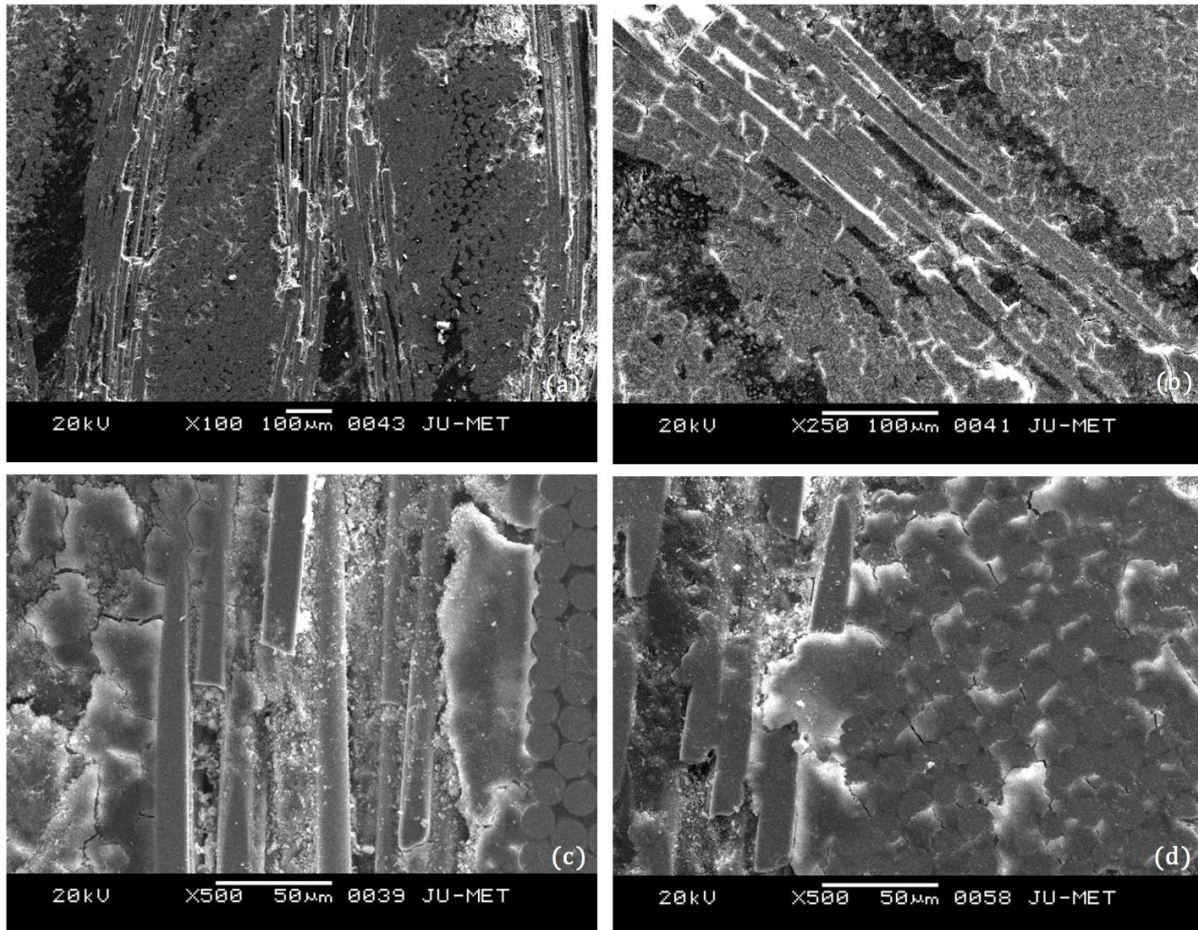

Figure 5.18 SEM images of worn 5AlGE sample surface under normal load of 30 N and sliding speed of 1 m/s for different sliding distances of (a) 600 m, (b) 1800 m, (c) 2400 m, (d) 3000 m.

indicates that at the end of 600 m distance run there is clear indication of exposed vertical and horizontal fibers but matrix in some portion is still adhere, this may be because of the unworn surface oxidization effect by way of formation of a thin artificial oxide film. Further increase of sliding distance from 600 to 1800 m (Figure 5.19 b), fiber exposure is more prominent and it is extended out of the matrix system as shown in Figure 5.9. Debris formation and its agglomeration of

different region is clearly noticed. Cracks initiation around the vertical fibers and its possible downward propagation is to occur at this stage. At this distance run as a result of which friction coefficient reaches to its highest value which validates the experimental result presented in Figure 5.7. Figure 5.19 (c) shows further crack propagation around the vertical fibers and accumulation of iron particles among the gap of the fibers (light grey colour). Some protrudated out aluminium particles even in oxide forms are also noticed (white colour). All these
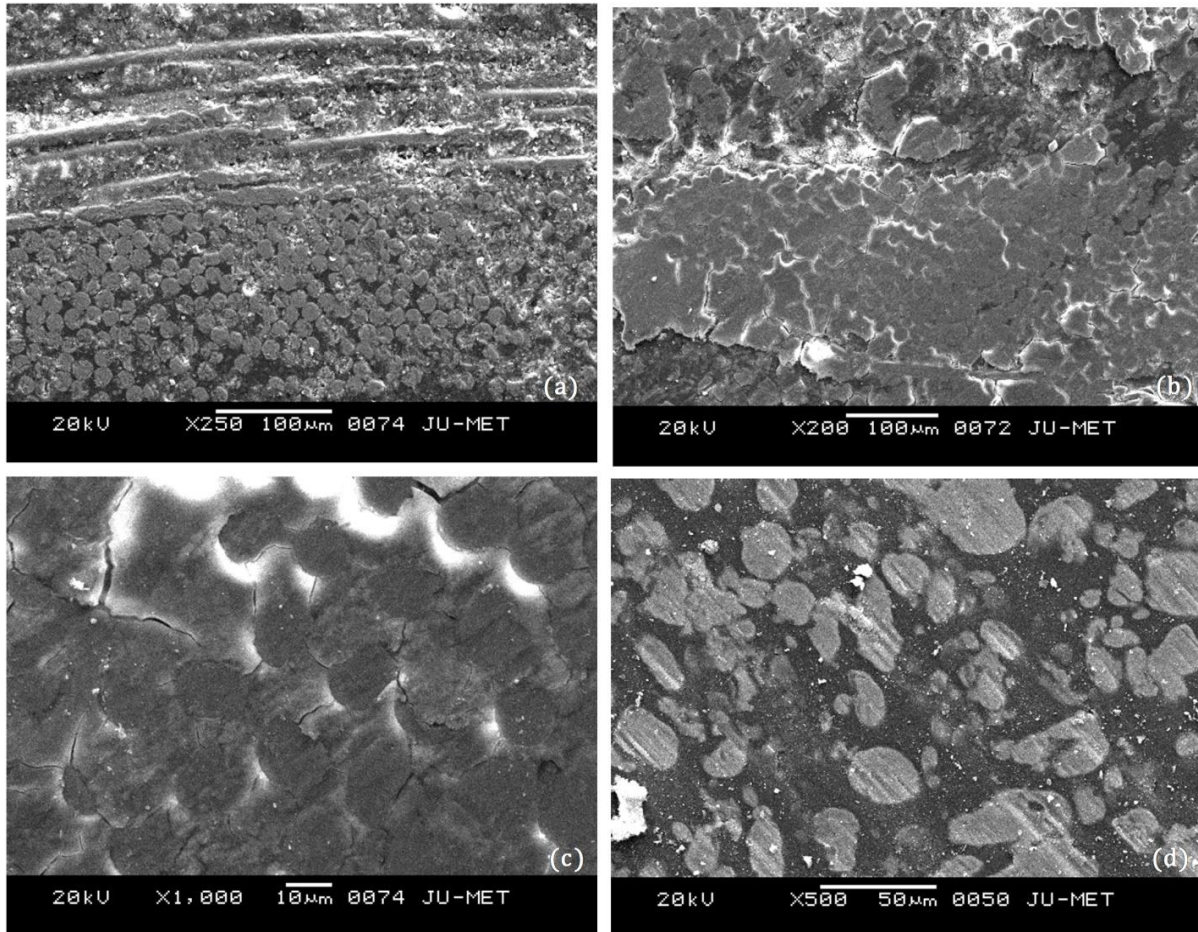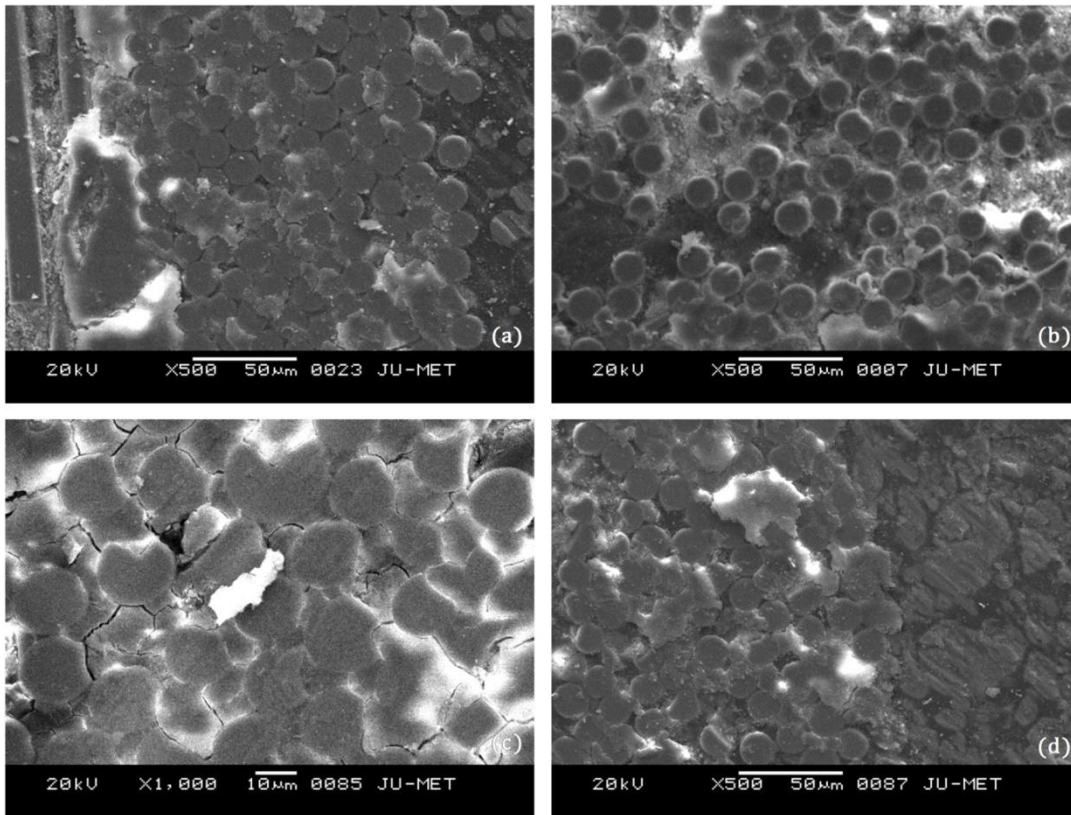

Figure 5.19 SEM images of worn 10AlGE sample surface under normal load of 30 N and sliding speed of 1 m/s for different sliding distances of (a) 600 m, (b) 1800 m, (c) 2400 m, (d) 3000 m.

particles along with the debris (matrix and fiber) fill the gap among the fibers, As a result of which surface at this stage behaves as a smooth one which corroborates the result as presented in Figure 5.7. Figure 5.19 (d) shows the plastically deformed aluminium particles because of the much more adhesion between the two comparatively smooth contacting surfaces. Most of the particles

are eroded. Oxide particles are also seen along with the debris formation at a distance of 3000 m run for 10AlGE sample. SEM micrograph for 15AlGE samples at different run distances has been shown in Figure 5.20. For better understanding of the worn surface features at different distances of sliding of 15AlGE test samples, the unworn surface feature is shown in Figure 5.18 is taken under consideration. It clearly shows the accumulation of a thin oxide layer on the test surface. During sliding contact with disc counterface, the oxide layer is to wear out first within a certain distance of sliding followed by the actual test surface. At 600 m distance run, Figure 5.20 (a) shows the corresponding surface features. The artificial layer on the sliding face of the sample is still exists and due to the existence of light, soft and porous layer, the friction coefficient as well as the wear not increase much which support the friction and wear data presented earlier. Only partial fiber exposure is noticed. Figure 5.20 (b) represents the SEM features at 1800 m distance run. Actual test surface is in contact with counter disc. Horizontal fibers are full exposed. Cavity formation is clearly noticed, it indicates fibers are out of the matrix bonding. On repeated loading, catering action at the interface will enhance the fiber delamination. Wear debris tendency is to agglomerate in the gap of fibers in the direction of sliding (diagonally left hand upword). With further increase of the sliding distance to 2400 m, Figure 5.20 (c) shows the features like fibers erosion and well spread debris in large quantity is observed. Oxide particles (light colour) in different shapes is available. Extended out delaminated fibers are well eroded which is in good tuning with the result as shown in Figure 5.7 and Figure 5.11. At a sliding distance of 3600 m, Figure 5.20 (d) represents the respective surface features. Random fiber erosion and fragmented along with huge quantity of debris formation are clearly seen. At the inter face, fibers are seen to be loosely fitted with the matrix.

Figure 5.21 and Table 5.2 show the EDX analysis for 5 wt% aluminium filled glass epoxy composite at 2400 m distance run. Elements present on the surface clearly

indicate the erosion of steel disc which in turn agree with the result as shown in Figure 5.7.
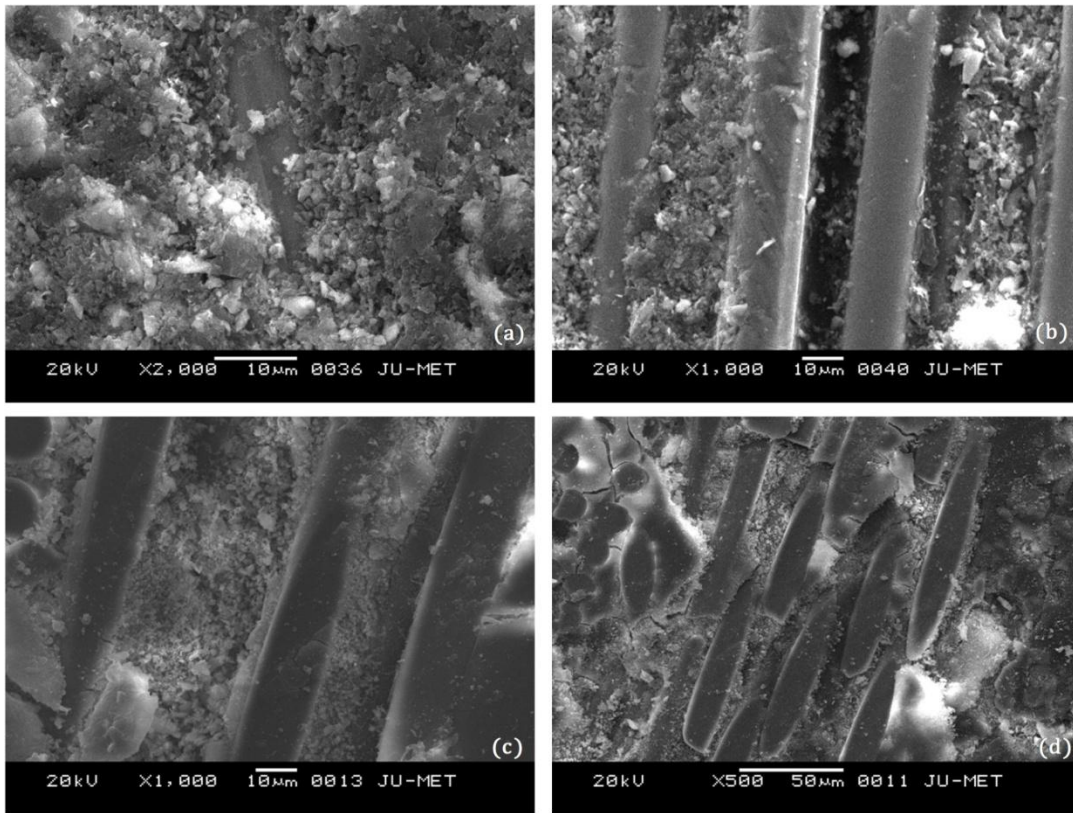

Figure 5.20 SEM images of worn 15AlGE sample surface under normal load of 30 N and sliding speed of 1 m/s for different sliding distances of (a) 600 m, (b) 1800 m, (c) 2400 m, (d) 3600 m.
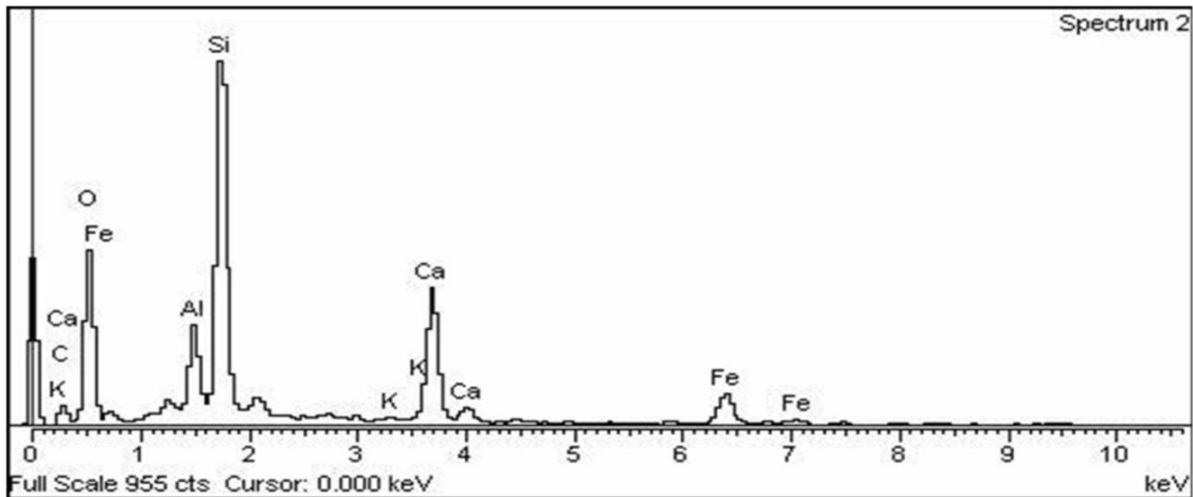

Figure 5.21 EDX spectra of elemental composition of worn surface of unfilled glass epoxy Composite, GE sample at 72 m distance run

Table 5.2 Chemical composition of unfilled glass epoxy composite at 72 m distance run

Elements	C	O	Al	Si	K	Ca	Fe	Total
Weight%	6.27	47.69	5.07	21.91	0.37	11.50	7.18	100

Figure 5.21 and Table 5.2 show the EDS analysis for 5 wt% aluminium filled glass

6. SUMMARY AND CONCLUSIONS

6.1 Summary of research findings

➢ The performance of an engineering material is judged by its properties and behavior under tensile, compressive, shear and other static or dynamic loading conditions in both normal and adverse test environments. This information becomes essential for selecting the proper material in a given application as well as for designing a composite component/structure with the selected material. To this end, the present work has reported the performance of a new class of polymer based composites with emphasis on the general trends observed in their properties and behavior. A wealth of property data has been generated for a series of glass epoxy, aluminium epoxy and glass epoxy composites filled with aluminium powder. These material properties have been determined by conducting physical and mechanical tests under controlled laboratory conditions.

➢ In the present investigation, it is noticed that the composites with aluminium particulate filler have higher void fraction compared to the unfilled composites. Among the aluminium powder filled glass epoxy composites, least value of void content is recorded for the composites with 5 wt% aluminium content. The presence of pores and voids in the composite structure significantly affect some of the mechanical properties and even the friction and wear performance of the composites. Higher void contents

usually mean lower fatigue resistance, greater susceptibility to water penetration and weathering. However, presence of void is unavoidable in composite making particularly through hand-lay-up route.

➢ Hardness values have been found to have improved invariably for all the composites on addition of aluminium powder. The reduction in tensile strength and the improvement in hardness with the incorporation of aluminium can be explained as follows: under the action of a tensile force, the filler-matrix interface is vulnerable to debonding depending on interfacial bond strength and this may lead to a break in the composite. But in case of hardness test, a compression or pressing stress is in action. So the polymeric matrix phase and the solid filler phase would be pressed together and touch each other more tightly. Thus, the interface can transfer pressure more effectively although the interfacial bond may be poor. This might have resulted in an enhancement of hardness.

➢ Inclusion of fiber in neat epoxy improved the load bearing capacity (tensile strength) and the ability to withstand bending (flexural strength) of the composites. But with the incorporation of aluminium powder, the tensile strengths of the composites are found to be decreasing in most of the cases whereas tensile modulus of the composite increases at 10 wt% aluminium content and it declines with 5 and 15 wt% filler addition in comparison to unfilled composite. The decline in tensile strength may be attributed to two reasons- one possibility is that due to the presence of pores at the interface between the filler particles and the matrix, the interfacial adhesion may be too weak to transfer the tensile stress; the other is that the corner points of the irregular shaped particulates result in stress concentration in the matrix body. For the explanation regarding tensile modulus, previous reports demonstrate that normally the fiber in the composite restrain the

deformation of the matrix polymer, reducing the tensile strain (Fu and Lauke, 1998; Thomason et al., 1996). So even if the strength decreases with filler addition, the tensile modulus of the composite is expected to increase for a certain wt% of aluminium powder addition as has been observed in the present investigation.

➢ The flexural property is observed to improve upto the aluminium content of 10 wt% in glass epoxy system. The highest improvement in flexural strength with 5 wt% of aluminium content is recorded whereas 15 wt% aluminium filled glass epoxy composite shows the lowest strength. Composite with 10 wt% of aluminium powder shows the better performance than 0 wt% filled glass epoxy composite but less than the 5 wt% aluminium filled composite. The improvement in the flexural strength of the composites with filler content (upto 10 wt%) is probably caused by good compatibility of the particulates and the epoxy matrix, leading to increase in interfacial bonding. The lower values of flexural properties (as 15AlGE) may also be attributed to fiber to fiber interaction, voids and dispersion problems. It is evident from this study that as far as the flexural strength is concerned, quantity of the aluminium powder as filler material plays a very significant role.

➢ In reciprocating contact condition, the friction coefficient of glass epoxy composites in general decreases with the addition of aluminium powder up to a level of 10 wt% and further addition of aluminium powder results in increase of friction coefficient. This may be explained from the fact that addition of up to 10 wt% of aluminium powder increases the hardness and strength of the composite due to better interfacial bonding of the composite constituents. Friction coefficient increases in general with sliding speed but the behavior is controlled by the amount of aluminium particle in the composite system. Friction coefficient of composites with a level of 10 wt%

aluminium concentration decreases with normal load due to formation of thin film at contact as a result of plastic deformation of matrix. Further higher aluminium concentration in composite (15 wt%) shows the reverse trend at higher loads because of the agglomeration of wear debris in reciprocating truck for the limited stroke length. Friction coefficient increases with reciprocating distances initially but subsequently gets reduced to a stable low value due to formation of thin film at contact as a result of plastic deformation of matrix.

➤ In reciprocating contact, wear of glass epoxy and aluminium filled composites increases with increase in reciprocating frequency, normal load and reciprocating distances. Wear performance of glass epoxy composite is improved with up to a level of 10 wt% aluminium addition and composite with 5 wt% aluminium shows less wear for all experimental combination of frequency and load and with respect to reciprocating distances. This may be attributed as the increase of strength and thermal conductivity of composites with the limited addition of aluminium powder. Composite with higher aluminium concentration (as in 15AlGE) shows the severe wear even more than the unfilled glass epoxy composite because of the agglomeration of aluminium particles leading less material strength and integrity. Addition of aluminium powder needs to be maintained at the optimum level in order to have better tribological characteristics.

➤ In sliding contact condition, the friction coefficient of epoxy based composites decreases with the addition of glass fiber reinforcement and 60 wt% fiber reinforced epoxy composite shows the lowest friction at all experimental conditions. Further addition of fiber reinforcement in epoxy, friction coefficient increases. This may be because of the presence of balance proportion of glass fiber and epoxy matrix in 60 wt% fiber reinforced

composite. In aluminium epoxy composites, friction coefficient of 100E, 5AlE, and 10AlE increases with increase of sliding speed whereas friction of 15AlE decreases with the sliding speed. Among the aluminium epoxy composites, 10AlE shows the lowest friction coefficient in most of the cases. In aluminium particulate glass epoxy composites up to a level of 10 wt% aluminium concentration, friction coefficient increases with increase of sliding speed whereas 10 wt% above aluminium concentration, friction shows the reverse trend i. e, it decreases with increase of sliding speed. With respect to normal load, friction of glass epoxy and aluminium particulate glass epoxy composites decreases due to formation of thin film at contact as a result of plastic deformation of matrix. Addition of aluminium powder in glass epoxy system is observed to be beneficial to reduce friction than the glass epoxy composite. This benefit is limited upto 10 wt% aluminium concentration and above of which friction coefficient increases. This may be explained from the fact that addition of up to 10 wt% of aluminium powder increases the hardness and strength of the composite due to better interfacial bonding of the composite constituents. Friction coefficient increases with sliding distances initially but subsequently gets reduced to a stable low value due to formation of thin film at contact as a result of plastic deformation of matrix. Wear of neat epoxy and glass epoxy composites with increase of sliding speed and normal load increases and with the addition of fiber reinforcement in epoxy wear decreases, the lowest wear value is recorded of the composite with 60 wt% fiber reinforcement. In neat epoxy and aluminium epoxy composites, wear increases with increase of sliding speed and normal load. With the addition of aluminium powder with epoxy wear decreases and the lowest value is recorded for the aluminium epoxy composite with 10 wt% aluminium concentration. Wear of glass epoxy and aluminium particulate glass epoxy composites increases with the increase of both sliding speed and

normal load. With the incorporation of aluminium powder up to the level of 10 wt% in glass epoxy system, wear performance improves than the unfilled glass epoxy composite and further incorporation of aluminium powder, wear performance shows the reverse trend. Overall, 5 wt% aluminium filled, 5AlGE composite yields less friction coefficient and high wear resistance. Addition of aluminium powder needs to be maintained at the optimum level in order to have better tribological characteristics.

6.2 Conclusions

This experimental investigation on glass epoxy, aluminium epoxy and aluminium powder filled glass epoxy composites has led to the following specific conclusions:

1. Successful fabrication of aluminium epoxy composite has been done with varying wt% of aluminium concentration in open mould process. Glass epoxy with varying fiber wt% and glass epoxy with fixed wt% of fiber reinforcement, filled with varying wt% of aluminium powder (0-15 wt%) composites are made in conventional hand layup followed by light compression moulding technique.

2. The density, micro-hardness, tensile strength, tensile modulus, flexural strength of the composites are greatly influenced by the amount of aluminium powder content. In aluminium filled glass epoxy composites up to the level of 10 wt% of aluminium possess higher hardness values compared to the glass-epoxy composite whereas for aluminium epoxy composites, hardness improves than neat epoxy. However, while fabricating a composite of specific requirements, there is a need for the choice of appropriate fiber and filler and their content for optimizing the desired property of composite.

3. In reciprocating and sliding both contact conditions, among the glass epoxy composites, 60 wt% fiber reinforced composite is found to be stable and lowest frictional material. This may be explained as the balance proportion of fiber and epoxy in composite. For lower wt% of fiber content, there is much adhesion at the contact surface due to epoxy enrichment, resulting to increase of friction coefficient and for higher wt% of fiber content, presence of pulverized glass particle at the contact zone may be the reason of higher friction coefficient. Though for reciprocating contact condition at the lower combination of experimental frequency and load of 15 Hz and 0.4 Kg condition, 50GE reports the lowest friction and it increases with the fiber reinforcement (Bahadur and Zheng, 1990).

4. In neat epoxy and aluminium epoxy composites for continuous sliding contact condition, the friction coefficient of aluminium powder filled epoxy composites decreases with the addition of aluminium powder up to 10 wt% and further addition of aluminium powder results in increase of friction coefficient at lower speed levels whereas for higher speed levels friction coefficient decreases. This may be explained from the fact that addition of up to 10 wt% of aluminium powder increases the hardness and strength of the composite due to better interfacial bonding of the composite constituents. Friction coefficient of 100E, 5AlE and 10AlE decreases with normal load due to formation of thin film at contact as a result of plastic deformation of matrix. Friction coefficient increases in general with sliding speed for but the behavior is controlled by the amount of aluminium particle in the composite system. Regarding wear loss, aluminium epoxy composites with up to 10 wt% aluminium addition shows less wear but with further addition of aluminium powder there is a considerable increase in wear. Overall, 10 wt% aluminium filled, 10AlE composite yields less friction coefficient and   high wear

resistance. Addition of aluminium powder needs to be maintained at the optimum level in order to have better tribological characteristics.

5. In reciprocating and continuous contact conditions, the friction coefficient of aluminium powder filled glass epoxy composites decreases with the addition of aluminium powder up to 10 wt% and further addition of aluminium powder results in increase of friction coefficient. Regarding wear loss, 60 wt% woven glass fiber reinforced epoxy composite with up to 10 wt% aluminium addition shows less wear for all load, frequency/speeds and all sliding distances but with further addition of aluminium powder there is a considerable increase in wear than the unfilled glass epoxy composite. Overall, 5 wt% aluminium filled, 5AlGE composite yields less friction coefficient and high wear resistance. Addition of aluminium powder needs to be maintained at the optimum level in order to have better tribological characteristics.

6. This study reveals that the composites with highest wt% of fiber or aluminium powder report the highest value of friction and wear. So for the better tribological behavior, amount of fiber reinforcement or addition of aluminium powder required to be at the optimum level.

7. Several wear mechanisms have been observed microscopically which explained the way glass epoxy and glass epoxy filled with aluminium powder respond to wear. For glass fiber epoxy composites, severe deterioration of both fiber and matrix, micro ploughing in the matrix, transverse shearing, stripping and fibrillation of fiber are identified as the predominant damage mechanisms. Whereas for aluminium glass epoxy composites, aluminium particles protrude out and its possible much harder oxide particle formation,

fiber matrix debonding, fiber-pulling and fracture are the characteristic features of wear.

8. The presence of aluminium powder as particulate filler in these composites improves their friction and wear performances and this improvement depends on the content of the filler in epoxy and glass epoxy system. Hence the use of aluminium filler in composite as tribo material is beneficial for the applications where friction and wear both are the critical issue.

6.3 Recommendations for potential applications

The glass epoxy and aluminium powder filled glass fiber reinforced composites fabricated and experimented upon in this investigation are found to have adequate potential for a wide variety of applications particularly in dry reciprocating and continuous sliding environment. When wear is not the predominant factor, only glass epoxy composites without any particulate filler can be recommended. Manufacturing of light weight sports goods such as: cricket bat, tennis racquets etc. are few such examples. Of course, the weight fraction of fiber in the composite is to be decided from the view point of required strength. If the place of use is involved with the tribological loading conditions then aluminium powder filled glass fiber reinforced composites are to be preferred due to their reasonably improved friction and wear resistance. The present study has established that aluminium powder be excellent candidate as particulate filler in glass epoxy composites. However, the content of filler is to be decided judiciously keeping the strength and wear in mind. Use of these composites, in general, may also be recommended for applications where relative motion exists like light weight vehicles etc.

REFERENCES

Agarwal, B.D., Broutman, L.J. and Chandrashekhara, K., 2006. Analysis and Performance of Fiber Composites. John Wiley & Sons, New York.

Alam, S., Habib, F., Irfan, M., Iqbal, W. and Khalid, K., 2010. Effect of orientation of glass fiber on mechanical properties of GRP composites. Journal of the Chemical Society of Pakistan, 32(3), pp.265-269.

Almeida, J.H.S., Amico, S.C., Botelho, E.C. and Amado, F.D.R., 2013. Hybridization effect on the mechanical properties of curaua/glass fiber composites. Composites Part B: Engineering, 55, pp.492-497.

Aramide, F.O., Atanda, P.O. and Olorunniwo, O.O., 2012. Mechanical properties of a polyester fiber glass composite. International Journal of Composite Materials, 2(6), pp.147-151.

Araujo, E.M., Araujo, K.D., Pereira, O.D., Ribeiro, P.C. and de Melo, T.J., 2006. Fiberglass wastes/polyester resin composites: mechanical properties and water sorption. Polímeros, 16(4), pp.332-335.

Archard, J., 1953. Contact and rubbing of flat surfaces. Journal of applied physics, 24(8), pp.981-988.

ASM Hand Book (1992). ASM International Materials Park, Ohio, USA.

Atas, C. and Liu, D., 2008. Impact response of woven composites with small weaving angles. International Journal of Impact Engineering, 35(2), pp.80-97.

Bahadur, S. and Zheng, Y., 1990. Mechanical and tribological behavior of polyester reinforced with short glass fibers. Wear, 137(2), pp.251-266.

Barbero, E.J., 2010. Introduction to Composite Materials Design. CRC press, New York.

Baucom, J.N. and Zikry, M.A., 2005. Low-velocity impact damage progression in woven E-glass composite systems. Composites Part A: Applied Science and Manufacturing, 36(5), pp.658-664.

Bhattacharya, S.K., 1986. Metal Filled Polymers (Vol. 11). CRC Press, New York.

Bhushan, B., 2013. Principles and Applications of Tribology. John Wiley & Sons, New Jersey.

Bijwe, J., Tewari, U.S. and Vasudevan, P., 1989. Friction and wear studies of a short glass-fiber-reinforced polyetherimide composite. Wear, 132(2), pp.247-264.

Chen, Y., Jallo, L., Quintanilla, M.A. and Dave, R., 2010. Characterization of particle and bulk level cohesion reduction of surface modified fine aluminium powders. Colloids and Surfaces A: Physicochemical and Engineering Aspects, 361(1), pp.66-80.

Chen, Z., Liu, X., Lü, R. and Li, T., 2006. Mechanical and tribological properties of PA66/PPS blend. III. Reinforced with GF. Journal of Applied Polymer Science, 102(1), pp.523-529.

Chung, S., Im, Y., Kim, H., Park, S. and Jeong, H., 2005. Evaluation for micro scale structures fabricated using epoxy-aluminium particle composite and its application. Journal of Materials Processing Technology, 160(2), pp.168-173.

Crouse, C.A., Pierce, C.J. and Spowart, J.E., 2010. Influencing solvent miscibility and aqueous stability of aluminium nanoparticles through surface functionalization with acrylic monomers. ACS Applied Materials & Interfaces, 2(9), pp.2560-2569.

Dandekar, D.P., Hall, C.A., Chhabildas, L.C. and Reinhart, W.D., 2003. Shock response of a glass-fiber-reinforced polymer composite. Composite Structures, 61(1), pp.51-59.

Debnath, K., Singh, I. and Dvivedi, A., 2013. Dry sliding wear behaviour of glass fiber reinforced epoxy composites filled with natural fillers. Reason-A Technical Journal, 12, pp.61-68.

Dong, C. and Davies, I.J., 2013. Flexural properties of E glass and TR50S carbon fiber reinforced epoxy hybrid composites. Journal of Materials Engineering and Performance, 22(1), pp.41-49.

El-Sayed, A.A., El-Sherbiny, M.G., Abo-El-Ezz, A.S. and Aggag, G.A., 1995. Friction and wear properties of polymeric composite materials for bearing applications. Wear, 184(1), pp.45-53.

El-Tayeb, N.S.M., Yousif, B.F. and Brevern, P.V., 2005. On the effect of counterface materials on interface temperature and friction coefficient of GFRE composite under dry sliding contact. American Journal of Applied Sciences, 2(11), pp.1533-40.

Friedrich, K., 1986. Wear of reinforced polymers by different abrasive counterparts. Friction and Wear of Polymer Composites, 1, pp.233-287.

Friedrich, K. and Reinicke, P., 1998. Friction and wear of polymer-based composites. Mechanics of Composite Materials, 34(6), pp.503-514.

Friedrich, K. ed., 2012. Friction and wear of polymer composites (Vol. 1). Elsevier

Fu, S.Y. and Lauke, B., 1998. Characterization of tensile behaviour of hybrid short glass fibre/calcite particle/ABS composites. Composites Part A: Applied Science and Manufacturing, 29(5), pp.575-583.

Goud, G. and Rao, R.N., 2012. Mechanical and electrical performance of Roystonea regia/glass fiber reinforced epoxy hybrid composites. Bulletin of Materials Science, 35(4), pp.595-599.

Hamed, G.M., 2009. Study the tensile strength for epoxy composite reinforced with fibers particles. Journal of University of Anbar for Pure Science, 3(2).

Hufenbach, W.A., Stelmakh, A., Kunze, K., Böhm, R. and Kupfer, R., 2012. Tribo-mechanical properties of glass fiber reinforced polypropylene composites. Tribology International, 49, pp.8-16.

Jallo, L.J., Schoenitz, M., Dreizin, E.L., Dave, R.N. and Johnson, C.E., 2010. The effect of surface modification of aluminium powder on its flowability, combustion and reactivity. Powder Technology, 204(1), pp.63-70.

Jang, B.Z., 1994. Advanced polymer composites: principles and applications. ASM International, Materials Park, OH 44073-0002, USA.

Kim, H.J., Jung, D.H., Jung, I.H., Cifuentes, J.I., Rhee, K.Y. and Hui, D., 2012. Enhancement of mechanical properties of aluminium/epoxy composites with silane functionalization of aluminium powder. Composites Part B: Engineering, 43(4), pp.1743-1748.

Kim, J., Kang P. H and Nho Y.C, 2004. Positive temperature coefficient behavior of polymer composites having a high melting temperature. Journal of Applied Polymer Science, 92(1), pp. 394-401.

Kim, S.S., Shin, M.W. and Jang, H., 2012. Tribological properties of short glass fiber reinforced polyamide 12 sliding on medium carbon steel. Wear, 274, pp.34-42.

Kukureka, S.N., Hooke, C.J., Rao, M., Liao, P. and Chen, Y.K., 1999. The effect of fiber reinforcement on the friction and wear of polyamide 66 under dry rolling–sliding contact. Tribology International, 32(2), pp.107-116.

Kumar, S., Joshi, A. and Gangil, B., 2013. Physico-Mechanical and Tribological Properties of Glass Fiber based Epoxy Hybrid Natural Composite. In Proceedings of International Conference on Emerging Trends in Engineering and Technology, 3, pp. 378-383.

Leonard LWH, Wong KJ, Low KO, 2009. Fracture behavior of glass fiber reinforced polyester composite. Journal of Material Design and Application, 223, pp. 83–89.

Lhymn, C. and Light, R., 1987. Effect of sliding velocity on wear rate of fibrous polymer composites. Wear, 116(3), pp.343-359.

Li, D.X., Deng, X., Wang, J., Yang, J. and Li, X., 2010. Mechanical and tribological properties of polyamide 6–polyurethane block copolymer reinforced with short glass fibers. Wear, 269(3), pp.262-268.

Mansor, M.R., Sapuan, S.M., Zainudin, E.S., Nuraini, A.A. and Hambali, A., 2013. Hybrid natural and glass fibers reinforced polymer composites material selection using Analytical Hierarchy Process for automotive brake lever design. Materials & Design, 51, pp.484-492.

Martin, M., Hanagud, S. and Thadhani, N.N., 2007. Mechanical behavior of nickel+ aluminium powder-reinforced epoxy composites. Materials Science and Engineering: A, 443(1), pp.209-218.

Mathew, M.T., Padaki, N.V., Rocha, L.A., Gomes, J.R., Alagirusamy, R., Deopura, B.L. and Fangueiro, R., 2007. Tribological properties of the directionally oriented warp knit GFRP composites. Wear, 263(7), pp.930-938.

Mimaroglu, A., Unal, H. and Arda, T., 2007. Friction and wear performance of pure and glass fibre reinforced poly-ether-imide on polymer and steel counterface materials. Wear, 262(11), pp.1407-1413.

Mohammed Selleb H. 2009. Studying the flexural characteristics of the epoxy reinforced by Al and Cu particles. The Iraqi Journal for Mechanical and Material Engineering, 9(2), pp.239-248.

Mohan, N., Mahesha, C.R. and Raja, R., 2014. Tribo-mechanical behaviour of SiC filled glass-epoxy composites at elevated temperatures. International Journal of Engineering, Science and Technology, 6(5), pp.44-56.

Mohan, N., Natarajan, S. and KumareshBabu, S.P., 2011. Investigation on sliding wear behaviour and mechanical properties of jatropha oil cake-filled glass-epoxy composites. Journal of the American Oil Chemists' Society, 88(1), pp.111-117.

Nikkeshi, S., Kudo, M and Masuko, T., 1998. Dynamic viscoelastic properties and thermal properties of powder-epoxy resin composites, Journal of Applied Polymer Science, 69(13), pp. 2593-2598.

Nuruzzaman, D.M., Rahaman, M.L. and Chowdhury, M.A., 2012. Friction coefficient and wear rate of polymer and composite materials at different sliding speeds. International Journal of Surface Science and Engineering, 6(3), pp.231-245.

Ozturk, B., Arslan, F. and Öztürk, S., 2013. Effects of different kinds of fibers on mechanical and tribological properties of brake friction materials. Tribology Transactions, 56(4), pp.536-545.

Patnaik, A., Satapathy, A. and Biswas, S., 2010. Investigations on three-body abrasive wear and mechanical properties of particulate filled glass epoxy composites. Malaysian Polymer Journal, 5(2), pp.37-48.

Peng, G., Gao, L., Zhan, Z., Wang, H. and Hao, W., 2009. Wear behavior of Al $(OH)_3$-GF/epoxy composites in low velocity. Polymer Bulletin, 63(6), pp.911-919.

Petrucci, R., Santulli, C., Puglia, D., Sarasini, F., Torre, L. and Kenny, J.M., 2013. Mechanical characterisation of hybrid composite laminates based on basalt fibers in combination with flax, hemp and glass fibers manufactured by vacuum infusion. Materials & Design, 49, pp.728-735.

Pıhtılı, H. and Tosun, N., 2002. Investigation of the wear behaviour of a glass-fiber-reinforced composite and plain polyester resin. Composites Science and Technology, 62(3), pp.367-370.

Raja, G.M. and Hari, A.N.R., 2013. Effect of an angle-ply orientation on tensile properties of kevlar/glass hybrid composites. International Journal on Theoretical and Applied Research in Mechanical Engineering, 2(3), pp.63-67.

Raju, B.R., Suresha, B., Swamy, R.P. and Kanthraju, B.S.G., 2013. Investigations on mechanical and tribological behaviour of particulate filled glass fabric reinforced epoxy composites. Journal of Minerals and Materials Characterization and Engineering, 1, pp.160-167.

Ramesh, M., Palanikumar, K. and Reddy, K.H., 2013. Mechanical property evaluation of sisal–jute–glass fiber reinforced polyester composites. Composites Part B: Engineering, 48, pp.1-9.

Reis, J.M.L., Coelho, J.L.V. and da Costa Mattos, H.S., 2013. A continuum damage model for glass/epoxy laminates in tension. Composites Part B: Engineering, 52, pp.114-119.

Rout, A.K. and Satapathy, A., 2012. Study on mechanical and tribo-performance of rice-husk filled glass–epoxy hybrid composites. Materials & Design, 41, pp.131-141.

Sampathkumaran, P., Seetharamu, S., Vynatheya, S., Murali, A. and Kumar, R.K., 2000. SEM observations of the effects of velocity and load on the sliding wear characteristics of glass fabric–epoxy composites with different fillers. Wear, 237(1), pp.20-27.

Sampathkumaran, P., Seetharamu, S., Thomas, P. and Janardhana, M., 2005. A study on the effect of the type and content of filler in epoxy–glass composite system on the friction and slide wear characteristics. Wear, 259(1), pp.634-641.

Sampathkumaran, P., Seetharamu, S., Murali, A. and Kumar, R.K., 2001. On the SEM features of glass–epoxy composite system subjected to dry sliding wear. Wear, 247(2), pp.208-213.

Sawyer, W., G, Freudenberg, K., D, Praveen, B and Schadler, L., S, 2003. A study on the friction and wear behavior of PTFE filled with alumina nanoparticles, Wear, 254(5), pp. 573-580.

Sen, M., Sarkar, P., Modak, N. and Sahoo, P., 2015. Woven E-glass fiber reinforced epoxy composite–preparation and tribological characterization. International Journal of Materials Chemistry and Physics, 1(2), pp. 189-197.

Senthilkumar, N., Kalaichelvan, K. and Elangovan, K., 2012. Mechanical behaviour of aluminium particulate epoxy composite–experimental study and numerical simulation. International Journal of Mechanical and Materials Engineering, 7 (3), pp.214-221.

Shivamurthy, B. and Prabhuswamyc, M.S., 2009. Influence of SiO_2 fillers on sliding wear resistance and mechanical properties of compression moulded glass epoxy composites. Journal of Minerals and Materials Characterization and Engineering, 8(7), pp. 513-530.

Shokrieh, M.M., Torabizadeh, M.A. and Fereidoon, A., 2012. Progressive failure analysis of glass/epoxy composites at low temperatures. Strength of Materials, 44(3), pp.314-324.

Srivastava, V.K. and Wahne, S., 2007. Wear and friction behaviour of soft particles filled random direction short GFRP composites. Materials Science and Engineering: A, 458(1), pp.25-33.

Srivastava, V.K., Pathak, J.P. and Tahzibi, K., 1992. Wear and friction characteristics of mica-filled fiber-reinforced epoxy resin composites. Wear, 152(2), pp.343-350.

Srivastava, V.K. and Hogg, P.J., 1998. Moisture effects on the toughness, mode-I and mode-II of particles filled quasi-isotropic glass–fiber reinforced polyester resin composites. Journal of Materials Science, 33(5), pp.1129-1136.

Suh, N.P., 1986. Tribophysics. Pretice-Hall, Englewood Cliffs, New Jersey, USA.

Sumer, M., Unal, H. and Mimaroglu, A., 2008. Evaluation of tribological behaviour of PEEK and glass fiber reinforced PEEK composite under dry sliding and water lubricated conditions. Wear, 265(7), pp.1061-1065.

Suresha, B. and Chandramohan, G., 2008. Three-body abrasive wear behaviour of particulate-filled glass–vinyl ester composites. Journal of Materials Processing Technology, 200(1), pp.306-311.

Suresha, B., Chandramohan, G. and Jawali, N.D., 2007. Effect of short glass fiber content on three-body abrasive wear behaviour of polyurethane composites. Journal of Composite Materials, 41(22), pp.2701-2713.

Suresha, B., Chandramohan, G. and Renukappa, N.M., 2007. Mechanical and tribological properties of glass–epoxy composites with and without graphite particulate filler. Journal of Applied Polymer Science, 103(4), pp.2472-2480.

Suresha, B., Chandramohan, G., Samapthkumaran, P., Seetharamu, S. and Vynatheya, S., 2006. Friction and wear characteristics of carbon-epoxy and glass-epoxy woven roving fiber composites. Journal of Reinforced Plastics and Composites, 25(7), pp.771-782.

Suresha, B., Chandramohan, G., Rao, P.S., Sampathkumaran, P., Seetharamu, S. and Venkateswarlu, V., 2006a. Friction and slide wear characteristics of glass-epoxy and glass-epoxy filled with SiCp composites. Indian Journal of Engineering and Materials Sciences, 13(6), p.535.

Suresha, B., Chandramohan, G., Samapthkumaran, P. and Seetharamu, S., 2007. Three-body abrasive wear behaviour of carbon and glass fiber reinforced epoxy composites. Materials Science and Engineering: A, 443(1), pp.285-291.

Suresha, B., Chandramohan, G., Prakash, J.N., Balusamy, V. and Sankaranarayanasamy, K., 2006b. The role of fillers on friction and slide wear characteristics in glass-epoxy composite systems. Journal of Minerals and Materials Characterization and Engineering, 5(01), pp.87-101.

Suresha, B., Chandramohan, G., Samapthkumaran, P. and Seetharamu, S., 2007. Investigation of the friction and wear behavior of glass-epoxy composite with and without graphite filler. Journal of Reinforced Plastics and Composites, 26(1), pp.81-93.

Thomason J. L, Vlug M. A, Schipper G and Krikor H. G., 1996. Influence of fibre length and concentration on the properties of glass fibre reinforced polypropylene: Part 3. Strength and strain at failure, Composites Part A: Applied Science and Manufacturing, 27(11), pp.1075-1084.

Unal, H., Mimaroglu, A. and Arda, T., 2006. Friction and wear performance of some thermoplastic polymers and polymer composites against unsaturated polyester. Applied Surface Science, 252(23), pp.8139-8146.

Unal, H., Sen, U. and Mimaroglu, A., 2004. Dry sliding wear characteristics of some industrial polymers against steel counterface. Tribology International, 37(9), pp.727-732.

Vasconcelos, P.V., Lino, F.J., Baptista, A.M. and Neto, R.J., 2006. Tribological behaviour of epoxy based composites for rapid tooling. Wear, 260(1), pp.30-39.

Vasconcelos, P.V., Lino, F.J., Magalhaes, A. and Neto, R.J.L., 2005. Impact fracture study of epoxy-based composites with aluminium particles and milled fibers. Journal of Materials Processing Technology, 170(1), pp.277-283.

Vishwanath, B., Verma, A.P. and Rao, C.K., 1993. Effect of reinforcement on friction and wear of fabric reinforced polymer composites. Wear, 167(2), pp.93-99.

Voss, H. and Friedrich, K., 1985. The wear behavior of short-fiber reinforced thermoplastics sliding against smooth steel surfaces. Wear of Materials, pp.742-750.

Voss, H. and Friedrich, K., 1987. On the wear behaviour of short-fibre-reinforced PEEK composites. Wear, 116(1), pp.1-18.

Wan, Y.Z., Chen, G.C., Raman, S., Xin, J.Y., Li, Q.Y., Huang, Y., Wang, Y.L. and Luo, H.L., 2006. Friction and wear behavior of three-dimensional braided carbon fiber/epoxy composites under dry sliding conditions. Wear, 260(9), pp.933-941.

Ward, R., 1970. A comparison of reciprocating and continuous sliding wear. Wear, 15(6), pp.423-434.

Yang, B., Kozey, V., Adanur, S. and Kumar, S., 2000. Bending, compression, and shear behavior of woven glass fiber–epoxy composites. Composites Part B: Engineering, 31(8), pp.715-721.

Yousif, B.F., 2013. Design of newly fabricated tribological machine for wear and frictional experiments under dry/wet condition. Materials & Design, 48, pp.2-13.

Yousif, B.F. and El-Tayeb, N.S.M., 2008a. Wear and friction characteristics of CGRP composite under wet contact condition using two different test techniques. Wear, 265(5), pp.856-864.

Yousif, B.F., El-Tayeb, N.S.M. and Yusaf, T., 2008b. Influence of material structure properties on sliding contact performance of CGRP composite. International Journal for Manufacturing Science and Technology, 10(1), pp.1-7.

Zaretsky, E. and Perl, M., 2004. The response of a glass fibers reinforced epoxy composite to an impact loading. International Journal of Solids and Structures, 41(2), pp.569-584.

Zeng, H., He, G. and Yang, G., 1987. Friction and wear of poly (phenylene sulphide) and its carbon fibre composites: I unlubricated. Wear, 116(1), pp.59-68.

Zhou, W., 2011. Effect of coupling agents on the thermal conductivity of aluminium particle/epoxy resin composites. Journal of Materials Science, 46(11), pp.3883-3889.

Zhou, W. and Yu, D., 2011. Effect of coupling agents on the dielectric properties of aluminium particles reinforced epoxy resin composites. Journal of Composite Materials, 45(19), pp.1981-1989.

Zhou, X.H., Sun, Y.S. and Wang, W.S., 2009. Influences of carbon fabric/epoxy composites fabrication process on its friction and wear properties. Journal of Materials Processing Technology, 209(9), pp.4553-4557.

Zunjarrao, S.C. and Singh, R.P., 2006. Characterization of the fracture behavior of epoxy reinforced with nanometer and micrometer sized aluminium particles. Composites Science and Technology, 66(13), pp.2296-2305.

****

Professor
Department of Aerospace Engineering
and Applied Mechanics
Indian Institute of Engineering
Science and Technology, Shibpur
Howrah - 711 103, INDIA

Professor
Department of Aerospace Engineering
and Applied Mechanics
Indian Institute of Engineering
Science and Technology, Shibpur
Howrah - 711 103, INDIA